PRESSURE DROP IN A PEBBLE BED REACTOR

A Thesis

by

CHANGWOO KANG

Submitted to the Office of Graduate Studies of
Texas A&M University
in partial fulfillment of the requirements for the degree of

MASTER OF SCIENCE

August 2010

Major Subject: Nuclear Engineering

PRESSURE DROP IN A PEBBLE BED REACTOR

A Thesis

by

CHANGWOO KANG

Submitted to the Office of Graduate Studies of
Texas A&M University
in partial fulfillment of the requirements for the degree of

MASTER OF SCIENCE

Approved by:

Chair of Committee,	Yassin A. Hassan
Committee Members,	William H. Marlow
	Kalyan Annamalai
Head of Department,	Raymond J. Juzaitis

August 2010

Major Subject: Nuclear Engineering

ABSTRACT

Pressure Drop in a Pebble Bed Reactor. (August 2010)

Changwoo Kang, B.S., Korea Military Academy

Chair of Advisory Committee: Dr. Yassin A. Hassan

Pressure drops over a packed bed of pebble bed reactor type are investigated. Measurement of porosity and pressure drop over the bed were carried out in a cylindrical packed bed facility. Air and water were used for working fluids.

There are several parameters of the pressure drop in packed beds. One of the most important factors is wall effect. The inhomogeneous porosity distribution in the bed and the additional wetted surface introduced by the wall cause the variation of pressure drop. The importance of the wall effects and porosity can be explained by using different bed-to-particle diameter ratios. Four different bed-to-particle ratios were used in these experiments (D/d_p = 19, 9.5, 6.33 and 3.65).

A comparison is made between the predictions by a number of empirical correlations including the Ergun equation (1952) and KTA (by the Nuclear Safety Commission of Germany) (1981) in the literature. Analysis of the data indicated the importance of the bed-to-particle size ratios on the pressure drop. The comparison between the present and the existing correlations showed that the pressure drop of large bed-to-particle diameter ratios (D/d_p = 19, 9.5and 6.33) matched very well with the original KTA correlation. However the published correlations cannot be expected to predict accurate pressure drop

for certain conditions, especially for pebble bed with D/d_p (bed-to-particle diameter ratio) ≤ 5. An improved correlation was obtained for a small bed-to-particle diameter ratio by fitting the coefficients of that equation to experimental database.

DEDICATION

This work is dedicated to the following:

I want to thank my parents and sisters for their understanding and encouragement. In addition, I dedicate it to the Korea Army that supported me for two years.

ACKNOWLEDGEMENTS

I would like to thank my committee chair, Dr. Yassin A. Hassan, and my committee members, Dr. William H. Marlow and Dr. Annamalai Kalyan, for their guidance and support throughout the course of this research.

Thanks also go to my friends and colleagues and the department faculty and staff for making my time at Texas A&M University a great experience. I also want to extend my gratitude to the Korea Army, which supported my study for two years, and to all of the lab friends and Korean students in nuclear engineering department who were willing to give advice in my research.

TABLE OF CONTENTS

CHAPTER Page

LIST OF FIGURES

Page

Page

LIST OF TABLES

Page

Page

CHAPTER I

INTRODUCTION

The importance of research

Pebble Bed Modular Reactor (PBMR), developed in South Africa, is type of packed bed. Mechanisms of heat and mass transfer, and the flow and pressure drop of the fluid through the bed of beads are considered for design of PBMR. Among these factors, pressure drop in a pebble bed reactor is important for design of PBMR and related to the pumping power and cost. The right description of the pressure drop explains the energy requirements of the pumps and compressors. Therefore an accurate correlation of pressure drop is required for a wide range of Reynolds number in packed bed. However, fluid velocity and pressure profile cannot be obtained easily for such packed column, particularly if the flow is turbulent. For such systems, experimental data can be used to build correlations of dimensionless variables that can give pressure profile in packed column. In addition, the porosity of the bed is an important factor for these mechanisms. Because the porosity gives affection to the velocity of the wall flow. The pressure loss due to friction in packed beds is part of the total pressure loss. Therefore, in this work, it is chosen to show pressure drop correlation in packed beds.

This thesis follows the style of *International Journal for Numerical Methods in Fluids.*

Review of literature

There have been two main approaches for developing friction factor expressions for packed columns. In one method the packed column is visualized as a bundle of tangled tubes of weird cross section; the theory is then developed by applying the previous results for single straight tubes to the collection of crooked tubes. In the second method the packed column is regarded as a collection of submerged objects, and the pressure drop is obtained by summing up the resistances of the submerged particles. The tube bundle theories have been somewhat more successful.

A variety of materials may be used for the packing in column: spheres, cylinders, Berl saddles, and so on. It is assumed throughout the following discussion that the packing is statistically uniform, so that there is no "channeling" (in actual practice, channeling frequently occurs, and then the development given here does not apply). It is further assumed that the diameter of the packing is contained, and that the column diameter is uniform.

The friction factor for the packed column is

$$f = \frac{1}{4}\left(\frac{d_p}{L}\right)\left(\frac{\Delta P}{\frac{1}{2}\rho v^2}\right) \tag{1}$$

in which L is the length of the packed column, d_p is the effective particle diameter, and v is the superficial velocity. This is the volume flow rate divided by the empty column cross section.

$$v = \frac{\dot{m}}{\rho A} \tag{2}$$

The pressure drop through a representative tube in the tube bundle model is written as

$$\Delta P = \frac{1}{2}\rho \langle v \rangle^2 \left(\frac{L}{R_h}\right) f_{tube} \tag{3}$$

in which the friction factor for a single tube, f_{tube} , is a function of the Reynolds number.

$$\mathrm{Re}_h = 4R_h \langle v \rangle \frac{\rho}{\mu} \tag{4}$$

When this pressure difference is substituted, then the following equation is derived.

$$f = \frac{1}{4}\frac{d_p}{R_h}\frac{\langle v \rangle^2}{v^2} f_{tube} = \frac{1}{4\varepsilon^2}\frac{d_p}{R_h} f_{tube} \tag{5}$$

In the second expression, we have introduced the void fraction, ε, the fraction of space in the column not occupied by the packing. Then v = <v>ε, which results from the definition of the superficial velocity.

The hydraulic radius, R_h, can be expressed in terms of the void fraction, ε, and the wetted surface per unit volume of bed as follows:

$$R_h = \frac{\text{cross section available for flow}}{\text{wetted perimeter}} = \frac{\text{volume available for flow}}{\text{total wetted surface}} = \frac{\left(\frac{\text{volume of void}}{\text{volume of bed}}\right)}{\left(\frac{\text{wetted surface}}{\text{volume of bed}}\right)} = \frac{\varepsilon}{d} \tag{6}$$

The quantity a is related to the "specific surface", a_v (total particle surface per volume of particles) by

$$a_v = \frac{a}{1-\varepsilon} \tag{7}$$

The quantity, a_v, is in turn used to define the mean particle diameter d_p as follows:

$$d_p = \frac{6}{a_v} \tag{8}$$

This definition is chosen because, for spheres of uniform diameter, d_p, is exactly the diameter of a sphere. From the last three expressions we find that the hydraulic radius is

$$R_h = \frac{d_p \varepsilon}{6(1-\varepsilon)} \tag{9}$$

Then, the friction factor is written as

$$f = \frac{3}{2}\left(\frac{1-\varepsilon}{\varepsilon^3}\right) f_{tube} \tag{10}$$

We now adapt this result to laminar and turbulent flows by inserting appropriate expressions for f_{tube}.

(a) For laminar flow, $f_{tube} = 16/Re_h$. This is exact for circular tubes only. To account for the non-cylindrical surfaces and tortuous fluid paths encountered in typical packed-column operations, it has been found that replacing 16 by 100/3 allows the tube bundle model to describe the packed-column data. When this method expression is used for the tube friction facto, then the friction factor becomes

$$f = \frac{3}{2}\left(\frac{(1-\varepsilon)^2}{\varepsilon^3}\right)\frac{75}{d_p \rho v / \mu} \tag{11}$$

This f is used to get pressure difference, then

$$\frac{\Delta p}{L} = 150\left(\frac{\mu v}{d_p^2}\right)\left(\frac{(1-\varepsilon)^2}{\varepsilon^3}\right) \tag{12}$$

Which is the Blake–Kozeny equation.

It is good for $\mathrm{Re_m} = \frac{\rho v d_p}{\mu(1-\varepsilon)} < 10 \quad and \quad \varepsilon < 0.5$

(b) For highly turbulent flow, a treatment similar to the above can be given. We begin again with the expression for the friction factor definition for flow in a circular tube. This time, however, it is noted that, for highly turbulent flow in tubes with any appreciable roughness, the friction factor is a function of the roughness only, and is independent of Reynolds number. If it is assumed that the tubes in all packed columns have similar roughness characteristics, then the value of f_{tube} may be taken to be the same constant for all systems. Taking $f_{tube} = 7/12$ proves to be an acceptable choice. When this is inserted into eq.(10), then

$$f = \frac{7}{8}\left(\frac{1-\varepsilon}{\varepsilon^3}\right) \tag{13}$$

When this is substituted into eq.(1), then

$$\frac{\Delta p}{L} = \frac{7}{4}\left(\frac{\rho v^2}{d_p}\right)\left(\frac{1-\varepsilon}{\varepsilon^3}\right) \tag{14}$$

which is the Burke-Plummer equation, valid for $Re_m = \frac{\rho v d_p}{\mu(1-\varepsilon)} > 1000.$

(c) For the transition region, after superposition of the pressure drop expressions for (a) and (b) above to get

$$\frac{\Delta p}{L}=180\left(\frac{\mu v}{d_p^2}\right)\left(\frac{(1-\varepsilon)^2}{\varepsilon^3}\right)+1.8\left(\frac{\rho v^2}{d_p}\right)\left(\frac{1-\varepsilon}{\varepsilon^3}\right) \tag{15}$$

For very small v, this simplifies to the Blake-Kozeny equation, and for very large v, to the Burke-Plummer equation. Such empirical super-positions of asymptotes often lead to satisfactory results. Again, it is rearranged to form dimensionless groups:

$$\left(\frac{\Delta p\rho}{G^2}\right)\left(\frac{d_p}{L}\right)\left(\frac{\varepsilon^3}{1-\varepsilon}\right)=150\left(\frac{1-\varepsilon}{d_pG/\mu}\right)+\frac{7}{4}=\frac{150}{\mathrm{Re}_m}+\frac{7}{4} \tag{16}$$

The most widely used correlation is the Ergun equation(1952) [1].

$$\frac{\Delta p}{L}=150\left(\frac{\mu v}{d_p^2}\right)\left(\frac{(1-\varepsilon)^2}{\varepsilon^3}\right)+1.75\left(\frac{\rho v^2}{d_p}\right)\left(\frac{1-\varepsilon}{\varepsilon^3}\right) \tag{17}$$

This equation is comprised of the pressure drop as the sum of the pressure losses coming from the viscous energy loss and the inertial energy loss. Therefore it is valid for laminar, turbulent as well as transitional region. It is also very simple and convenient to use and gives good results for predicting the pressure drop. However, the coefficients (150 and 1.75) in the Ergun equation [1] are not constants and don't have physical meanings but depend on many factors such as the Reynolds number, the porosity, and particle shape. Moreover, the obtained pressure drop results from the Ergun equation [1] are mostly less than other's data in the low Reynolds number regimes($\frac{\mathrm{Re}}{(1-\varepsilon)} \leq 10$). Otherwise, the Ergun's predictions are larger than some experimental data by other researchers. Plus, one of their limitation is that their equation is mainly applicable for spherical particles in the porosity range of 0.35~0.55. Therefore, researchers are in

agreement with the fact that the values of the Ergun constants should be determined empirically for each bed and many have tried to make proper correlations.

One of the most used correlations for predicting pressure drop through the pebble bed type reactor is the KTA(1981) correlation [2]. They performed an extensive investigation to give an empirical correlation for the pressure loss coefficient due to friction. KTA correlation [2] is valid for wide range of Modified Reynolds number($10^0 < Re_m < 10^5$). However their valid range of porosity(ε) is from 0.36 to 0.42.

There are several influencing parameters of the pressure drop in packed beds. One of the most important factors is wall effect. The inhomogeneous porosity distribution in the bed and the additional wetted surface introduced by the wall cause the variation of pressure drop. The opinions about the resultant wall effect are contradictory. Some researchers found increase of the pressure drop due to the wall effect. But others said they have obtained a reduction due to the wall effect. Many researchers have concluded the following: The pressure drop can be increased by wall friction or decreased by an increase in porosity near the wall based on the type of flow regime. In the lower Reynolds number regime, the wall friction is highly affected. In the high Reynolds number regime, the porosity effect is dominant [3]. Some other published paper on the influence of the tube to particle diameter ratio shows that the increasing pressure drop due to the wall effect are based on experiments under streamline flow conditions or in the transitional range[4],[5],[6],[7]. Otherwise, the decreasing pressure drop due to the wall effect is measured at high Reynolds numbers[4],[8],[9],[10]. The general conclusion is that the Ergun equation[1] (with average values of porosity and superficial

velocity) is applicable down to tube-to-particle-diameter ratios of D/d_p >10. He tested with the tube-to-particle-diameter ratio higher than 10, so the experimentally determined Ergun constants should not be affected by the reactor column wall.

Mehta and Hawley(1969)[7] redefined the equivalent diameter in Ergun equation[1] and introduced the modified Ergun equation to use for the finite beds with wall effects. The hydraulic radius is shown as a characteristic length of the packed bed and it should depend on the wall for small bed-to-particle diameter ratios. And they used the wall correction factor that explains the effect of the bed-to-particle diameter ratios on the hydraulic diameter. This factor is used for modifying the hydraulic diameter. However, their result is only valid for the limited Reynolds number regimes ($Re_m < 10$).

R.E Hicks(1970)[11] also said that two coefficients are not constants but they are the functions of Reynolds number. Also, he found a friction factor. It is not intended as a general equation for packing beds but emphasized that the Ergun equation [1] is not valid for values of Reynolds number less than 500.

Reichelt(1972)[12] modified Mehta and Hawley's correlation[1] and redefined a wall modified hydraulic radius and corresponding wall modified parameters.

Macdonald et al.(1979)[13] also changed two coefficients of the Ergun's equation[1]. Moreover, using $\varepsilon^{3.8}$, instead of ε^3 is considered to make better fit to the data point. He divided the various published model into three categories: phenomenological model, model based on the conduit flow (a. geometrical model, b. statistical model, c. model utilizing the complete Navier-Stokes equation), and models based on flow around

submerged objects. Their equation is also valid for only limited Reynolds number regime.

R.M. Fand and R. Thinakaran(1990)[14] expressed their correlation with the respect to the porosity and the flow parameters as functions of the bed-to-particle diameter ratios. But their experiments were limited within circular cylinders.

Comiti and Renaud(1989)[15] generated the correlation of a capillary type model. Their correlation for the pressure drop has two terms like many correlations. The first term of the model explains the wall friction in the pore as well as at the bed wall, while the second one accounts for the energy loss and wall effects. Each term of the equation of the model is shown as a function of three structural parameters that are the porosity, the dynamic specific surface area, and the tortuosity.

Foumeny et al.(1993)[8] provided a correlation for mean porosity in packed beds of spherical particles. They have mentioned that one of common source of error is the assumption the mean porosity of packed beds with spherical particles is nearly equal to 0.4. And they tried to solve the problem of existing pressure drop correlations that didn't account for the strong wall effect of the low bed-to-particle diameter ratio. In addition, their porosity equation follow a general rule, decreasing the particle size reduces the mean porosity of the bed and, therefore, increases the pressure drop. Their approach has followed from this paper.

Shijie Liu et al.(1994)[16] showed the fluid has different chances for mixing and less curvature effects is considered to the flow near the wall. A near the wall, the particle has less possibilities of fluid mixing due to less faces of incoming flow. They considered and

assumed that the mixing and the curvature effects are equally affected by the wall. The limitation of their equation is validation for limited Reynolds number.

R.E. Hayes(1995)[17] reported the Darcy law is available for low Reynolds number less than one. His new correlation for the permeability of a packed bed has been presented. Capillary and the cell models are applied for modeling pressure drop in porous media. The proposed porous micro structure of a square channel is not affordable for a physical model of a porous medium is filled with uniform spherical particles.

Eisfeld and Schnitzlein(2001)[3] made an improved correlation that accounts for the wall effect. For the inertial pressure loss term, they manipulated the coefficients of the wall correction factor. They mentioned the boundary layer theory that indicates the wall friction. The wall friction factor is restricted to a small boundary layer at high Reynolds numbers and it reaches further into the reactor at low Reynolds numbers. They concluded that the pressure drop can be increased by wall friction or decreased by an increase in porosity near the wall. In the low Reynolds number regime, the wall friction effects in more important and it causes the pressure drop to decrease. Otherwise, the porosity is more influential that the wall friction factor in the high Reynolds number regime and the pressure drop increases. They also explained that the predominance of one effect depends on fluid velocity. According to Foumeny et al.[8], their wall correction factor for the inertial pressure loss term doesn't come from physical reasoning and it is based on curve-fitting model. Moreover their equation makes a larger inertial pressure loss term that that of the Ergun equation[1] for the bed of D/d_p.

Niven(2002)[18] discusses a model of pore conduits consisting of alternating expanding and contracting sections can be used for analyzing of Ergun equation[1]. They obtained a model for the pressure drop in packed beds even though it has too many parameters to be determined.

Di Felice and Gibilaro(2004)[19] also suggested a model which explains the wall effect in packed beds. They used a corrected average superficial fluid velocity to predict the pressure drop. The parallel flow of fluid through two zones, the bulk zone and the wall zone, is indicated in their results. By using their simple model, the unusual trend of pressure loss - increasing with increasing of wall effects in the viscous flow regime and decreasing with increasing wall effects in the inertial flow regime - is explained. The limitation of their results is poor predictions in the high Reynolds number regime.

Agnes Montillet(2004)[20] mentioned the experimental pressure drop is lower than that predicted by classical models and it seems difficult to give a physical explanation to this phenomenon. The influence of the wall effect decreases with the bed-to-particle diameter ratio, but this influence is hard to estimate at large Reynolds numbers for the bed-to-particle diameter ratios more than 10. Their work indicated the pressure drop in a finite bed is not a power 2 terms in velocity for the turbulent flow regime. A correlating equation for $f(\varepsilon)$ of Rose correlation[21], which account for the effect of the bed-to-particle diameter ratio, is proposed in their results.

Nemec and Levec(2005)[22] studied the effect of particle shapes and sizes and bed packing techniques on the single phase pressure drop in packed bed.

Y.S. Choi et al.(2008)[23] developed a semi-empirical pressure drop equation for the packed beds of spherical particles with small bed-to-particle diameter ratios. They used capillary-orifice model which treats a packed bed as a bundle of capillary tubes with orifice plates to explain a wall correction factor for the inertial pressure loss term.

Jinsui Wu. et al.(2008)[24] evaluated that the effect of the bed height on the pressure drop with constant ball diameter. It is found that the pressure drop increases with increasing of the bed height and the fluid velocity. The average hydraulic radius model and the contracting-expanding channel model are also used for their model.

The previously discussed correlations are obtained by limited empirical experiments. Table 1 Shows the pressure drop correlations, porosity ranges, bed-to-particle diameter ratios and Reynolds number ranges found in the literature. These correlations are limited in the sense of a narrow range of Reynolds number and limited porosity range used. This causes a problem when the use of a wide range of Reynolds number and porosities is needed.

The purposes of this paper are to verify the KTA correlation [2] that is used for Gas Cooled Pebble Bed Reactor and to formulate an accurate correlation for pressure drop that includes wall effect. This work also presents data for CFD validation. For these purpose, we made experimental set up of cylindrical packed bed and annular packed bed. The real pebble bed reactor geometry was changed from a cylindrical bed ($D/d_p = 61.7$) to annular bed($D_o - D_i$)/$2d_p$ =14.17). These present experiments that were considering of real packed geometries would give good directions for predicting of pressure drop.

Table 1. Pressure drop correlations, porosity, diameter ratios and Reynolds number found in the literature.

Author	Pressure drop equation	ε	d_p(cm)	D/d_p	Re or Re_m
Ergun(1952)	$\frac{\Delta p}{L}=150\left(\frac{\mu v}{d_p^2}\right)\left(\frac{(1-\varepsilon)^2}{\varepsilon^3}\right)+\frac{7}{4}\left(\frac{\rho v^2}{d_p}\right)\left(\frac{1-\varepsilon}{\varepsilon^3}\right)$				1<Re<10^3
Handley/Heggs(1968)	$\frac{\Delta p}{L}=368\left(\frac{(1-\varepsilon)^2}{\varepsilon^3}\right)\left(\frac{\mu v}{d_p^2}\right)+1.24\left(\frac{\rho v^2}{d_p}\right)\left(\frac{1-\varepsilon}{\varepsilon^3}\right)$	0.390	3.17 9.52	8 24	399<Re<3985
Reichelt(1972)	$\frac{\Delta p}{L}=\left(\frac{154A_w^2\mu(1-\varepsilon)}{\rho v d_p}+\frac{A_w}{B_w}\right)\left(\frac{\mu v}{d_p^2}\right)\left(\frac{(1-\varepsilon)^2}{\varepsilon^3}\right)$ $A_w=1+\left(\frac{2}{3\frac{D}{d_p}(1-\varepsilon)}+1\right)^2$ $B_w=\left(1.15\left(\frac{d_p}{D}\right)^2+0.87\right)$	0.366~0.485	9.71~24.05	3.32~14.32	0.01<Re<17635
Foumeny(1993)	$\frac{\Delta p}{L}=130\left(\frac{(1-\varepsilon)^2}{\varepsilon^3}\right)\left(\frac{\mu v}{d_p^2}\right)+\left(\frac{D/d_p}{(0.335(D/d_p)+2.28)}\right)\left(\frac{\rho v^2}{d_p}\right)\left(\frac{1-\varepsilon}{\varepsilon^3}\right)$	0.386~0.456	2.1~15.48	3.23~23.8	5<Re_m<8500
Yu(2002)	$\frac{\Delta p}{L}=203\left(\frac{\mu v}{d_p^2}\right)\left(\frac{(1-\varepsilon)^2}{\varepsilon^3}\right)+1.95\left(\frac{\rho v^2}{d_p}\right)\left(\frac{1-\varepsilon}{\varepsilon^3}\right)$	0.364~0.379	12~20	30	797<Re<2449
Montillet(2004)	$\frac{\Delta p}{L}=\left(\frac{1410}{\mathrm{Re}}+16+\frac{45}{\mathrm{Re}^{0.45}}\right)\left(\frac{\rho v^2}{d_p}\right)$	0.367	4.92	12.2	30<Re<1500
Y.S.Choi(2008)	$\frac{\Delta p}{L}=150\left(\frac{\mu M^2 v}{d_p^2}\right)\left(\frac{(1-\varepsilon)^2}{\varepsilon^3}\right)+1.75\left(\frac{\rho M C_w v^2}{d_p}\right)\left(\frac{1-\varepsilon}{\varepsilon^3}\right)$			3.2~91	0.01<Re<10^3
J.Wu(2008)	$\frac{\Delta p}{L}=72\tau\left(\frac{\mu v}{d_p^2}\right)\left(\frac{(1-\varepsilon)^2}{\varepsilon^3}\right)+\frac{3}{4}\tau\left(\frac{\rho v^2}{d_p}\right)\left(\frac{1-\varepsilon}{\varepsilon^3}\right)\left(\frac{3}{2}+\frac{1}{\beta^4}-\frac{5}{2\beta^2}\right)$ $\beta=\frac{1}{1-\sqrt{1-\varepsilon}}$	0.42	10		0<Re_m<4000
Leva(1951)	$\frac{\Delta p}{L}=200\left(\frac{\mu v}{d_p^2}\right)\left(\frac{(1-\varepsilon)^2}{\varepsilon^3}\right)+\frac{7}{4}\left(\frac{\rho v^2}{d_p}\right)\left(\frac{1-\varepsilon}{\varepsilon^3}\right)$	0.354~0.651		1.624 ~13.466	1<Re<17635

Table 1. continued

Author	Pressure drop equation	ε	d_p(cm)	D/d_p	Re or Re_m
Wentz and Thodos(1963)	$\frac{\Delta p}{L}=\left(\frac{\mu v}{d_p^2}\right)\left(\frac{(1-\varepsilon)^2}{\varepsilon^3}\right)\left(\frac{0.396\,\mathrm{Re}_m}{\mathrm{Re}_m^{0.05}-1.20}\right)$	0.354~0.882	3.1242	11.382	1460<Re<7661
Tallmadge(1970)	$\frac{\Delta p}{L}=\left(\frac{\mu v}{d_p^2}\right)\left(\frac{(1-\varepsilon)^2}{\varepsilon^3}\right)\left(150+4.2\,\mathrm{Re}_m^{0.833}\right)$				0.1<Re<10^5
Hicks(1970)	$\frac{\Delta p}{L}=6.8\left(\frac{(1-\varepsilon)^{1.2}}{\varepsilon^3}\right)\left(\frac{\rho^{1.2}v^{1.8}\mu^{0.2}}{d_p^{1.2}}\right)$				300<Re_m<60000
R.E. Hayes(1994)	$\frac{\Delta p}{L}=\left(\frac{\mu v}{d_p^2}\right)\left(\frac{(1-\varepsilon)^2}{\varepsilon^3}\right)\left\{\frac{1}{\tau}\left[456+\frac{17.8(3\tau-1)}{\tau(1-\varepsilon)(1-\tau)}\mathrm{Re}\right]^{0.5}\frac{1}{\varepsilon}+1.3\left(\frac{\tau}{3\tau-1}\right)\mathrm{Re}_m\right\}$	0.402, 0.408,0.427, 0.385	2.97, 4.82, 6.01, 2.5		3<Re<1000
KTA(1981)	$\frac{\Delta p}{L}=\left(\frac{320}{\mathrm{Re}/(1-\varepsilon)}+\frac{6}{(\mathrm{Re}/(1-\varepsilon))^{0.1}}\right)\left(\frac{1-\varepsilon}{\varepsilon^3}\right)\left(\frac{\rho v^2}{d_p}\right)\left(\frac{1}{2\rho}\right)$	0.36 ~0.42			10<Re_m<10^5
Brauer(1960	$\frac{\Delta p}{L}=\left(160+3.1\mathrm{Re}_m^{0.9}\right)\left(\frac{\mu v}{d_p^2}\right)\left(\frac{(1-\varepsilon)^2}{\varepsilon^3}\right)$				2<Re_m<20000
Foscolo(1982)	$\frac{\Delta p}{L}=1.73\left(\frac{1-\varepsilon}{\varepsilon^{4.8}}\right)\left(\frac{\mu v}{d_p^2}\right)+0.336\left(\frac{1-\varepsilon}{\varepsilon^{4.8}}\right)\left(\frac{\rho v^2}{d_p}\right)$				0.2<Re<500
Macdonald(1979)	$\frac{\Delta p}{L}=150\left(\frac{\mu v}{d_p^2}\right)\left(\frac{(1-\varepsilon)^2}{\varepsilon^3}\right)+\frac{7}{4}\left(\frac{\rho v^2}{d_p}\right)\left(\frac{1-\varepsilon}{\varepsilon^3}\right)$				
Shijie Liu(1994)	$\frac{\Delta p}{L}=\left(\frac{\mu v}{d_p^2}\right)\left(\frac{(1-\varepsilon)^2}{\varepsilon^{11/3}}\right)$ $\left\{85.2\left(1+\frac{\pi(d_p/D)}{6(1-\varepsilon)}\right)^2+0.69\left(1-\frac{\pi^2(d_p/D)}{24}(1-0.5(d_p/D))\right)\mathrm{Re}_m\frac{\mathrm{Re}_m{}^2}{16^2+\mathrm{Re}_m{}^2}\right\}$	0.6007	3.184	1.4039	1328 < Re_m < 4081
Carman(1970)	$\frac{\Delta p}{L}=(180+2.87\,\mathrm{Re}_m^{0.9})\left(\frac{\mu v}{d_p^2}\right)\left(\frac{(1-\varepsilon)^2}{\varepsilon^3}\right)$				
Rose(1949)	$\frac{\Delta p}{L}=f(\varepsilon)\left(\frac{1000}{\mathrm{Re}}+\frac{60}{\mathrm{Re}^{1/2}}+12\right)\left(\frac{\rho v^2}{d_p}\right)$ f(ε) is 1 for ε = 0.4	0.373 0.480	1.12 3.10	10.25 2.7	1000<Re<6000
Morcom(1946)	$\frac{\Delta p}{L}=\left(\frac{800}{\mathrm{Re}}+14\right)\left(\frac{\rho v^2}{d_p}\right)$	0.425 ~0.450	0.56~1.01		100<Re<500

Theoretical consideration

There are several influencing parameters of pressure drop in packed beds.

Wall effect and porosity are especially considered in this work.

Wall effect

The wall effect exists for packed beds. The inhomogeneous porosity distribution in the bed and the additional wetted surface introduced by the wall cause the variation of pressure drop. It is important to predict the wall effect.

The opinions about the resultant wall effect are contradictory. Some researchers found increase of the pressure drop due to the wall effect. But others said they have got a reduction due to the wall effect.

Many researchers have concluded as follows : The pressure drop can be increased by wall friction or decreased by an increase in porosity near the wall. The flow regimes affect the predominance of one effect over the other. The wall friction effect is more important than the increased porosity effect in the low Reynolds number regime. On the other hand, the porosity effect is dominant in the high Reynolds number regime [3]. Some other published paper on the influence of the tube to particle diameter ratio shows that the increasing pressure drop due to the wall effect are based on experiments under streamline flow conditions or in the transitional range [4],[5],[6],[7]. Otherwise, the decreasing pressure drop due to the wall effect is measured at high Reynolds numbers[4],[8],[9],[10]. There are some efforts to account for the wall effect. The first

attempt to address the wall effect was made by Crman(1937)[5]. He considered that the wall effect on the inertial term is negligible and only the viscous term(Darcy's flow) needs to be corrected. Recent experimental studies showed that Carman's treatment is inadequate.

One of the main researchers is Metha and Hawley(1969)[7]. They defined a hydraulic radius,

$$R_H = \frac{\varepsilon}{6(1-\varepsilon)M} \tag{18}$$

Where, $M = 1 + \frac{2}{3}\left[\frac{d_p}{D(1-\varepsilon)}\right]$.

Their conclusion is that wall effects are not significant if the diameter ratio is greater than 50.

Fand et al.(1990)[14] said that experimental data obtained by Metha and Hawley(1969)[7] indicates that this last conclusion is somewhat overly conservative. Finally they concluded that wall effects are not significant if the diameter ratio is greater than 40.

Riechelt(1972)[12] modified Metha and Hawley's correlation[7], and he defined a wall modified hydraulic radius,

$$R_{hw} = \frac{R_H}{M} \tag{19}$$

He also yielded corresponding "wall-modified" parameters:

$$f_w = \frac{f'}{M} \tag{20}$$

$$\mathrm{Re}_w = \frac{\mathrm{Re}'}{M} \tag{21}$$

At last, he obtained the following modification equation,

$$f_w = A_w / \mathrm{Re}_w + B_w; \qquad A_w = 150, \quad \frac{1}{\sqrt{B_w}} = \frac{1.5}{(D/d_p)^2} + 0.88 \tag{22}$$

Fand et al.(1990)[14] reported that, for cylindrical ducts packed with spheres, the "wall effect" becomes significant for $D/d_p < 40$, and consequently the flow parameters become functionally dependent upon D/d_p for $D/d_p < 40$.

Foumeny(1993)[8] also concluded that the wall effect is important when the diameter ratio, D/d_p, is less than 50, and it is pronounced at values less than 12.

The general conclusion of all above works is that the Ergun equation[1](with average values of porosity and superficial velocity) from a practical point of view is applicable down to quite low tube-to-particle-diameter ratios($D/d_p \geq 10$). They tested with the tube-to-particle-diameter ratio higher than 10, so the experimentally determined Ergun constants should not be affected by the reactor column wall.

Porosity

The pressure drop is extremely sensitive to changes in the mean void fraction, ε , This influence is described either empirically, using dimensional analysis [21], or theoretically, most often employing the hydraulic radius concept [1],[5]. The porosity, ε,

defined as the fraction of the total volume of a porous medium represented by the voids in its matrix, is a primary controlling geometry of the matrix of the medium. For the case of spherical particles contained in a circular cylinder, the porosity tends toward unity upon approach to the cylinder wall [14].

The constants of Ergun equation [1], A and B, can vary from macroscopic bed to bed even if repacked with the same batch of particles. If the repacking of the bed changes the values of the Ergun constants this could mean that the porosity is not adequately taken into account by the capillary model [22].

Rumph and Gupte(1971) [25] have analyzed the effect of various distributions of spherical particles over a relatively wide range of porosities($0.35 < \varepsilon < 0.70$) and proposed a different dependence upon porosity. For the region of packed bed reactor relevance ($0.35 < \varepsilon < 0.55$) does not differ very much from that of the capillary model, considering an average difference of only about 10%. Other porosity functions like the one determined by Liu et al.(1994)[26] in general yield values between those of the capillary model and the empirical model proposed by Rumph and Gupte(1971) [25]. Furthermore, it has to be pointed out that the results of Rumph and Gupte(1971) [25] have been obtained from media created with higher porosities than normally encountered in beds composed of spherical particles and could therefore lead to non-uniformly packed beds giving us the wrong impression. Thus, it was deemed necessary to recheck the porosity effect on pressure drop with more natural particle distributions.

Some additional differences between the porosities of beds, despite the same packing procedures, were due to wall effect. One can conclude that the porosity dependence

seems to be well described by the capillary model, reflected by the fact that all the data lay on a single curve for all packed beds. This is in agreement with a number of works for the viscous regime reviewed by Carman(1937)[5] as well as a more recent one of Endo et al.(2002)[27]. With regards to the porosity dependence within the inertial regime, Hill et al.(2001)[28] reported, on the basis of theoretical simulations of flow through random arrays of spheres, that the porosity function is also well taken into account as long as the porosity is around 0.4 as is indeed the case for packed bed reactors when made up of spheres. Ergun(1952)[1] also made an interesting point that if a transformation of his equation is made employing the fundamental expressions for the shear stress, hydraulic radius and interstitial velocity, this leads to complete elimination of porosity, in the field of aerodynamics. Therefore, the porosity function of the capillary model can be assumed as an accurate one within the region of interest($0.35<\varepsilon<0.55$) as the arguments for overweight those against [22].

CHAPTER II

EXPERIMENTAL METHODOLOGY

This chapter explains the channel flow facility, experimental techniques and detailed methods used for this investigation.

A pressure drop experimental setup had been designed for studying single-phase flow studies. The basic components of the test rig were the test section(column), different kinds of pump, reservoir water tank, hot film manometer to measure velocity of working fluid, several flow meters(electrical flow meter, Dwyer rate master flow meter and Hi-volume air flow rate calibrator), different kinds of pressure measurer (Pressure transducers, Magnehelic differential pressure gages, Inclined-Vertical manometer and Digital manometer) and electrical thermometer. A cylindrical packed bed and an annular type packed bed were used for these experiments. Also, four different sizes of spherical particles were used for air and water test.

Properties of working fluids

The working fluids are air and water. Tables 2 and 3 show the properties of working fluids, air and water.

Table 2. Air properties

Temperature(°C)	Density (kg/m3)	Dynamic Viscosity (kg/m·s)
28	1.204	0.0000182

Table 3. Water properties

Temperature(°C)	Density (kg/m3)	Dynamic Viscosity (kg/m·s)
25	997.13	0.000891
26	996.86	0.000871
27	996.59	0.000852
28	996.31	0.000833
29	996302	0.000815
30	995.71	0.000798
31	995.41	0.000781
32	995.09	0.000765
33	994.76	0.000749
34	994.43	0.000734
35	994.08	0.000720
36	993.73	0.000705
37	993.37	0.000692
38	993.00	0.000678
40	992.63	0.000666
39	992.25	0.000653

Instruments for cylindrical bed experiments

A test rig

The column is a cylindrical bed. The diameter of column is 4.75" (0.12065m). The length is 60" (1.534m). It has five tabs to measure pressure. Thin aluminum grids were placed at the column inlet and outlet to serve as a filter.

Beads

The column was filled with spherical balls randomly. Four different sizes of sphere beads were used for this experiment. These sizes were 0.635cm, 1.27cm, 1.905cm and 3.302cm. By using these particles, pressure drops over the bed were measured. And each different bed-to-particle ratios gave different porosities. It affected the velocity on the bed wall. As the size of particles increases, a high Reynolds number was presented at same flow rate because of diameter of the particle as well as porosity affections to the Reynolds number.

Pipes, valves, and unions

The diameter of cylindrical pipes that were used for these experiments were 1.5 inches (3.81cm). Fluid flows were controlled by using valves. Unions were also used for connection of pipes.

A reservoir tank

A Reservoir tank was used for water experiments. The water should be enough to make a loop. The shape of tank was rectangular parallelepiped.

Pumps (power source)

For water experiments: A 3 H.P. pump was used with Lancer GPD 502 that was pump controller. The RPM was 3450. The maximum frequency was 60Hz. The fluid was pumped from a reservoir tank through the packed bed using this centrifugal type pump.

For air experiments: Two different power sources were used for these experiments.

- Air compressor
- Blower(Hi-Q) (it sucked the air from the bottom of the column.)

Pressure instruments

4 different pressure instruments were used for these experiments in order to check wall pressures with high accuracy. It would be also good error estimator by comparing each result.

- Magnehelic differential pressure gages (6 different scale pressure gages)
- Inclined - Vertical Manometer (scale: 0 to 10 inches water)
- Digital Manometer (for 0 to 40 psi)
- Pressure transducer (5 sensors of the pressure transducer (for 0 to 30 psi))
- Model : NI-SCXI model (1600/1200/1000)

Flow meter

For water experiments, a magnetic electrical flow meters with a digital display was placed at the inlet of the channel to measure the bulk flow rate. The flow rate was checked by using a propeller type flow meter

For air experiments, 3 different flow meters were used.

- Dwyer rate master flow meter(scale)
- Hi-volume air flow rate calibrator: The HFC-XXC series units utilize a precision machined venturi tube coupled with a pressure differential gauge giving a direct reading in the volumetric units of our choice
- Hot-film manometer: It measures velocity of the pipe. By multiplying area to velocity, flow rate can be calculated.

Experimental techniques

Pressure transducer is a device capable of measure the pressure that is present at certain point with a cross sectional area, A. The basic definition of pressure is the ratio of the force applied to a body divided by the cross sectional area where the force is being applied. The differential pressure transducer measures the difference of pressure at two different locations or in two different directions. The differential pressure transducer used in this study is the validyne model DP103. This device utilizes a central diaphragm as a sensor element and is of the variable reluctance type.

A variable reluctance pressure transducer is perhaps best described as an inductive half-bridge, and consists of a pressure sensing diaphragm and two coils. The coils are wired in series and are mounted so their axes are normal to the plane of the diaphragm. Clamped tightly between the coil housings, the diaphragm is free to move in response to differential pressure.

The coils are supplied with an AC excitation, typically 5 Vrms at 3 or 5 KHz. The coils are matched so that their impedances are approximately equal. When a differential pressure is applied to the sensor, the diaphragm deflects away from one coil and towards the opposite. The diaphragm material is magnetically permeable, and its presence nearer the one coil increases the magnetic flux density around the coil. The stronger magnetic field of the coil, in turn, causes its inductance to increase, which increases the impedance of one coil. At the same time, the opposite coil is decreasing its impedance. The change

in coil impedances brings the half-bridge out of balance, and small AC signal appears on the signal line.

The change in coil impedance is directly proportional to the position of the diaphragm, so the amplitude of the signal is directly proportional to the applied pressure. The phase of the signal with respect to the excitation is determined by the direction of movement of the diaphragm."

Sensitivity to low pressures

Because the diaphragm need move only one or two thousandths of an inch to produce a full scale output, the thickness and area of the diaphragm determines the full-scale pressure range. A large diaphragm made of thin foil will respond to extremely low pressures. Conversely, a thick diaphragm with a small area responds to very high pressures.

Frequency response

The ability of a pressure sensor to respond accurately to rapid pressure changes is a function of three variables: the mechanical response of the sensor itself, the frequency response of the sensor electronics, and the natural frequency of the plumbing that brings the pressure waveform to the transducer. The mechanical response of the sensor depends on the construction of the sensing element. The electronics connected to a pressure transducer will mostly likely include damping, or a low pass filter on the output stage that may even be the most limiting factor in system response. The tubing that leads

up to the transducer from the pressure source will also have a resonant frequency that will limit the usable response of the pressure measuring system. Each of these factors must be considered in order to arrive at a good estimate of the accurate response of the pressure measurement system.

Sensor mechanical response

Almost all pressure-sensing technologies rely on a pressure-sensing diaphragm to transmit the dynamic pressure waveform to the electro-mechanical element of the pressure sensor. For sensing technologies other than variable reluctance, the sensing diaphragm is connected via linkages or other mechanical means to a strain gage, piezoelectric, capacitive, or some other electrical sensing element. The stiffness of the sensing diaphragm and the associated linkages create a mechanical spring-mass system whose natural frequency is usually specified by the manufacturer. If the sensor is under-damped, amplification and also dynamic error, of the incoming waveform occurs. If the sensor is over-damped, the incoming pressure waveform is attenuated. In either case, pressure measurement at or near the natural frequency of the sensor will result in undesirable distortion of the dynamic signal.

For variable reluctance pressure sensors, the only mechanical part that moves in response to pressure is the sensing diaphragm, and the total displacement over a full scale pressure excursion is less than 2 thousandths of an inch. There are no mechanical linkages or hydraulics inside the sensor to slow down the sensing element. The position of the diaphragm is measured inductively, and this is how the sensed pressure is

converted to an electrical signal. The natural frequency of variable reluctance transducer is a function of range. Because the sensing diaphragm is in contact with the flow being measured, the sensor is typically over-damped at its natural frequency.

Pressure transducer

Two PCI 6024 data acquisition boards from National Instruments acquire the analog-signal produced by the differential pressure transducer. This board counts with an A/C converter to convert the analog signal into a digital one. The internal clock board gives the maximum conversion rate for the A/D converter. A code program developed in Labview was the responsible for the data acquisition start, storage and process. Basically, this program waits for the trigger signal generated by the frame grabber PCI 1424 and then starts the acquisition of data. The program has the capability to choose the acquisition rate.

Porosity measurements

One of the most important parameters affecting the behavior of a packed bed is the accurate quantification of its porosity. However, its measurement is a challenging topic when talking about randomly packing beds due to the nature of the packing. Three independent methods were implemented in order to characterize the porosity or voids fraction in the column: water displacement, weighting and particle counting.

Water displacement method

This method consists in pouring water in the empty column and measuring the total water volume poured. The second step is to randomly pack the spheres into the column. Water is poured into the randomly packed bed until the whole column was completely filled. The column was shaken during the water pouring in order to let the trapped air between the pores to escape. The water is then collected into an accurate scaled container. The voids fraction is obtained by subtracting the amount of water measured in the container when the column is packed from the one obtained from the empty column. The procedure is repeated several times and the average porosity is quantified.

Weighting method

In this method the total number of spheres packed into the column is needed in addition to the volume of the empty column. The empty column volume is calculated using the cylinder dimensions. The total number of beads is obtained by weighting the randomly packing the beads in the column. The total bead's weight is calculated by subtracting the

empty column weight. In an independent procedure, the weight of groups of 5, 10, 15, 20 and 100 beads is measured in order to obtain an average weight per bead. The total number of beads in the column is calculated using the ratio of the total beads weight to an individual bead weight. Once the total number of spheres is known, the total volume occupied by the packing material is calculated using the volume of an individual sphere. The porosity value is calculated by subtracting the volume of the empty column from the volume occupied by the spheres. This method assumed that the beads are perfect spheres with tight tolerances in its diameter.

Particle counting method

This method consists in manually counting the total number of beads inside the column. The total volume occupied by the spheres is calculated by multiplying the number of spheres times the volume of an ideal sphere. The porosity is obtained by subtracting the total volume occupied by the spheres from the volume of the empty column. The method is repeated several times to obtain a good statistical value of the averaged porosity.

The last one was most accurate even though it was time consuming. The porosity was also compared with several porosity correlations to confirm the porosity and to get the regime of porosity error.

Comparison with existing porosity correlations

To compare present work for porosity measurements with existing porosity correlations, 6 correlations were chosen.

Fand and Thinakaran (1990) [14]

$$\varepsilon = \frac{0.151}{(\frac{D}{d_p} - 1)} + 0.360, \text{for } D/d_p \geq 2.033 \tag{23}$$

Beaver et al. (1973) [29]

Beaver et al.[29] said that the porosity increases with decreasing D/d_p for small beds. When D/d_p is greater than 15, the size of the bed appears to have no effect on the porosity. The average value of the porosity for all beds having D/d_p is greater than 15 was found to be 0.368, with a maximum deviation of less than 2 percent. They also reported that the trend of variation of ε with D/d_p can be predicted by employing a simple model first proposed by Rose. If it is assumed that the outer layer of spheres, to a depth of d/2 from the walls, has void fraction ε_w and that the inner core is randomly packed and has a void fraction ε_∞, then the porosity of the whole bed is given by

$$wh\varepsilon = [wh - (w - d_p)(h - d_p)]\varepsilon_w + [(w - d_p)(h - d_p)]\varepsilon_\infty \tag{24}$$

$$D_e = 2wh/(w+h) \tag{25}$$

where, $wh\varepsilon$ is the porosity of the whole bed.

D_e is the equivalent diameter of the bed.

h and w are, respectively, the height and width of the bed.

The term involving d_p is always very small and can be neglected. Then after rearrangement and introduction of D_e , there is obtained

$$\varepsilon = \varepsilon_\infty[1+2\frac{d_p}{D_e}(\frac{\varepsilon_w}{\varepsilon_\infty}-1)] \tag{26}$$

where, it has been assumed that $\varepsilon_\infty = 0.368$, and that layer of spheres next to the walls is close-packed so that $\varepsilon_w = 0.476$ [29].

Foumeny et al. (1993) [8]

A common source of error is the assumption that mean porosity of packed beds of spherical particles is approximately equal to 0.4. While this may be acceptable for beds with relatively large tube to particle diameter ratios, it is certainly not realistic tube to particle diameter ratios, it is certainly not realistic for low diameter ratios, $D/d_p<10.0$. [8]

$$\varepsilon = 1-\frac{2}{3}\left(\frac{1}{\frac{D}{d_p}}\right)^3 \frac{1}{\sqrt{\left(\frac{2}{\frac{D}{d_p}}-1\right)}}, \quad \text{for} \quad 1 \le D/d_p \le \sqrt{3}/2 \tag{27}$$

$$\varepsilon = 0.383 + 0.25\left(\frac{D}{d_p}\right)^{-0.923} \frac{1}{\sqrt{\left(0.723\frac{D}{d_p}-1\right)}}, \quad \text{for} \quad 1+\frac{\sqrt{3}}{2} \geq \frac{D}{d_p} \tag{28}$$

Sato (1973) [30]

Sato[30] made 3 different porosity correlations for different packing ways.

- Gently dumped (without external impact).

$$\varepsilon = 0.3517 + 0.4657\left(\frac{d_p}{D}\right), \quad \text{for} \quad \frac{d_p}{D} < 0.4 \tag{29}$$

- Dumped with simultaneous vibration.

$$\varepsilon = 0.3472 + 0.4417\left(\frac{d_p}{D}\right), \quad \text{for} \quad \frac{d_p}{D} < 0.4 \tag{30}$$

- One minute vibration after dumped.

$$\varepsilon = 0.3494 + 0.4381\left(\frac{d_p}{D}\right), \quad \text{for} \quad \frac{d_p}{D} < 0.4 \tag{31}$$

Zou and Yu(1995) [31]

- for the loose random packing

$$\varepsilon = 0.400 + 0.010(e^{10.686\left(\frac{d_p}{D}\right)} - 1), \quad \text{for} \quad \frac{d_p}{D} < 0.256 \tag{32}$$

$$\varepsilon = 0.8460 - 1.898\left(\frac{d_p}{D}\right) + 2.725\left(\frac{d_p}{D}\right)^2, \quad \text{for} \quad 0.256 < \frac{d_p}{D} < 0.538 \tag{33}$$

$$\varepsilon = 1 - \frac{2}{3} \times 1 \frac{\left(\frac{d_p}{D}\right)^3}{\sqrt{2\left(\frac{d_p}{D}\right) - 1}}, \quad \text{for} \quad 0.538 < \frac{d_p}{D} \tag{34}$$

- for the dense packing

$$\varepsilon = 0.372 + 0.002(e^{15.306\left(\frac{d_p}{D}\right)} - 1), \quad \text{for} \quad \frac{d_p}{D} < 0.253 \tag{35}$$

$$\varepsilon = 0.681 - 1.363\left(\frac{d_p}{D}\right) + 2.241\left(\frac{d_p}{D}\right)^2, \quad \text{for} \quad 0.253 < \frac{d_p}{D} < 0.530 \tag{36}$$

$$\varepsilon = 1 - \frac{2}{3} \times 1 \frac{\left(\frac{d_p}{D}\right)^3}{\sqrt{2\left(\frac{d_p}{D}\right) - 1}}, \quad \text{for} \quad 0.530 < \frac{d_p}{D} \tag{37}$$

Chu(1989) [32]

Their actual porosities data were used in order to compare with present porosities.

Table 4. Actual porosities data for Chu(1989)

D(cm)	d_p(cm)	D/ d_p	ε
0.273	0.095	2.873684	0.462
0.491	0.057	8.614035	0.407
0.957	0.095	10.07368	0.387
0.802	0.034	23.58824	0.386

Temperature measurements

A Density and viscosity of air and water are affected by temperature. Especially the properties of the water were sensitive to the temperature. Therefore, an exact temperature measurement at each experiment should be taken. As pump power increased, the temperature was also increased. On the previous experiments, average temperature was used for calculation of Reynolds number. However, properties of water were changed with temperature variation outstandingly. Instead of using of average temperature, the right temperatures at each flow rate measurement point were used to determine properties of water. Because an accurate temperature affects an exact Reynolds number at each point. Even small difference of viscosity's value gave different Reynolds number. It would be one of the error mechanisms.

Methods of experiment for the pressure drop

Air experiments with a cylindrical packed bed

For experiments with air, pumps and air compressor are used to give power.

With pump blower

The column is filled by slow feeding of the spherical particles of diameter is 0.635cm. While the particles were poured into the bed, the bed was shaken to make sure the beads were firm and filled very well. It was connected to pump on the bottom of the bed. Two blowers of the pump sucked air from bottom of the Bed. Then air entered the column from the top of the bed in a downward direction. On the top of the bed, flow meter and open pipe were connected. The bed has two knit-mesh at the end of both sides to prevent beads from leaving the bed as well as the uniform distribution of the air. By using flow meter on the inlet of the bed, the flow rate of air was measured. The flow rate was controlled by the main valve located at the side of the blower. Pressure gauges and inclined vertical manometer checked the pressure at each tab. Same procedures were used for different size particles.

With air compressor

The bed was connected to air compressor. The air compressor forced air into the column. Also rate mate flow meter checked flow rate. The flow rate was controlled by the main valve located at the top of the air compressor. Pressure gages and inclined vertical manometer checked the pressure at each tab. On the bottom of the bed, the air went out to the room. It was not the loop but open system. Also we did same experiments for different size particles with same way.

Water experiments with a cylindrical packed bed

The column was connected to flow meter, pump, and reservoir water tank. The water from the reservoir water tank went through the pump. Pump gave out the water to the column. The water flow rate was measured using flow meter. When the flow rate was constant, pressure transducer measured each pressure on the tabs. The Flow rate was controlled by Pump controller button. Also, an electronic thermometer was submerged into the reservoir tank to measure temperature of water. We did this experiment with different particle sizes and different bed set up(vertical and horizontal set up). For the vertical column set up, we did experiments for both flow directions (up-flow and down-flow). All these experiments were performed with a data rate acquisition system. Data was acquired different flow rate for single-phase flow. These experiments were carried out under various Reynolds numbers.

Fig. 1. and 2. show the particles that were used in these experiments. Fig. 3. indicates a diagram of facility of air experiment. Also, Fig. 4. show a picture of facility of air experiment. Otherwise, Fig. 5. indicates a diagram of facility of water experiment. Fig. 6. show a picture of facility of water experiment.

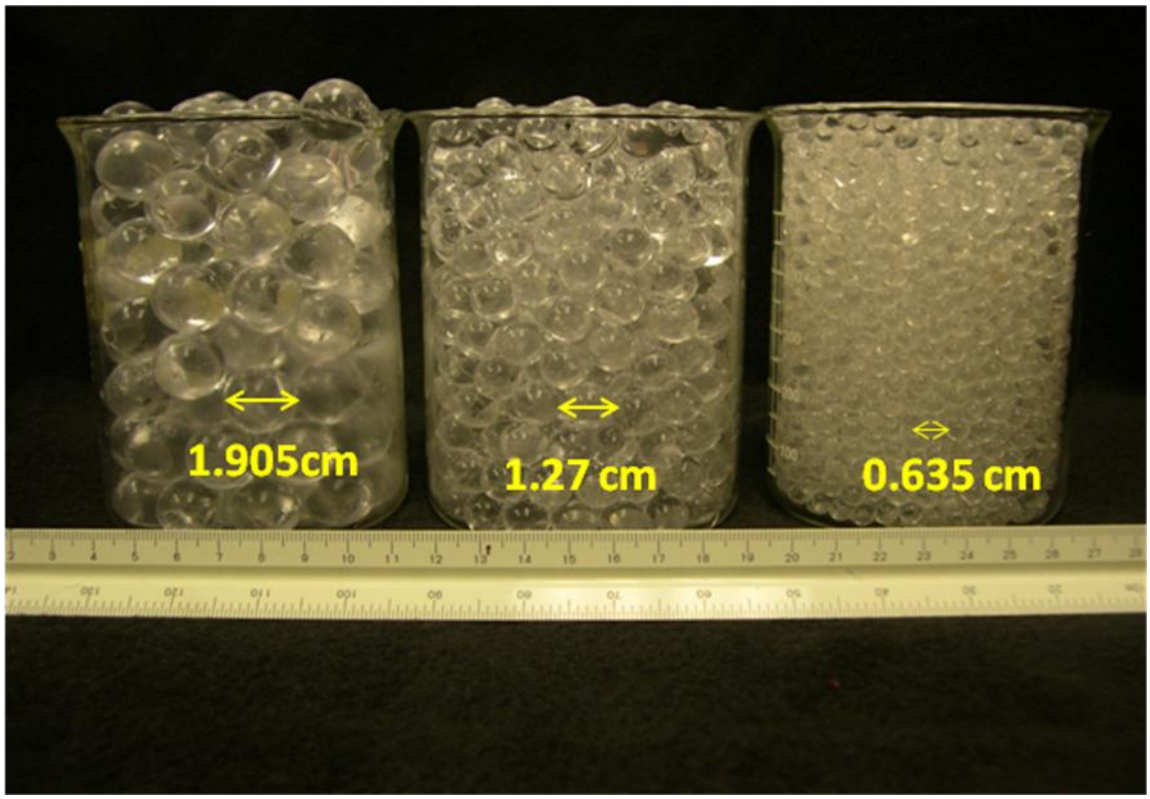

Fig. 1. Different size sphere particles (d_p = 0.635cm, 1.27cm and 1.905cm).

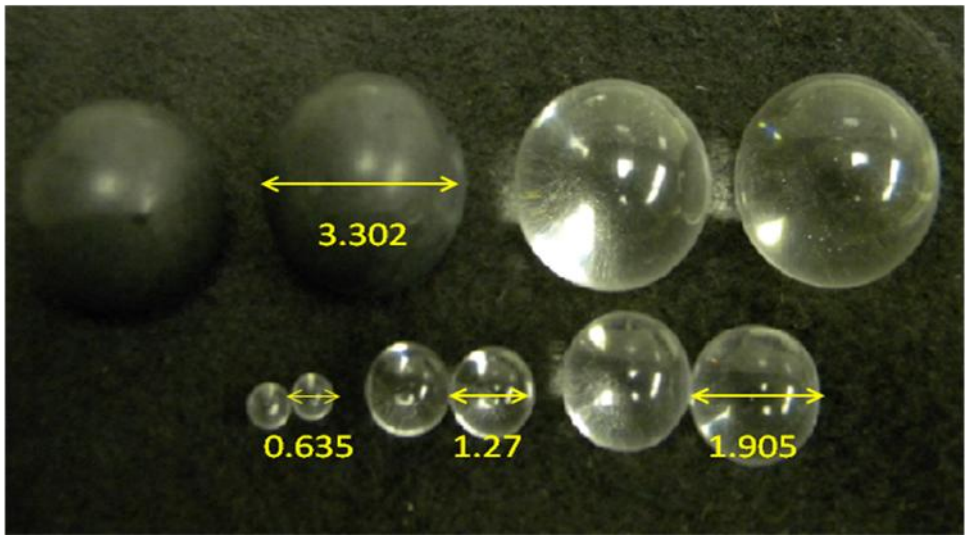

Fig. 2. Different size sphere particles (d_p = 0.635cm, 1.27cm,1.905cm and 3.302cm).

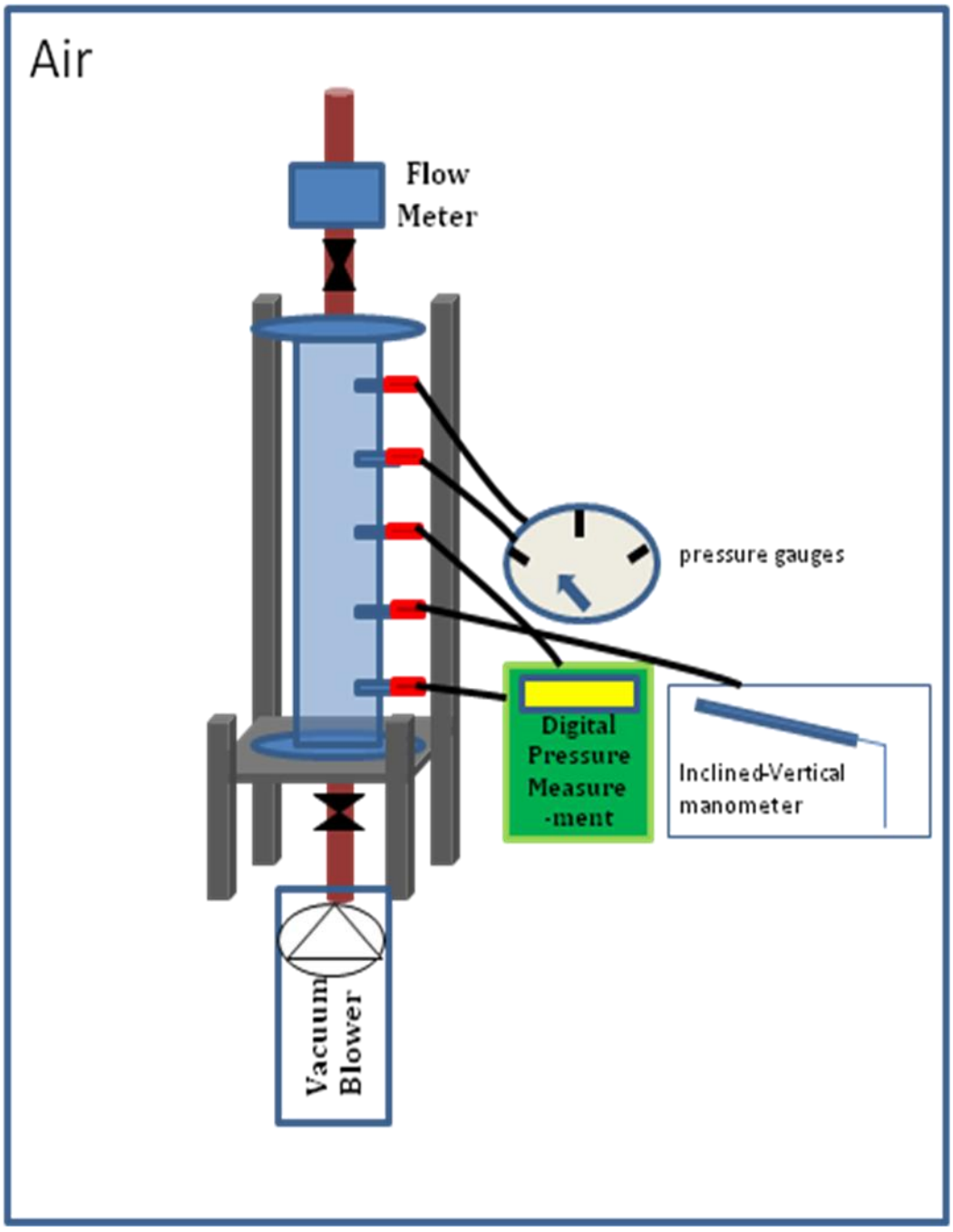

Fig. 3. A diagram of facility of air experiment.

Fig. 4. A picture of facility of air experiment.

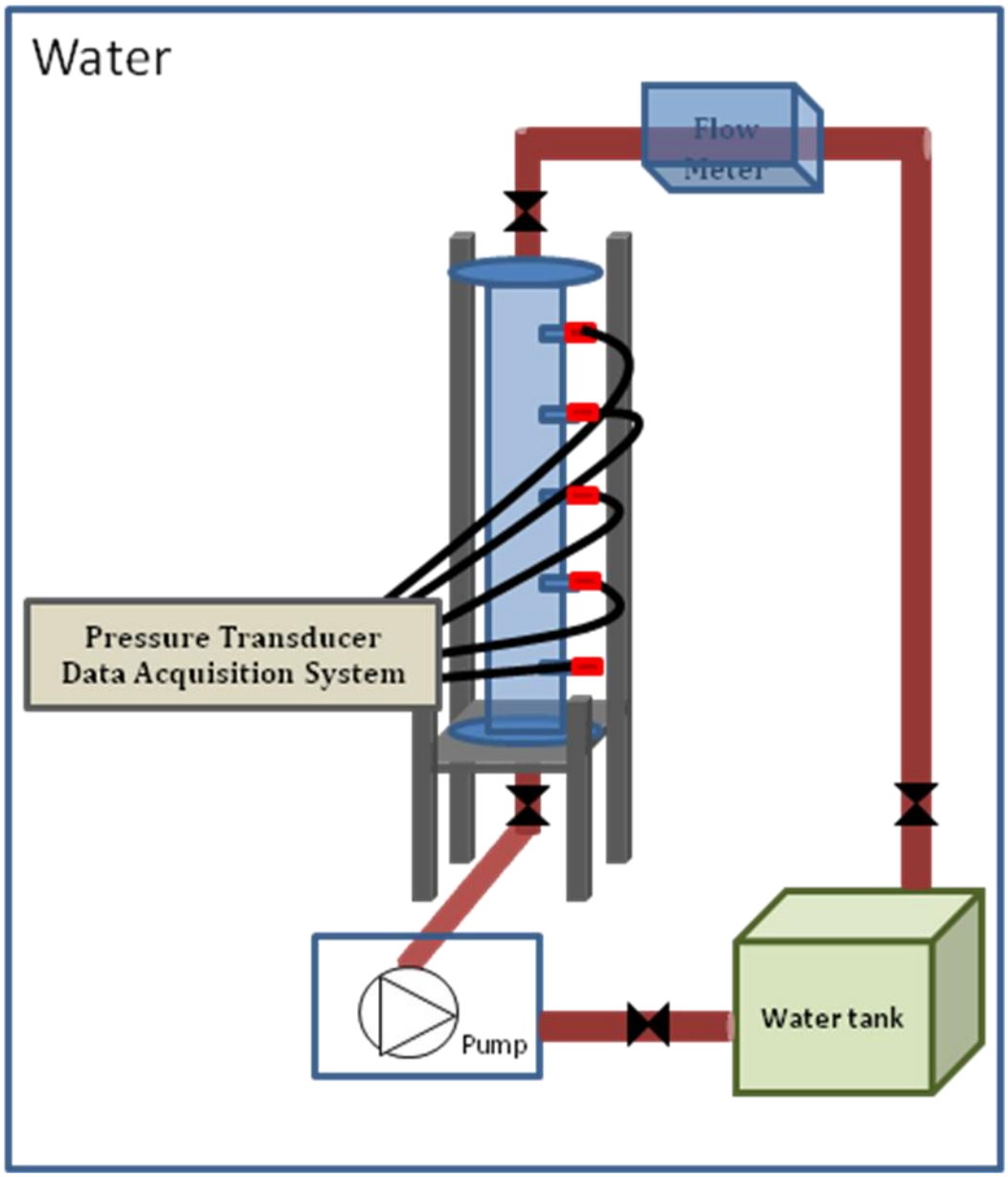

Fig. 5. A diagram of water experiment facility.

Fig. 6. A picture of water experimental facility.

CHAPTER III

DATA ANALYSIS AND RESULTS

The average porosity

Average porosities were measured from three different experiments. Table 5 indicates the average porosity at each bed-to-particle diameter ratios. The average porosity for D/d_p = 19 came from method 2, and the average porosity for D/d_p =9.5, 6.33 and 3.66 came from method 3. The results from method 2 and 3 did not have big differences. In case of D/d_p = 19, the number of particles is a lot, so it was hard to count all the particles.

Table 5. Bed-to-particle diameter ratios and each porosity.

D/d_p	19	9.5	6.33	3.66
ε	0.385	0.397	0.416	0.465

The average porosities from present experiments were compared with correlations found in the literature.

Again, the porosity measurements were like below.

- Water displacement method
- Weighting method
- Particle counting method

Water displacement method results

Table 6 shows water displacement method results for $D/d_p = 19$.

Table 6. Water displacement method results for $D/d_p = 19$.

	Measured volume of column with water (liter)	Volume of water with beads are filled (liter)	Porosity	Average Porosity
1	17.371	6.55	0.377	0.385
2	17.37	6.53	0.376	
3	17.36	6.57	0.378	
4	17.41	6.6	0.379	
5	17.4	6.9	0.396	

Weighting method results

Table 7 shows weighting method results for $D/d_p = 19$.

Table 7. Weighting method results for $D/d_p = 19$.

The number of beads	Weight(g)	1 bead weight(g)	Estimated total number of beads	Porosity
Total beads	12655g			
10	1.59	0.159	79591	0.387
25	3.96	0.1584	79892	0.385
100	15.85	0.1585	79842	0.386
110	17.44	0.15855	79819	0.386
210	33.3	0.15857	79806	0.386
245	38.84	0.15853	79826	0.386
345	54.59	0.15823	79977	0.385

Weighting method results and particle counting method results

Table 8 shows Weighting method results and Particle counting method results for $D/d_p = 9.5$.

Table 8. Weighting method results and Particle counting method results for $D/d_p = 9.5$.

The number of beads	Weight (g)	1 bead weight (g)	Estimated, the number of beads	Counted, the number of beads	Porosity	Average Porosity
Total	7546			5990	0.397	0.397
10	12.64	1.264	5970		0.399	
50	62	1.24	6085		0.387	

Table 9 shows Weighting method results and Particle counting method results for $D/d_p = 6.33$.

Table 9. Weighting method results and Particle counting method results for $D/d_p = 6.33$.

The number of beads	Weight (g)	1 bead weight (g)	Estimated, the number of beads	Counted, the number of beads	Porosity	Average Porosity
Total	8550			1990	0.416	0.416
10	43.05	4.305	1986.9		0.417	
50	212	4.24	2016.5		0.408	

Table 10 shows Weighting method results and Particle counting method results for $D/d_p = 3.65$.

Table 10. Weighting method results and Particle counting method results for $D/d_p = 3.65$.

The number of beads	Weight (g)	1 bead weight (g)	Estimated, the number of beads	Counted, the number of beads	Porosity
Total	10520			489	0.465
5	108	21.6	487.03		0.471
10	215	21.5			
20	430	21.5			
30	645	21.5			
40	860	21.5			

Porosities from existing correlations

Tables 11 and 12 show porosities from existing correlations.

Table 11. Porosities from existing correlations.

d_p (cm)	D (cm)	Foumeny	Beaver	R.M. Fand	Sato	Zou /Yu	Chu	Average experimental porosity
0.635	12.065	0.387	0.395	0.368	0.376 0.370 0.372	0.407 (Loose) 0.374 (Dense)	·	0.385
1.27	12.065	0.396	0.405	0.377	0.401 0.394 0.396	0.42 (Loose) 0.38 (Dense)	·	0.397
1.905	12.065	0.407	0.414	0.388	0.425 0.417 0.419	0.444 (Loose) 0.392 (Dense)	·	0.416
3.302	12.065	0.443	0.435	0.417	0.479 0.468 0.469	0.53 (Loose) 0.47 (Dense)	·	0.465

Table 12. Porosities from present work (Summary for porosities from present work).

d_p(cm)	D(cm)	D/d_p	d_p/D	ε(1)	ε(2)	ε(3)
0.635	12.065	19	0.053	0.381	0.385	
1.27	12.065	9.5	0.105		0.393	0.397
1.905	12.065	6.33	0.158		0.414	0.416
3.302	12.065	3.65	0.274		0.471	0.465

Pressure drop analysis and results

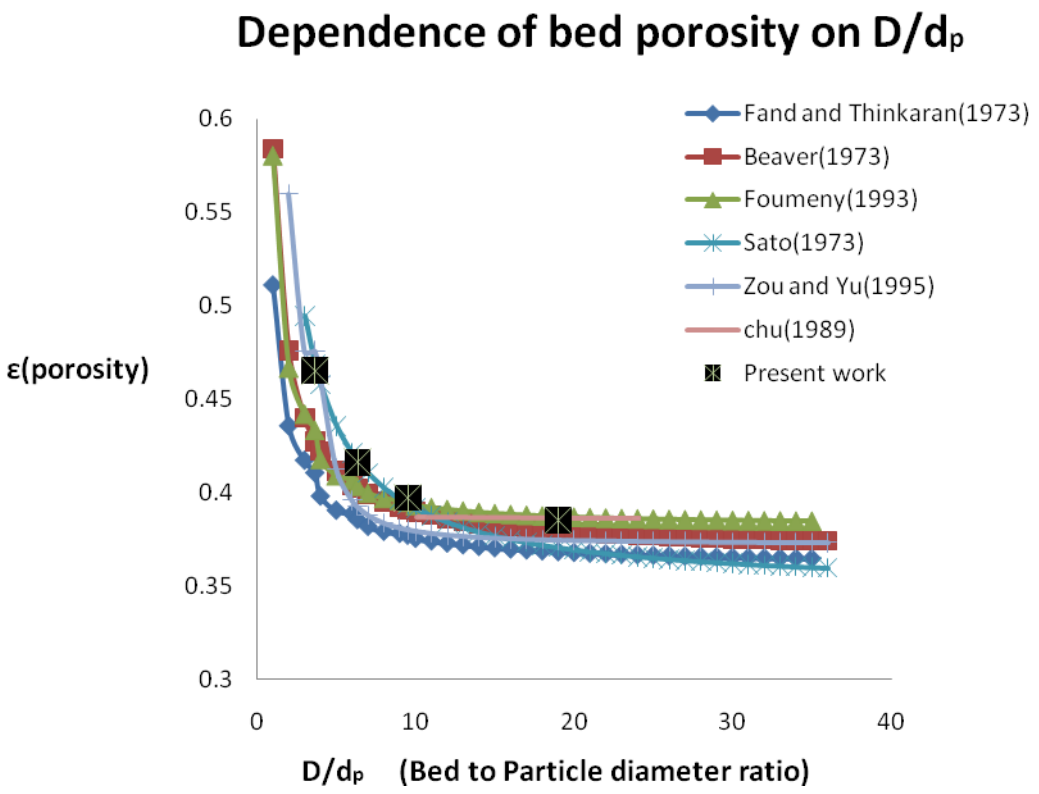

Fig. 7. Comparison of present work with existing correlations

(porosity as a function of bed-to-particle diameter ratios).

Fig. 7. shows porosities as a function of tube to particle diameter ratios. Present work is similar with Chu (1989)[32] for D/d_p =19 and other porosities(for D/d_p = 9.5, 6.33 and 3.66) are similar with Sato(1973)[30].

Small differences in the values of mean porosity can give rise to big differences in the constants A and B of the Ergun equation [1]. It is therefore important that the mean porosity of the bed is accurately known so that reliable pressure drop correlations can be

formulated. In order to obtain such information, the mean porosity values of the beds considered here have been determined experimentally using three different methods.

Fig. 7. shows present work for porosity with existing porosity correlations. For decreasing bed-to-particle diameter ratios, porosity also increases as seen in our calculations. The average porosity of D/d_p = 19 is 0.385 and it is most similar with the result of Foumeny(1993)[8], Chu(1989)[32]. And the average porosity of D/d_p = 9.5 is 0.397. This porosity is same value with the porosity from Sato(1973)[30]. The average porosity of D/d_p = 6.33 is 0.416 and it is also most similar with the result of Sato(1973) [30]. The average porosity of D/d_p = 3.65 is 0.465 and it is most similar with the result of Sato(1973) [30].

Table 13. The modified Reynolds number regimes for present work.

	D/d_p	19	9.5	6.33	3.66
Air	Re_m	528~1,197	646~3,797	1,118~8,010	
Water	Re_m	547~3,114	2,648~9,102	4,877~13,313	20,046~29,936

Fig. 8. indicates pressure drops per unit length as a function of the modified Reynolds numbers for air working fluid experiments. The pressure drop for large bed-to-particle diameter ratios (D/d_p= 19) has more pressure drop at a constant modified Reynolds number. And the pressure drop was decreased as the bed-to-particle diameter ratios was decreased. Fig. 9. depicts the modified friction factor as a function of the modified

Reynolds number for air working fluid experiments. The results are linear even D/ d_p is different.

$$\text{Where,} \quad f_m \text{ (the modified friction factor)} = \frac{\Delta p d_p^2 \varepsilon^3}{L \mu v (1-\varepsilon)^2}$$

$$\text{Re}_m \text{ (the modified Reynolds number)} = \frac{\rho v d_p}{\mu(1-\varepsilon)} \tag{38}$$

Fig. 10 indicates pressure drops per unit length as a function of the modified Reynolds numbers for water working fluid experiments. Like Fig. 8., the pressure drops were increased as D/ d_p were increased at a constant modified Reynolds number. Fig. 11. shows that the modified friction factors are linear with D/d_p is larger than 6.33. However, the slope of modified friction factor for D/ d_p = 3.65 is less than the slope of modified friction factor for other D/ d_p. From these results and Foumeny (1993)[8], in case of D/d_p is less than 5, the wall effect became an important factor.

Many correlations found in the literature considered wall effect. However, their consideration doesn't cover the small bed-to-particle diameter ratio (D/d_p) and their valid modified Reynolds number is low even though they considered it. This present work was compared with existing correlations. For this purpose, 20 correlations provided by Ergun(1952)[1], Foscolo(1983)[33], Handley and Heggs(1968)[34], Hicks(1970)[11], J.Wu(2008)[24], Leva(1947)[9], Macdonald(1979)[13], Montillet(2004)[20], Reichelt(1972)[12], Yu(2002)[35], Shijie Liu(19994)[16], Tallmadge(1970)[36], Brauer(1960)[37], Carman(1937)[5], Morcom(1946)[38], Foumeny(1993)[8], R.E.

Hayes(1995)[17], Rose(1949)[21], Wentz and Thodos(1963)[39] and KTA(1981)[2] were used. These correlations were plotted with their valid regime of the modified Reynolds number found in the literature. Fig. 12, 13 and 14 show comparison present work with correlations found in literatures at each bed-to-particle diameter ratios with air experiments. In these plots of Fig. 19 and 20, the Ergun[1] is matched well with present work for less than 1000 of $Re_{m.}$ The Ergun[1] is only valid for modified Reynolds number less than 1000. However, as the modified Reynolds number increases, the equation from Ergun does not match with present experiment results.

Fig. 15, 16, 17 and 18 indicate comparison present work of water working fluid with correlations in the literature at each bed-to-particle diameter ratios. KTA[2], Brauer[37], Carman[5] have similar trends with this present work for bed-to-particle diameter ratios of 19, 9.5, 6.33. However, for D/d_p = 3.66, present work has less value than other correlations. In this bed-to-particle diameter ratios and in this modified Reynolds number region, present work is similar with Hicks[11] and Tallmadge[36].

Fig. 21, 22 explain this phenomenon by comparing with the KTA[2]. KTA[2] modified friction factor is similar with present work for D/d_p = 19, 9.5 and 6.33. However, the modified friction factor of KTA[2] has higher values than present experiment results. KTA[2] porosity is from 0.36 to 0.42. It is limited and it is considered wall effect for relatively large bed-to-particle diameter ratios D/d_p = 6.33. However, as founded from Fig. 11, the wall effects become more important factors for pressure drop for D/d_p is less than 5. From KTA[2] paper, it was presented that KTA[2] .is valid for only 0.36~0.42 porosity regions. When D/d_p = 3.65, the porosity is 0.465. It means that KTA[2] could

not consider high wall effects from their experiments. Therefore, it is concluded that the wall effect makes the difference between KTA[2] and present experiment results. In addition, existing correlations proposed by low bed-to-particle diameter ratios ($D/d_p < 5$) has limited valid Reynolds number regimes. It signifies existing correlations couldn't apply widely. This present work is quite important, since the pressure drop of Gas Cooled Pebble Bed Reactor has to be predicted with high Reynolds numbers.

In case of $D/d_p < 5$, by fitting the KTA[2], in order to match with present work, a new correlation was derived.

$$f_m = \frac{\Delta p d_p^2 \varepsilon^3}{L \mu v (1-\varepsilon)^2} = \frac{\frac{D}{d_p}}{0.2\frac{D}{d_p}+3.6} \frac{\rho v d_p}{\mu(1-\varepsilon)} + 160 \tag{39}$$

This correlation is valid for $20{,}000 < Re_m < 29{,}936$ and $D/d_p < 5$.

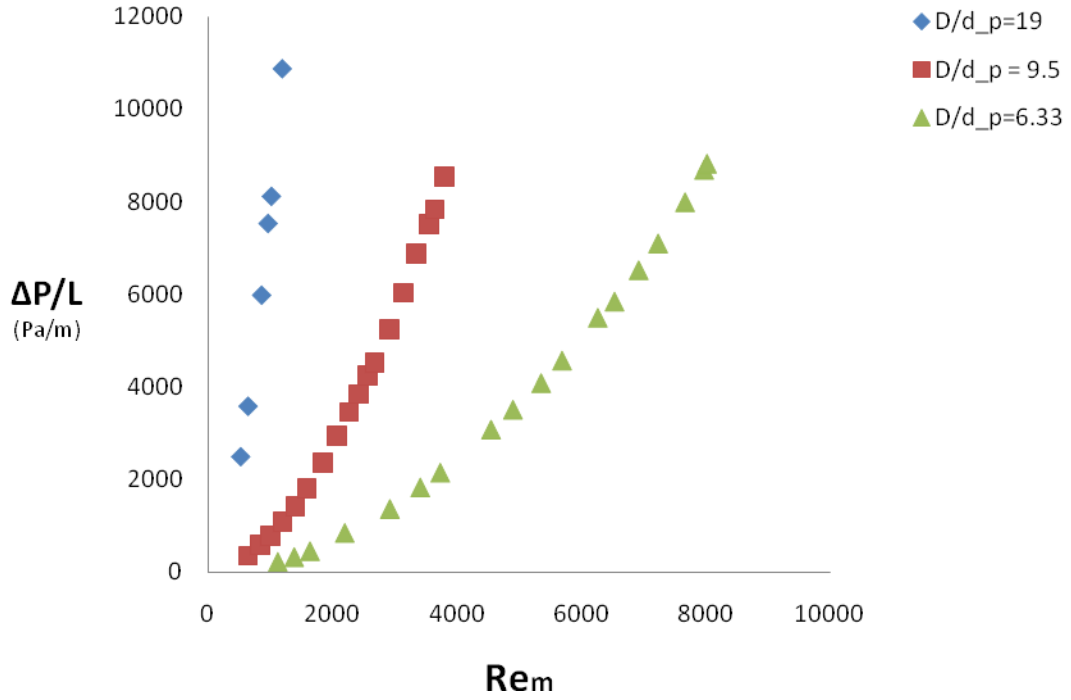

Fig. 8. Pressure drops per unit length as a function of the modified Reynolds numbers for air working fluid experiments.

It is evident that increasing the Reynolds number increases the pressure drop across the bed. It can be seen that, under similar hydrodynamic conditions, decreasing the particle size or increasing the bed-to-particle diameter ratio results in a very large increase in the pressure drop. Since the mean porosity of the bed goes down significantly as the particle size decreases, thereby increasing the resistance to flow of the fluid. For a given bed diameter, the wall effect increases with increasing particle size. Thus, the fluid experiences more channeling in a bed of large-size particles than small ones and, therefore, provides a lower pressure drop. As a general rule, decreasing the particle size reduces the mean porosity of the bed and, thereby, increases the pressure drop across it.

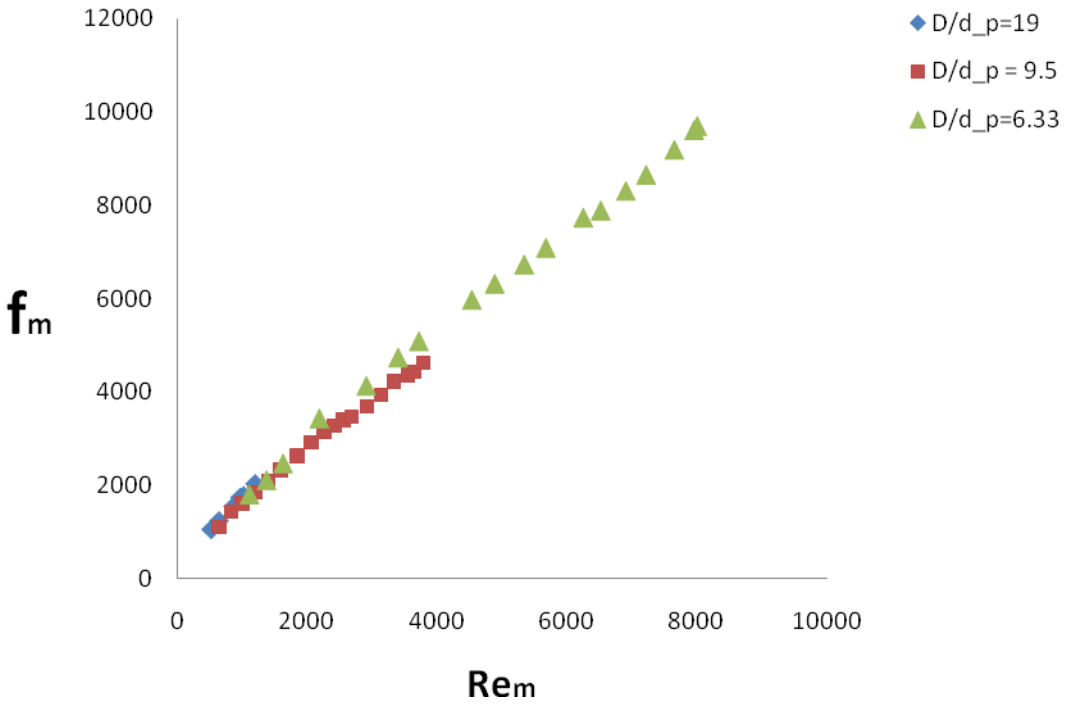

Fig. 9. The modified friction factor as a function of the modified Reynolds number for air working fluid experiments.

When the column diameter is much greater than the particle diameter, the wall should have little effect on the characteristic length. In this air pressure drop experiments, D/d_p = 19, 9.5 and 6.33. As we mensioned eariler, when D/d_p is less than 40, wall effects have to be considered for pressure drop. Therefore, the wall effects may be important for these present experiments.

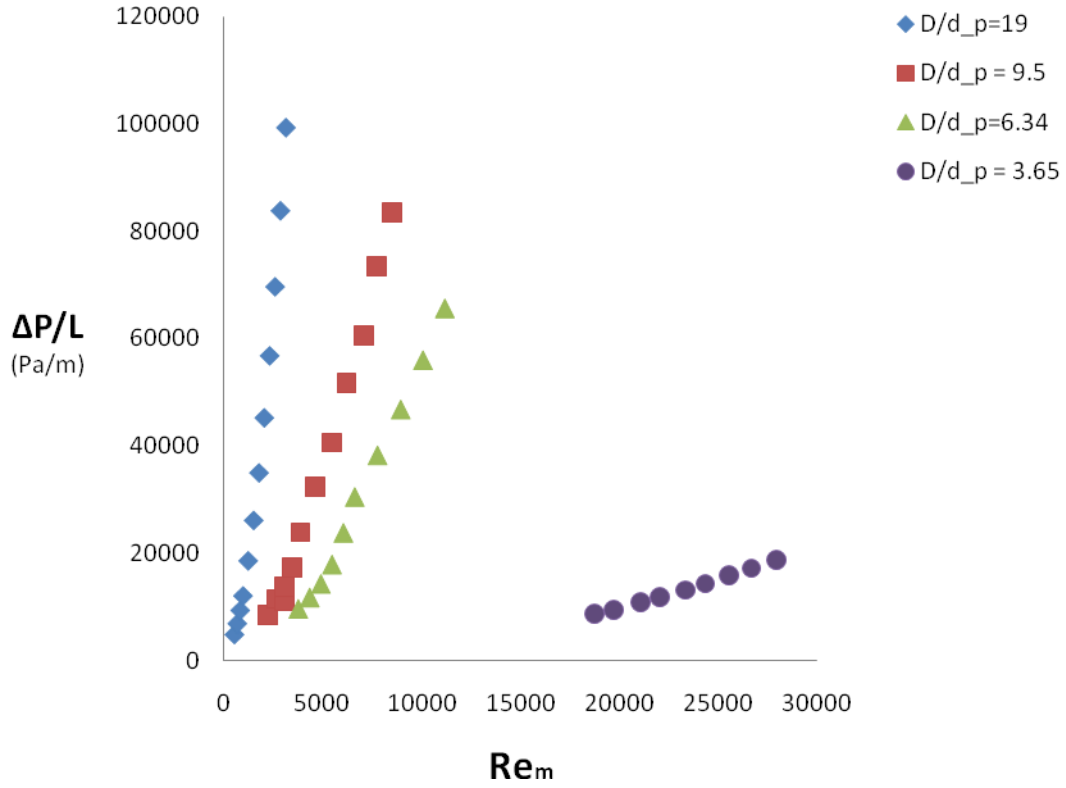

Fig. 10. Pressure drops per unit length as a function of the modified Reynolds numbers for water working fluid experiments

Like air results, in the case of water experiments, an increasing the Reynolds number increases the pressure drop across the bed. It can be also seen that, under similar hydrodynamic conditions, decreasing the particle size or increasing the bed-to-particle diameter ratio results in a very large increase in the pressure drop. Since the mean porosity of the bed goes down significantly as the particle size decreases, thereby increasing the resistance to flow of the fluid. In the case of $D/d_p = 3.65$, the average porosity is 0.465. This big increase of porosity causes small pressure drop as shown in Fig.10.

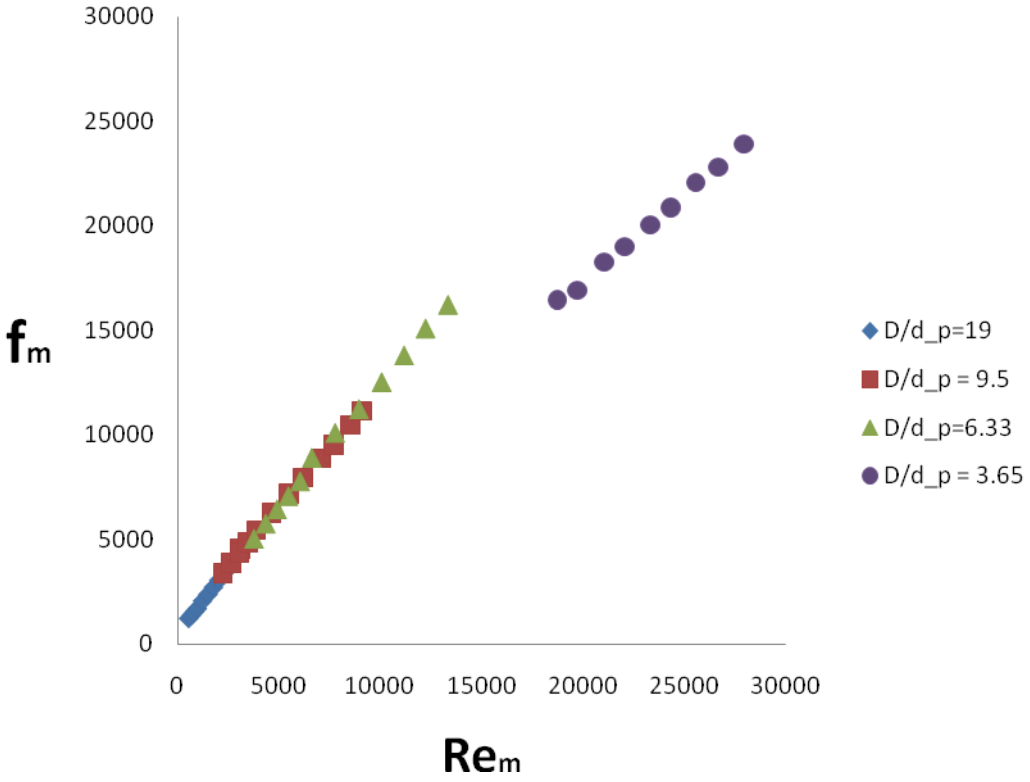

Fig. 11. The modified friction factor as a function of the modified Reynolds number for water working fluid experiments.

The pressure drop measurements for beds of spheres were plotted in the linear Ergun[1] manner, which in terms of dimensionless modified friction factor and the modified Reynolds number. The experimental pressure drop measurements should be affected by the presence of the wall, since the ratio of bed-to-particle diameter was small. In order to quantify the wall effect, the experiment was done at various bed-to-particle diameter ratios.

When the ratios of bed-to-particle diameter are 19, 9.5 and 6.33, the modified fricton factor, f_m, has a similar value at a constant modified Reynolds number, Re_m. However, the modified friction factor is different in the case of $D/d_p = 3.65$ at a constant modified Reynolds number, Re_m. It is found from the slope of the linear line in Fig. 11.

Such a behavior was also observed by Foumeny et al.(1993)[8]. In the Foumeny et al.(1993) [8], the slope changed very shaply from $D/d_p = 5.62$. Even though they also have differen slope between $D/d_p = 19$ to $D/d_p = 6.33$, the difference of that slope is not big. The cause of its difference reuslts between this work and Foumeny (1993) [8] is believed to be due to the experimental and fitting errors which tend to be more pronounced at extreme operating conditions. In addition, Foumeny[8] did experiments at a lower Reynolds number than these experiments. From this result and from Foumeny (1993) [8], it is concluded that the wall effect is important when the bed-to-particle diameter ratio is small, especially, when it is below around 5. Therefore, the wall effect causes less pressure drop.

Indeed, a closer inspection of several other publications on the influence of the bed-to-particle diameter ratio reveals that statements of an increasing pressure drop due to the wall effect are generally based on experiments under stream flow conditions or in the transitional range. In contrast, an independent or decreasing pressure drop due to the wall effect is reported mainly for measurements at high Reynolds numbers. At least for streamline flow, the wall effect is important only for bed-to-particle diameter ratios below 10, as stated frequently in the literature.

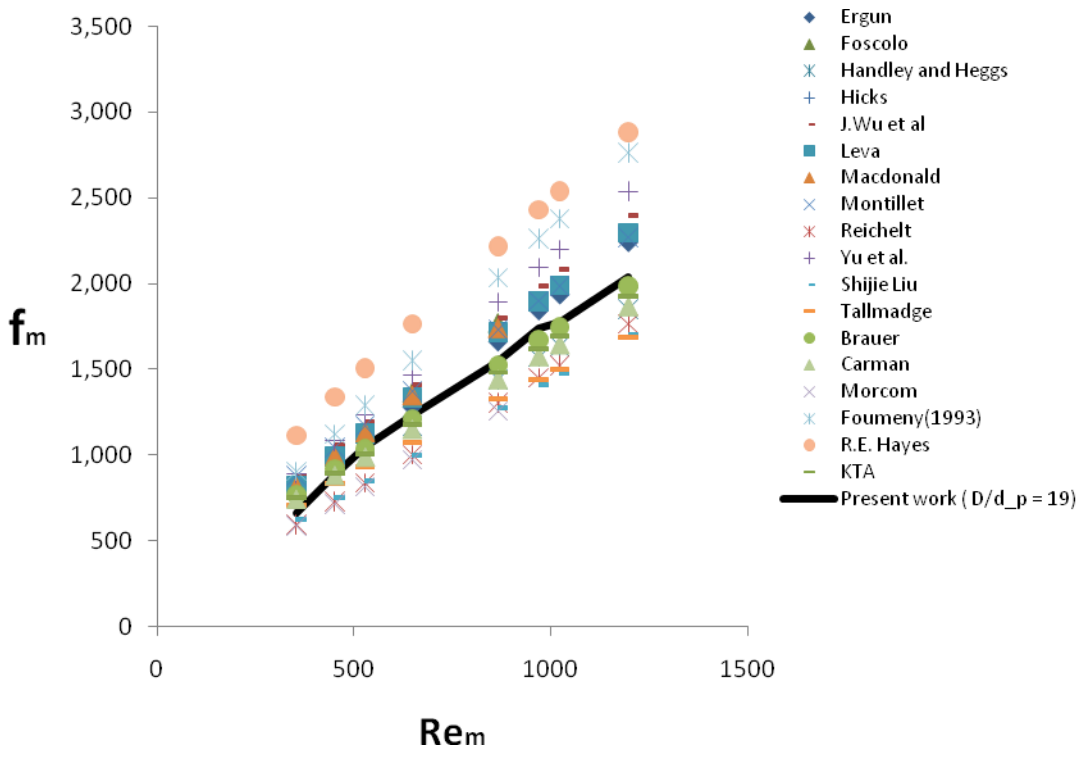

Fig. 12. The modified friction factor as a function of the modified Reynolds number for $D/d_p = 19$ with air working fluid.

It is desirable to compare the present work with existing correlations in the literature. For this purpose, 18 correlations provided by Ergun(1952) [1], Foscolo(1983) [33], Handley and Heggs(1968) [34], Hicks(1970) [11], J.Wu et al(2008) [24], Leva(2002) [9], Macdonald(1979) [13], Montillet(2004) [20], Reichelt(1972) [12], Yu et al(2002) [35], Shijie Liu(1994) [16], Tallmadge(1970) [36], Brauer(1960) [37], Carman(1970) [5], Morcom(1946) [38], Foumeny(1993) [8], R.E. Hayes(1995) [17] and KTA(1981) [2] were used.

Fig. 12 indicates the modified friction factor as a function of the modified Reynolds number, as defined by Ergun(1952) [1]. This figure shows the present experimental results as well as the published pressure drop correlations, with the following parameters of D = 12.065 cm, d_p = 0.635 cm, and ε = 0.385. Here, the bed-to-particle diameter ratio is 19. These parameters are plugged into the above correlations. In addition, the air property like as density and dynamic viscosity at room temperature were considered. In this plot, the modified Reynolds number range goes from 353 to 1197. The published correlations were plotted with their valid regime of modified Reynolds number found in the literature. As can be seen, all data points scatter around a general trend.

We observed that the current work (black line in the Figure X) agrees fairly well with the Brauer(1960) [37], Hicks(1970) [11], KTA(1981) [2], Ergun(1952) [1], Carman(1970) [5], Foumeny(1993) [8]. While R.E. Hayes(1995) [17], Handley and Heggs(1968) [34], Yu et al(2002) [35], J.Wu et al(2008) [24], Leva(2002) [9], Montillet(2004) [20] overpredict the present work in th entire range studied. This can be easily explained by the fact that the existing correlations were derived from experiments performed at high D/d_p that has less wall effect. On the other hand, Morcom(1946) [38], Shijie Liu(1994) [16], Tallmadge(1970) [36] and Reichelt(1972) [12] underpredict the current work. This reason is because these correlations were derived from experiments at low D/d_p and at high Re_m. This clearly signifies the limited applicability of the existing correlations.

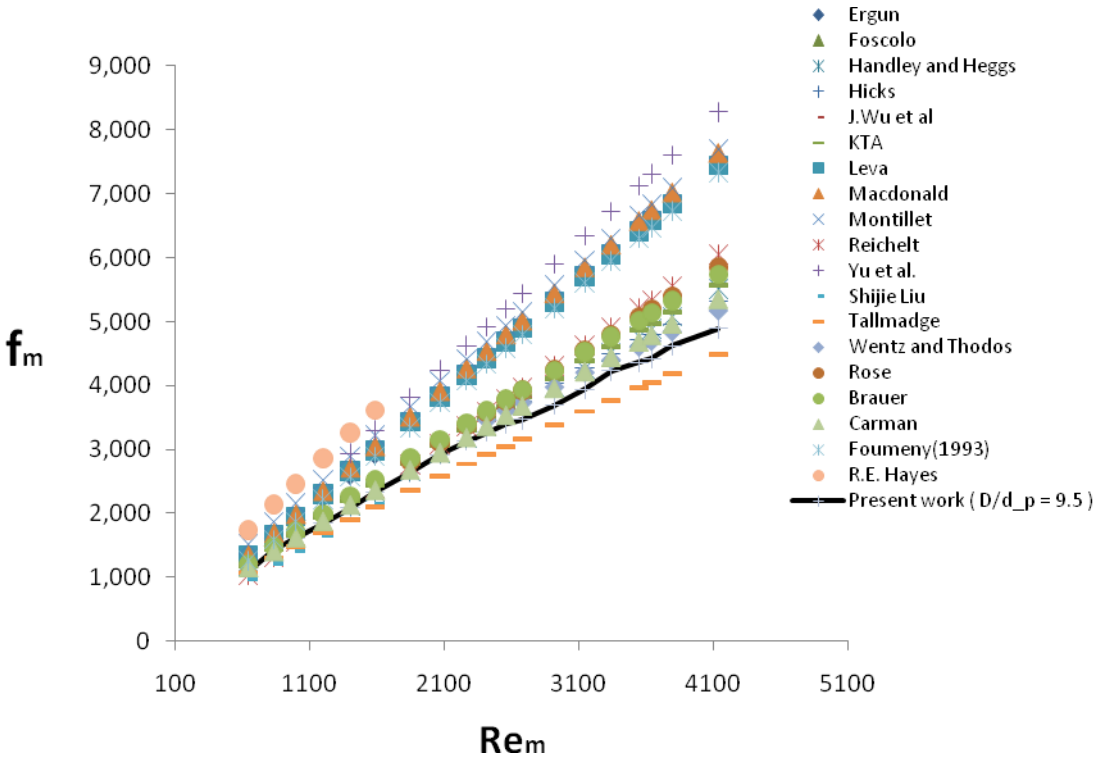

Fig. 13. The modified friction factor as a function of the modified Reynolds number for $D/d_p = 9.5$ with air working fluid.

In the case of $D/d_p = 9.5$, it was also compared with existing correlations. 19 correlations provided by Ergun(1952)[1], Foscolo(1983)[33], Handley and Heggs(1968)[34], Hicks(1970)[11], J.Wu(2008)[24], Leva(1947)[9], Macdonald(1979)[13], Montillet(2004)[20], Reichelt(1972)[12], Yu(2002)[35], Shijie Liu(19994)[16], Tallmadge(1970)[36], Brauer(1960)[37], Carman(1937)[5], Foumeny(1993)[8], R.E. Hayes(1995)[17], Rose(1949)[21], Wentz and Thodos(1963)[39] and KTA(1981)[2] were Considered for this comparison.

Fig. 13 indicates the modified friction factor as a function of the modified Reynolds number, as defined by Ergun(1952) [1]. This figure shows the present experimental results as well as the published pressure drop correlations, with the following parameters of D = 12.065 cm, d_p = 1.27 cm, D/d_p = 9.5 and ε = 0.397. In addition, the air property like as density and dynamic viscosity at room temperature were considered. These parameters are plugged into the above correlations. In this plot, the modified Reynolds number range goes from 647 to 4141. The published correlations were plotted with their valid regime of modified Reynolds number found in the literature. As can be seen, all data points scatter around a general trend.

We observed that the current work (black line in the Fig. 13) agrees fairly well with the Brauer(1960)[37], Hicks(1970)[11], KTA(1981)[2], Foumeny(1993)[8], Carman(1970) [5], Foumeny(1993) [8], Wentz and Thodos(1963) [39]. While Ergun(1952) [1] doesn't match with the present work. Ergun overestimates present work when the Reynolds number is larger than 1000.

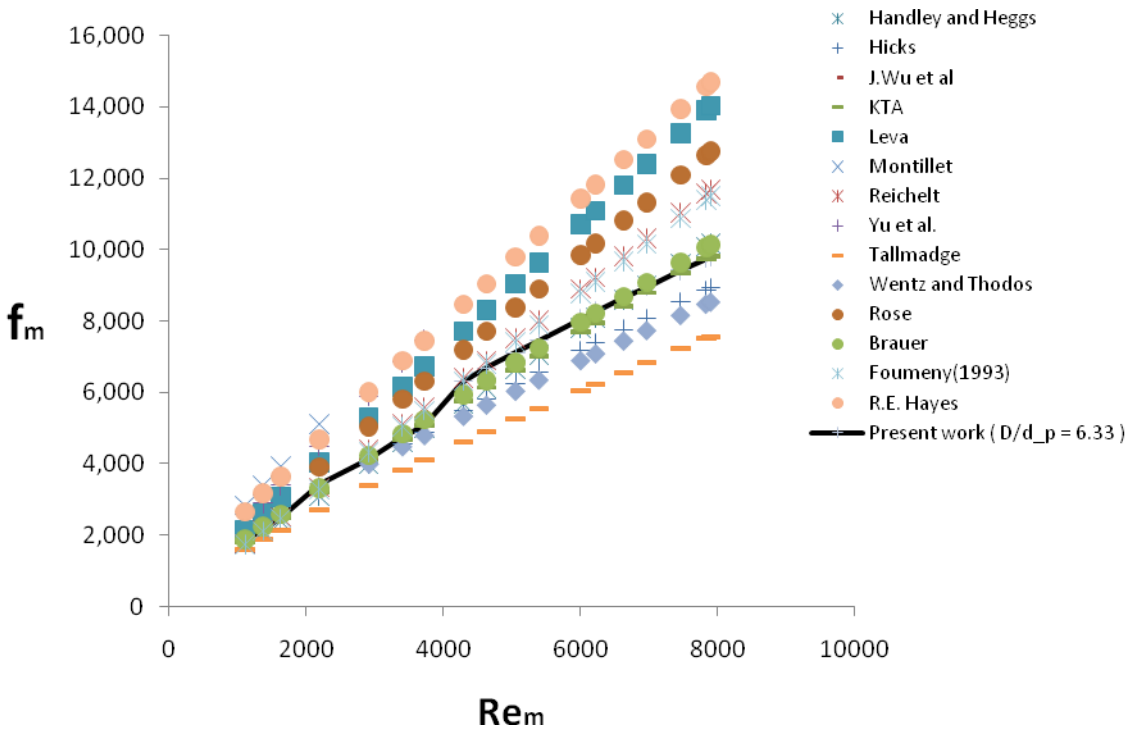

Fig. 14. The modified friction factor as a function of the modified Reynolds number for $D/d_p = 6.33$ with air working fluid.

In the case of $D/d_p = 6.33$, it was also compared with existing correlations. 14 correlations provided by Handley and Heggs(1968)[34], Hicks(1970)[11], J.Wu(2008)[24], Leva(1947)[9], Yu(2002)[35], Montillet(2004)[20], Reichelt(1972)[12], Rose(1949)[21], Tallmadge(1970)[36], Brauer(1960)[37], Foumeny(1993)[8], R.E. Hayes(1995)[17], Wentz and Thodos(1963)[39] and KTA(1981)[2] were Considered for this comparison.

Fig. 14 indicates the modified friction factor as a function of the modified Reynolds number, as defined by Ergun(1952) [1]. This figure shows the present experimental

results as well as the published pressure drop correlations, with the following parameters of D = 12.065 cm, d_p = 1.905 cm, D/d_p = 9.5 and ε = 0.416. In addition, the air property like as density and dynamic viscosity at room temperature were considered. These parameters are plugged into the above correlations. In this plot, the modified Reynolds number range goes from 1118 to 7901. The published correlations were plotted with their valid regime of modified Reynolds number found in the literature. As can be seen, all data points scatter around a general trend.

We observed that the current work (black line in the Fig. 14) agrees fairly well with the Handley and Heggs(1968) [34], Brauer(1960) [37], KTA(1981) [2].

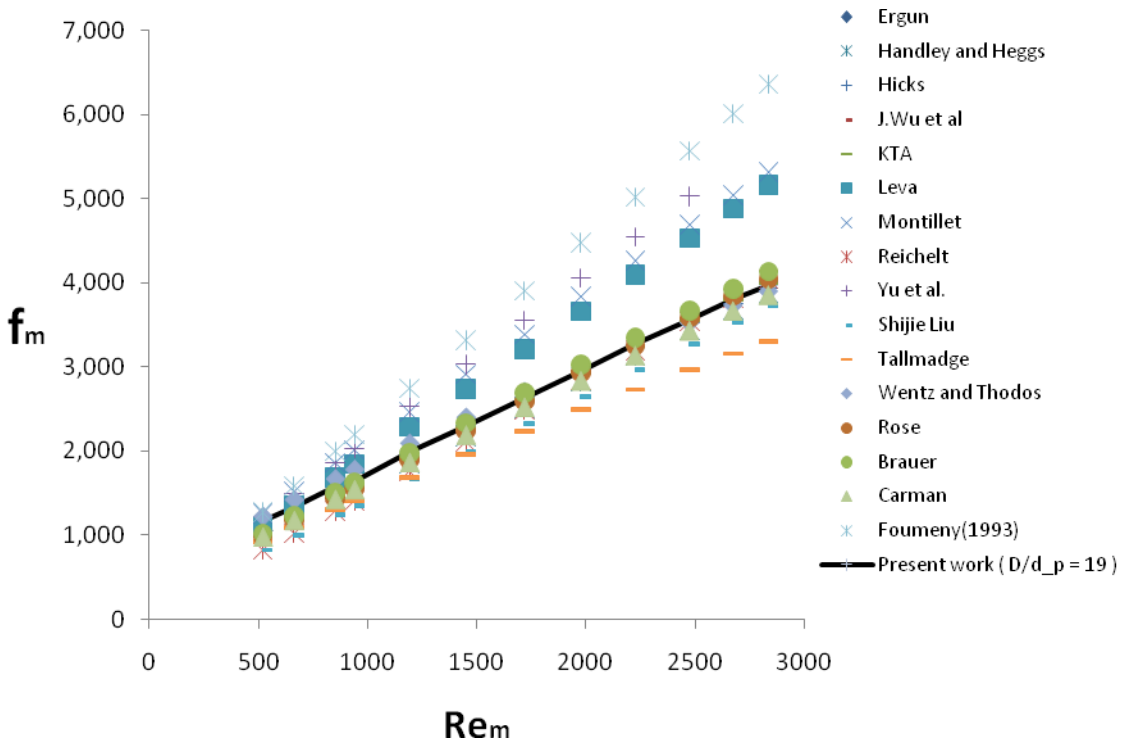

Fig. 15. The modified friction factor as a function of the modified Reynolds number for $D/d_p = 19$ with water working fluid.

It is desirable to compare the present work with existing correlations in the literature. For this purpose, 16 correlations provided by Ergun(1952)[1], Handley and Heggs(1968)[34], Hicks(1970)[11], J.Wu(2008)[24], Leva(1947)[9], Yu(2002)[35] Montillet(2004)[20], Reichelt(1972)[12], Shijie Liu(19994)[16], Tallmadge(1970)[36], Brauer(1960)[37], Carman(1937)[5], Foumeny(1993)[8], Rose(1949)[21], Wentz and Thodos(1963)[39] and KTA(1981)[2] were used.

Fig. 15 indicates the modified friction factor as a function of the modified Reynolds number, as defined by Ergun(1952) [1]. This figure shows the present experimental

results as well as the published pressure drop correlations, with the following parameters of D = 12.065 cm, d_p = 0.635 cm, and ε = 0.385 for water working fluid. Here, the bed-to-particle diameter ratio is 19. These parameters are plugged into the above correlations. In addition, the water property like as density and dynamic viscosity at measured temperature were considered. In this plot, the modified Reynolds number range goes from 353 to 1197. The published correlations were plotted with their valid regime of modified Reynolds number found in the literature. As can be seen, all data points scatter around a general trend.

We observed that the current work (black line in the Fig. 15) agrees fairly well with the Handley and Heggs(1968)[34], Hicks(1970)[11], Reichelt(1972)[12], Wentz and Thodos(1963)[39], Rose(1949)[21], Brauer(1960)[37], Carman(1937)[5], and KTA(1981)[2].

While Ergun(1952)[1], Yu(2002)[35], J. Wu(2008)[24], Leva(1947)[9], Montillet(2004)[20] overpredict the present work in th entire range studied. This can be easily explained by the fact that the existing correlations were derived from experiments performed at high D/d_p that has less wall effect.

On the other hand, Shijie Liu(19994)[16], Tallmadge(1970)[36] underpredict the current work. This reason is because these correlations were derived from experiments at low D/d_p and at high Re_m. This clearly signifies the limited applicability of the existing correlations.

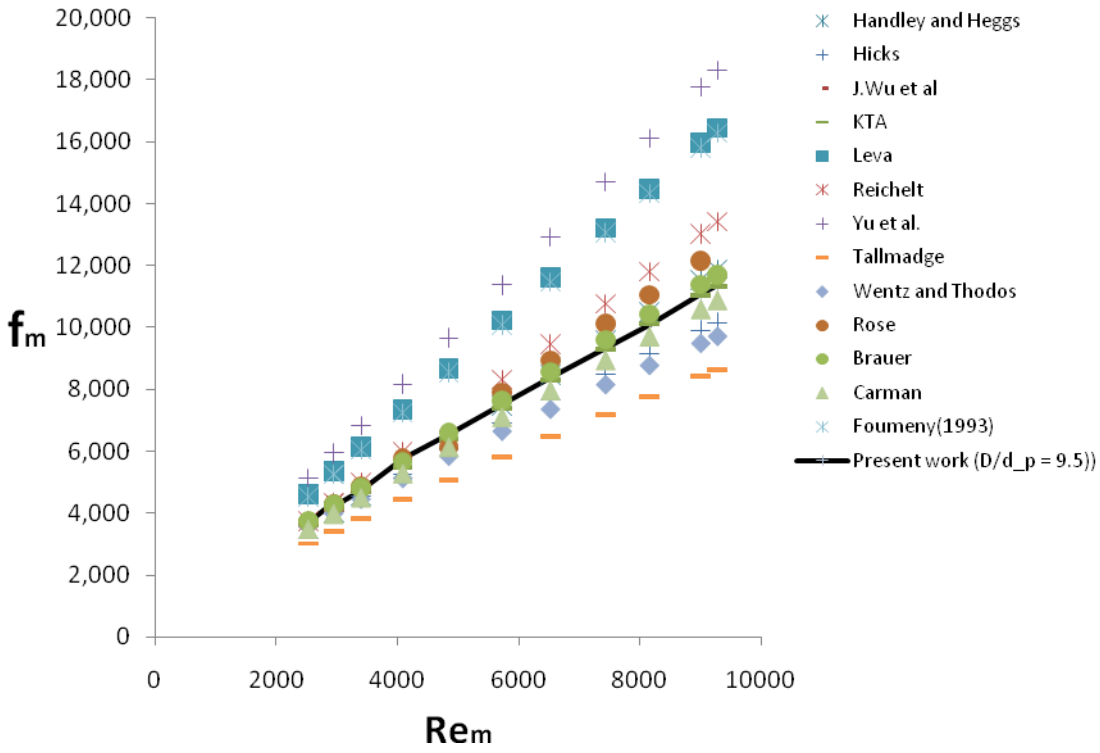

Fig. 16. The modified friction factor as a function of the modified Reynolds number for $D/d_p = 9.5$ with water working fluid.

13 correlations provided by Handley and Heggs(1968)[34], Hicks(1970)[11], J.Wu(2008)[24], Leva(1947)[9], Reichelt(1972)[12], Rose(1949)[21], Yu(2002)[35], Tallmadge(1970)[36], Brauer(1960)[37], Carman(1937)[5], Foumeny(1993)[8], Wentz and Thodos(1963)[39] and KTA(1981)[2] were used.

Fig. 16 indicates the modified friction factor as a function of the modified Reynolds number, as defined by Ergun(1952)[1]. This figure shows the present experimental results as well as the published pressure drop correlations, with the following parameters of $D = 12.065$ cm, $d_p = 1.27$ cm, and $\varepsilon = 0.397$ for water working fluid. Here, the bed-

to-particle diameter ratio is 9.5. These parameters are plugged into the above correlations. In addition, the water property like as density and dynamic viscosity at measured temperature were considered. In this plot, the modified Reynolds number range goes from 2524 to 9283. The published correlations were plotted with their valid regime of modified Reynolds number found in the literature. As can be seen, all data points scatter around a general trend.

We observed that the current work (black line in the Fig. 16) agrees fairly well with the Handley and Heggs(1968)[34], Brauer(1960)[37], Carman(1937)[5], and KTA(1981)[2].

While Reichelt(1972)[12], Yu(2002)[35], Rose(1949)[21], J.Wu(2008)[24], Leva(2002), Foumeny(1993)[8] overpredict the present work in th entire range studied. This can be easily explained by the fact that the existing correlations were derived from experiments performed at high D/d_p that has less wall effect.

On the other hand, Hicks(1970)[11], Wentz and Thodos(1963)[39], Tallmadge(1970)[36] underpredict the current work. This reason is because these correlations were derived from experiments at low D/d_p and at high Re_m. This clearly signifies the limited applicability of the existing correlations.

In the case of Rose(1949), it is matched very well by the modified Reynolds number is 6000. However, as it increases over $Re_m = 6000$, it over-predicts the present work.

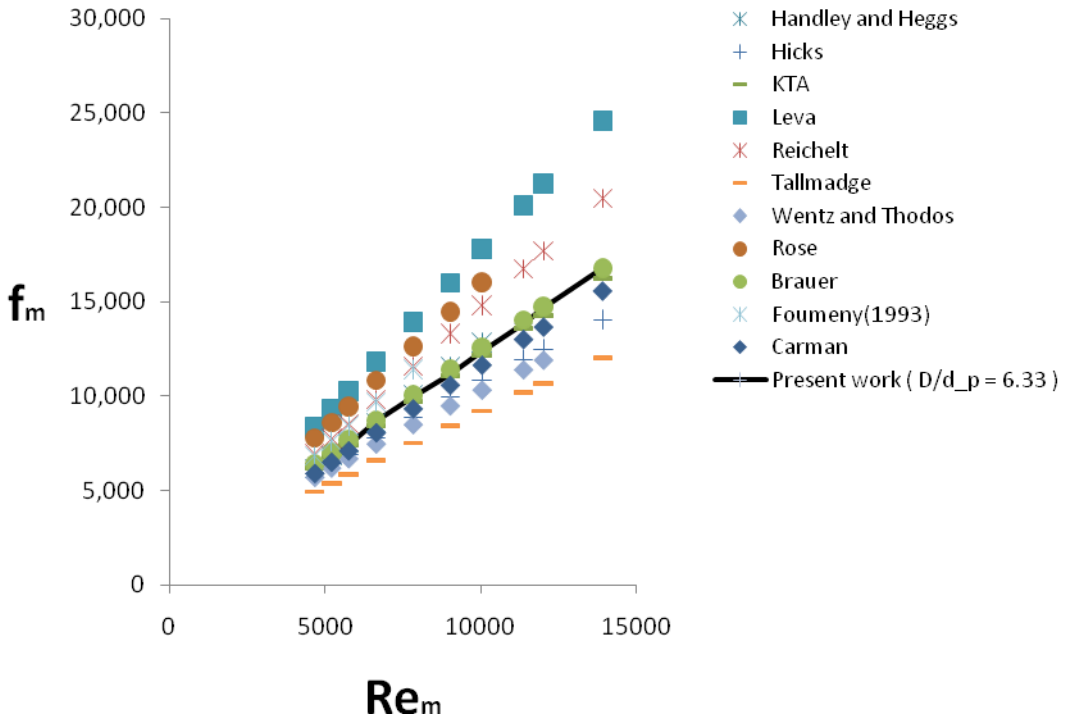

Fig. 17. The modified friction factor as a function of the modified Reynolds number for $D/d_p = 6.33$ with water working fluid.

For comparison of pressure drop in the case of $D/d_p = 6.33$, 11 correlations provided by Handley and Heggs(1968)[34], Hicks(1970)[11], Leva(1947)[9], Reichelt(1972)[12], Tallmadge(1970)[36], Wentz and Thodos(1963)[39], Rose(1949)[21], Brauer(1960)[37], Carman(1937)[5], Foumeny(1993)[8] and KTA(1981)[2] were used.

Fig. 17 indicates the modified friction factor as a function of the modified Reynolds number, as defined by Ergun(1952)[1]. This figure shows the present experimental results as well as the published pressure drop correlations, with the following parameters of $D = 12.065$ cm, $d_p = 1.27$ cm, and $\varepsilon = 0.397$ for water working fluid. Here, the bed-

to-particle diameter ratio is 9.5. These parameters are plugged into the above correlations. In addition, the water property like as density and dynamic viscosity at measured temperature were considered. In this plot, the modified Reynolds number range goes from 4667 to 13920. The published correlations were plotted with their valid regime of modified Reynolds number found in the literature. As can be seen, all data points scatter around a general trend.

We observed that the current work (black line in the Fig. 17) agrees fairly well with the Handley and Heggs(1968)[34], Brauer(1960)[37], and KTA(1981)[2].

While Reichelt(1972)[12], Rose(1949)[21], Leva(1947)[9], Foumeny(1993)[8] overpredict the present work in th entire range studied. This can be easily explained by the fact that the existing correlations were derived from experiments performed at high D/d_p that has less wall effect.

On the other hand, Hicks(1970)[11], Wentz and Thodos(1963)[39], Carman(1937)[5], Tallmadge(1970)[36] underpredict the current work. This reason is because these correlations were derived from experiments at low D/d_p and at high Re_m. This clearly signifies the limited applicability of the existing correlations.

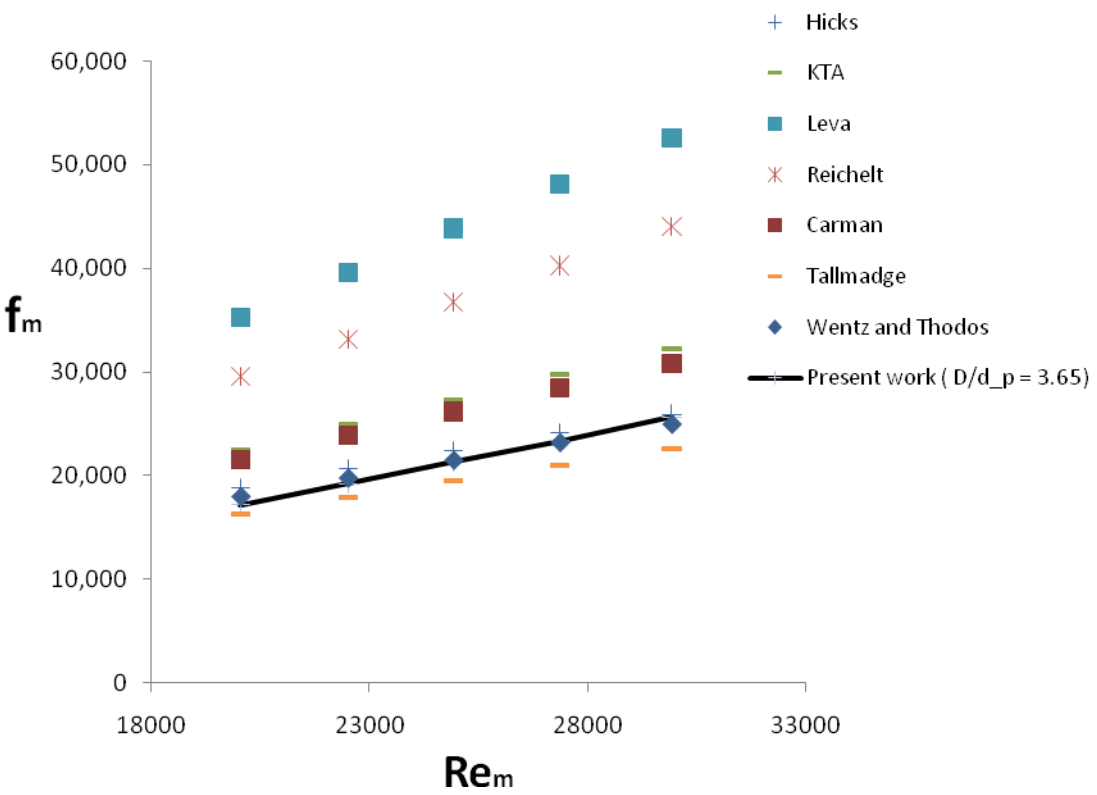

Fig. 18. The modified friction factor as a function of the modified Reynolds number for $D/d_p = 3.65$ with water working fluid.

For a bed-to-particle diameter ratio of 3.65, a corresponding porosity is 0.465 was found in Fig. 18. In this plot, the modified Reynolds number range goes from 20,036 to 29,936.

It is very difficult to do experiments with high Reynolds number. The reason is that there is not much of experiement results in the literature.

The pressure drop should be lower in this case, as a consequence of the existence of larger channels in the wall regions than those formed between spheres in the absense of a wall. The original Ergun equation[1] would thus overestimate the pressure drop. The

Ergun equation[1] wasn't plotted in Fig. 18. Because the modified Reynolds number is over their valid Re_m regime.

By previouse cases, D/d_p = 19, 9.5 and 6.33, Handley and Heggs(1968)[34], Brauer(1960)[37], and KTA(1981)[2] were matched very well with the present experiment work. However, Brauer(1960)[37] and KTA(1981)[2] didn't agree with the present work of D/d_p = 3.65 anymore because of large wall effects. Here, , Handley and Heggs(1968)[34] wasn't plottted in this figure due to their limitation Reynolds number.

However, the current work (black line in the Fig. 18) agrees well with Hicks(1970)[11], and Wentz and Thodos (1963)[39]. Unfortunately, their correlations didn't match with current work in all of previous cases. Hicks(1970)[11] correlations is not the results of their experiments. They just made a best matched correlation by comparing many correlations like as Ergun(1952)[1], Handley and Heggs(1968)[34], Carman(1937)[5], Wentz and Thodos(1963)[39] and Morcom(1946)[38]. Otherwise, Wentz and Thodos(1963)[39] did experiments with high porosities (ε = 0.354, 0.480, 0.615 and 0.728). Therefore, their experiments had large wall effects.

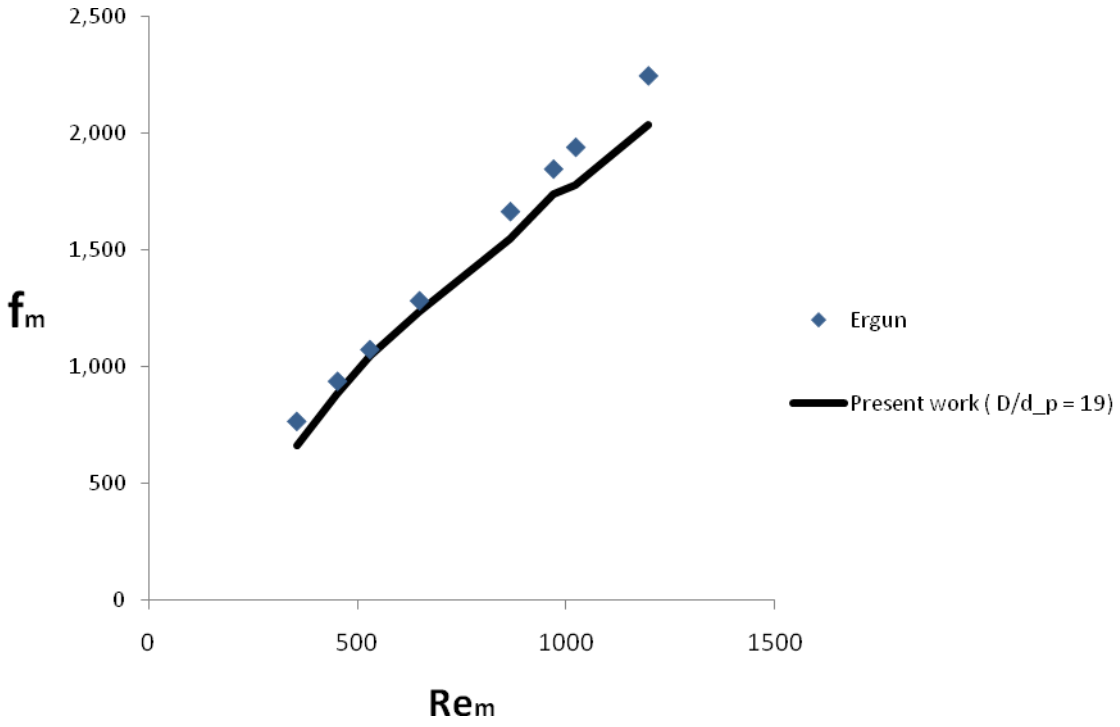

Fig. 19. Comparison of present work with Ergun equation (D/d_p = 19 with air).

As menstioned earlier, a couple of coefficients in Ergun's equation[1] have ever been disputed although this equation has been widely used in the engineering field.

The Ergun equation[1] predicts the experimental data well in the low modified Reynolds number as is shown in Fig. 19. and overpredicts the present work as the modified Reynolds is increased. And the discrepancy is increased at high modified Reynolds number as is shown in Fig. 20. The disagreement shown is probably due to the non consideration of wall effects in Ergun's equation[1]. A possible explanation is that, at high velocities, there is even more tendency for the flow to go through the larger channels close to the walls, where there is less friction.

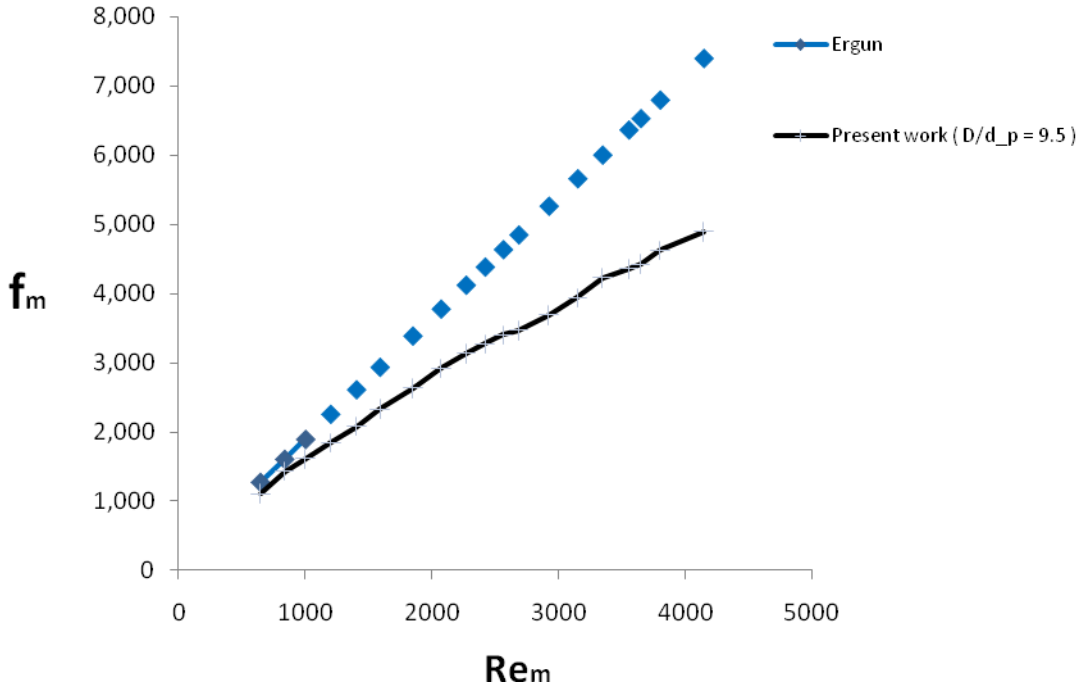

Fig. 20. Comparison of present work with Ergun equation (D/d_p = 9.5 with air).

For turbulent flow, the kinetic effects on the flow friction (second term in the right-hand side of Ergun's equation[1]) are preponderant over the viscous effects (the first term in the right hand side of Ergun's equation[1]). For laminar flow (low Reynolds number), when the viscous effects are predominant, the friction area of the channels plays a major role.

Fig. 21, 22. indicate comparison of present work with KTA[2]. KTA[2] modified friction factor is similar with present work for D/d_p = 19, 9.5 and 6.33. KTA[2] porosity is from 0.36 to 0.42. It is limited and it is considered wall effect for relatively large bed-to-particle diameter ratios D/d_p = 6.33.

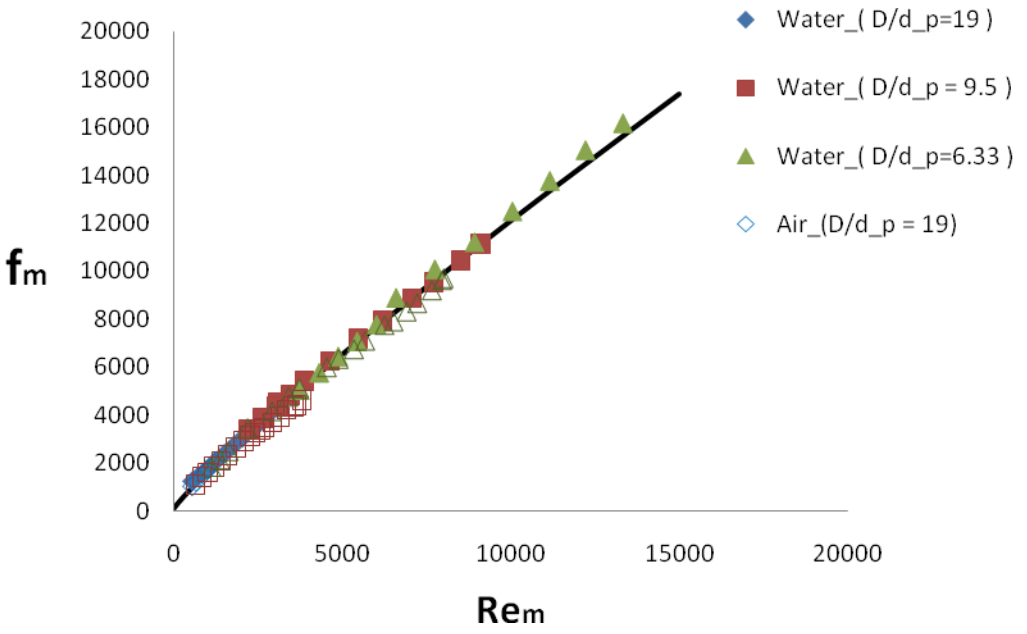

Fig. 21. Comparison of present work with KTA
(D/d_p = 19, 9.5 and 6.33 with air and water working fluids).

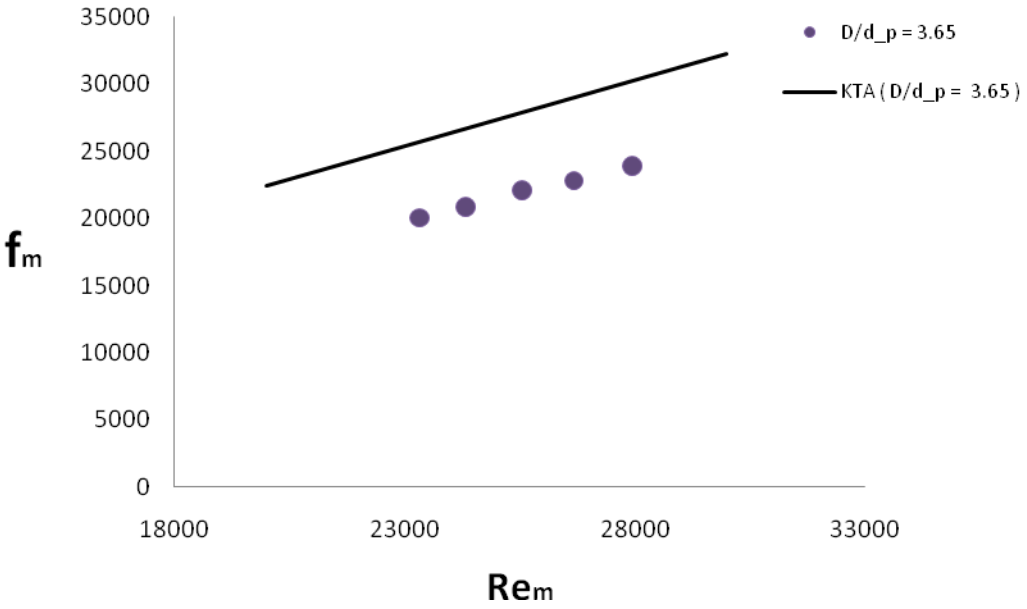

Fig. 22. Comparison of present work with KTA
(D/d_p = 3.65 with water working fluid).

Different friction factor

Many authors used modified friction factor to represent their result about pressure drop in packed beds. The modified friction factor came from the friction factor. The friction factor for packed bed is shown in equation 40.

$$\text{f (friction factor for packed bed)} = \frac{(\mathcal{P}_O - \mathcal{P}_L)\rho}{G^2}\left(\frac{d_p}{L}\right)\left(\frac{\varepsilon^3}{1-\varepsilon}\right) \tag{40}$$

And the relationship between the modified friction factor and the friction factor is shown as:

$$f_m(\text{Modified friction factor for packed bed}) = f \times Re_m \tag{41}$$

Where, f × Re is essentially a dimensionless velocity gradient averaged over the surface. Therefore, the modified friction factor can be like this equation 42.

$$\begin{aligned} f_m = f \times Re_m &= \frac{(\mathcal{P}_O - \mathcal{P}_L)\rho}{(\rho v)^2}\left(\frac{d_p}{L}\right)\left(\frac{\varepsilon^3}{1-\varepsilon}\right) \times \frac{\rho v d_p}{\mu(1-\varepsilon)} \\ &= \frac{(\mathcal{P}_O - \mathcal{P}_L){d_p}^2}{L\mu v}\left(\frac{\varepsilon^3}{(1-\varepsilon)^2}\right) \end{aligned} \tag{42}$$

The interesting thing is that KTA(1981)[2] used friction correlation, ψ by modifying the friction factor in their paper. KTA(1981)[2] pressure drop correlation is shown as:

$$\frac{\Delta P}{L} = \left\{\frac{320}{\left(\frac{Re}{1-\varepsilon}\right)} + \frac{6}{\left(\frac{Re}{1-\varepsilon}\right)^{0.1}}\right\}\left\{\left(\frac{(1-\varepsilon)}{\varepsilon^3}\right)\left(\frac{1}{d_p}\right)\left(\frac{1}{2\rho}\right)(\rho U)^2\right\} \tag{43}$$

The friction correlation for KTA(1981)[2] is shown as:

$$\psi(\text{friction correlation for KTA}) = \left\{ \frac{320}{\left(\frac{Re}{1-\varepsilon}\right)} + \frac{6}{\left(\frac{Re}{1-\varepsilon}\right)^{0.1}} \right\} \tag{44}$$

The relationship between the friction factor and the friction correlation for KTA is represented like shown as:

$$f = \frac{(p_o - p_L)\rho}{G^2}\left(\frac{d_p}{L}\right)\left(\frac{\varepsilon^3}{1-\varepsilon}\right) = \frac{1}{2}\left\{ \frac{320}{\left(\frac{Re}{1-\varepsilon}\right)} + \frac{6}{\left(\frac{Re}{1-\varepsilon}\right)^{0.1}} \right\} = \frac{1}{2}\psi \tag{45}$$

Based on these relationship, the KTA(1981) correlation[2] can be represented with the modified friction factor.

$$f_m = \frac{\Delta P d_p^2 \varepsilon^3}{L \mu U (1-\varepsilon)^2} = f \times Re_m = \frac{1}{2}\psi \times Re_m$$

$$= \frac{1}{2}\left\{ \frac{320}{\left(\frac{Re}{1-\varepsilon}\right)} + \frac{6}{\left(\frac{Re}{1-\varepsilon}\right)^{0.1}} \right\} \times Re_m = 160 + 3Re_m^{0.9} \tag{46}$$

Fig. 23 to 30 shows the comparison of present work with KTA by using the friction factor and the friction correlation that used in the KTA(1981)[2] paper.

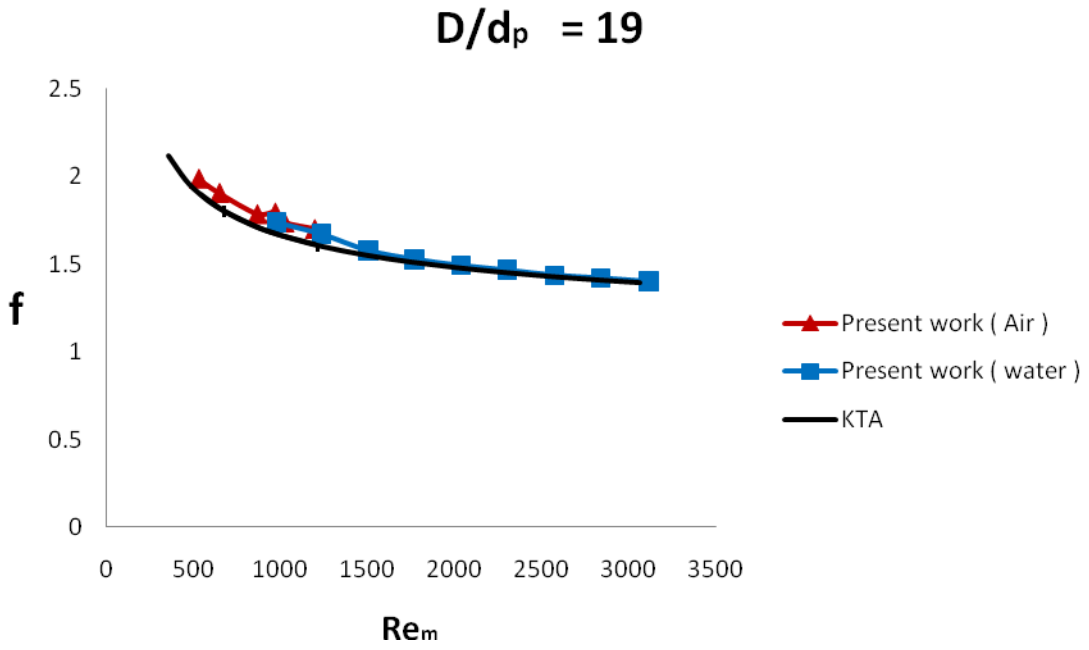

Fig. 23. The comparison of present work with KTA by using the friction factor ($D/d_p = 19$).

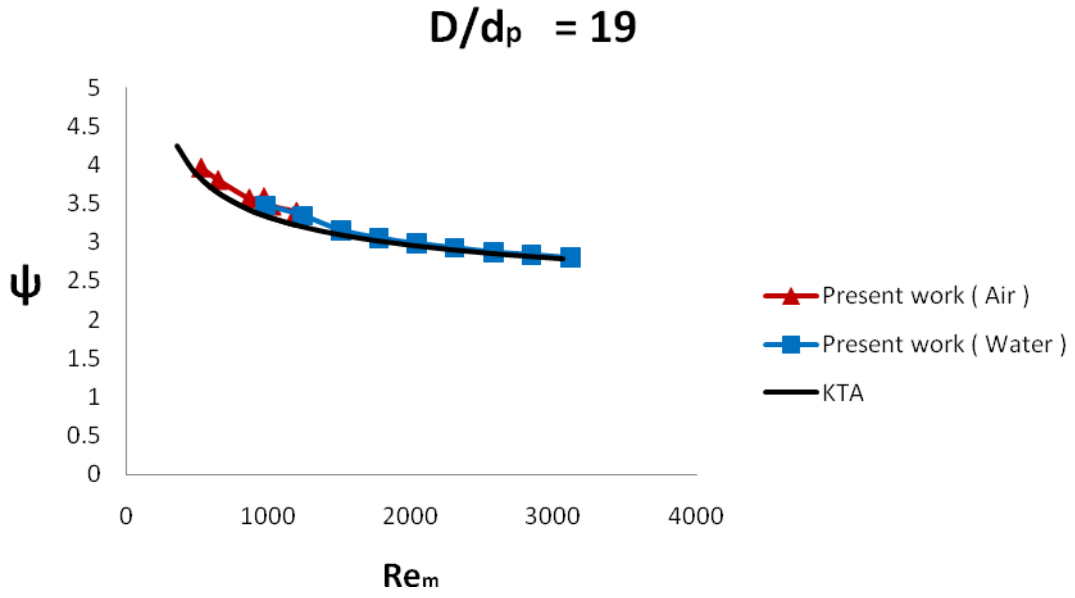

Fig. 24. The comparison of present work with KTA by using the friction correlation used in KTA ($D/d_p = 19$).

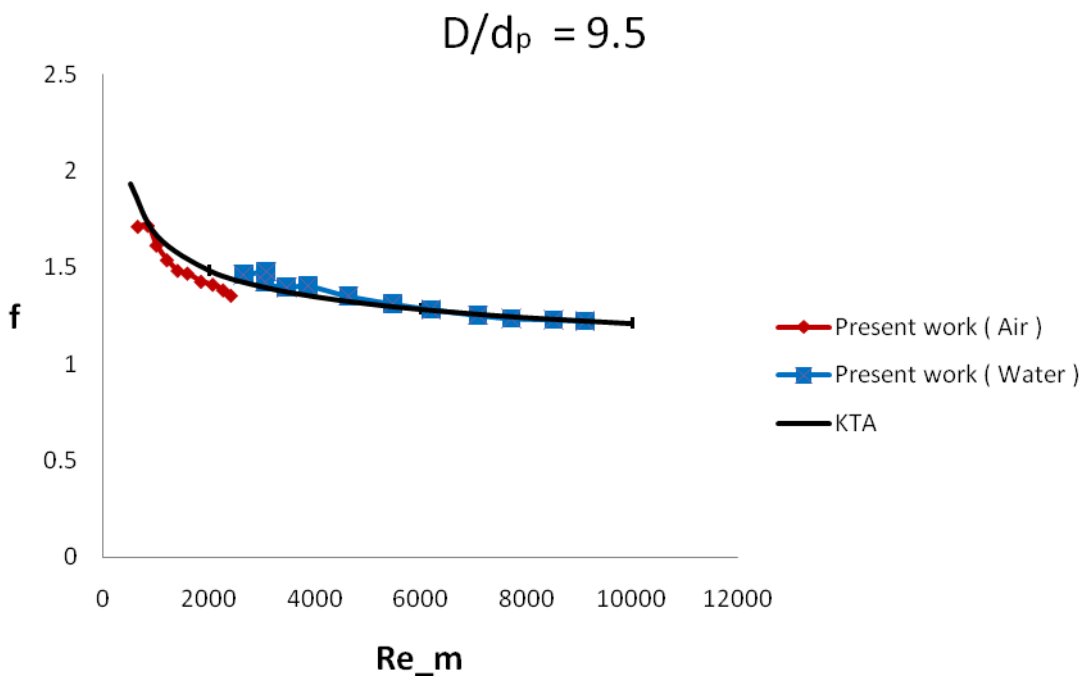

Fig. 25. The comparison of present work with KTA by using the friction factor ($D/d_p = 9.5$).

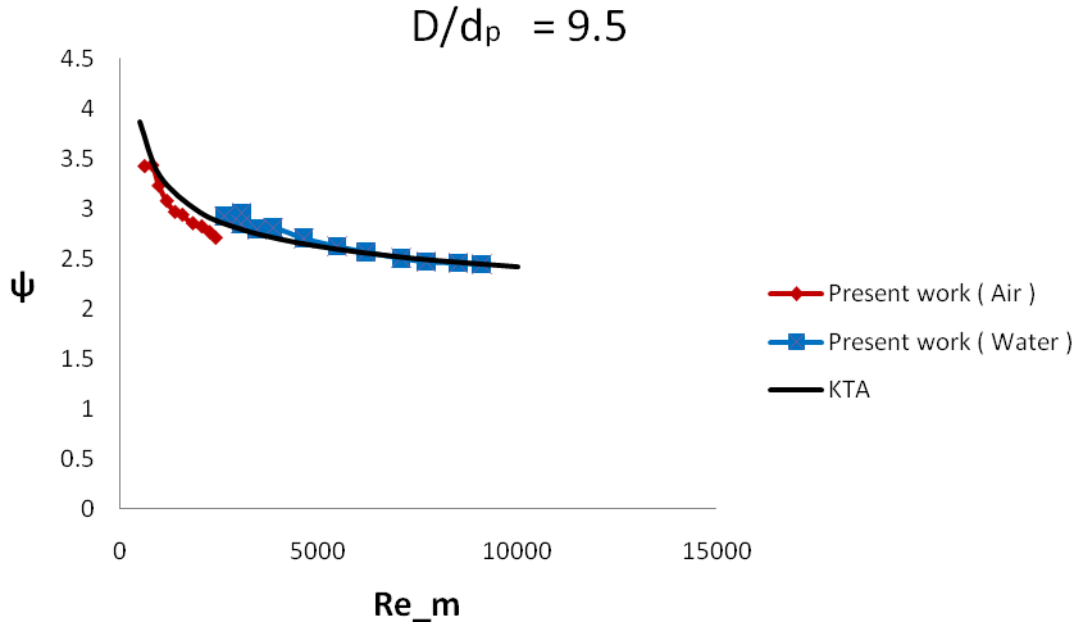

Fig. 26. The comparison of present work with KTA by using the friction correlation used in KTA ($D/d_p = 9.5$).

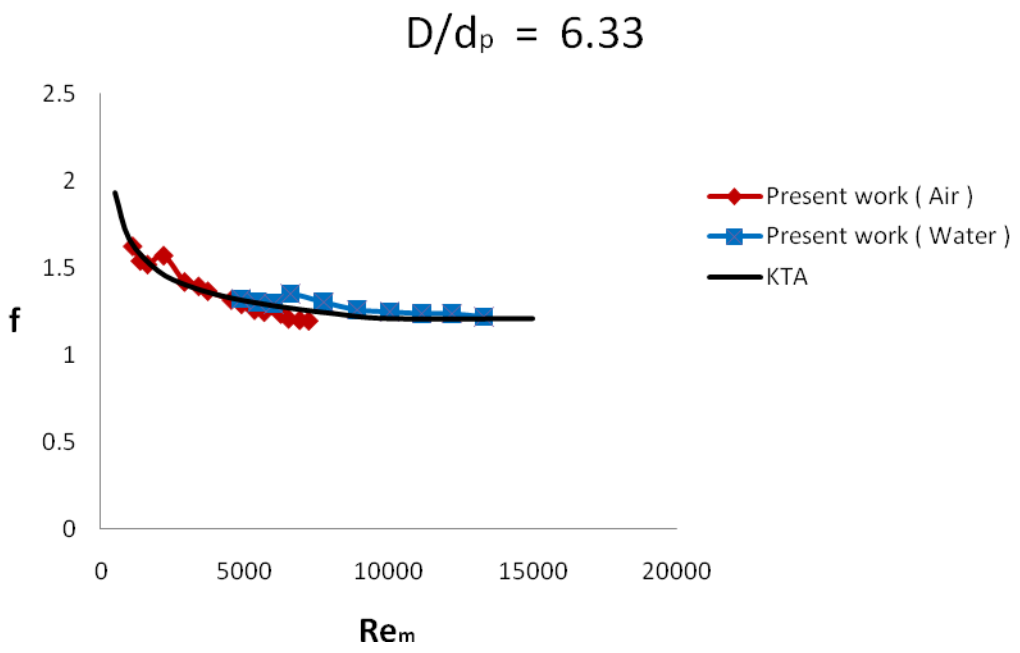

Fig. 27. The comparison of present work with KTA by using the friction factor (D/d_p=6.33).

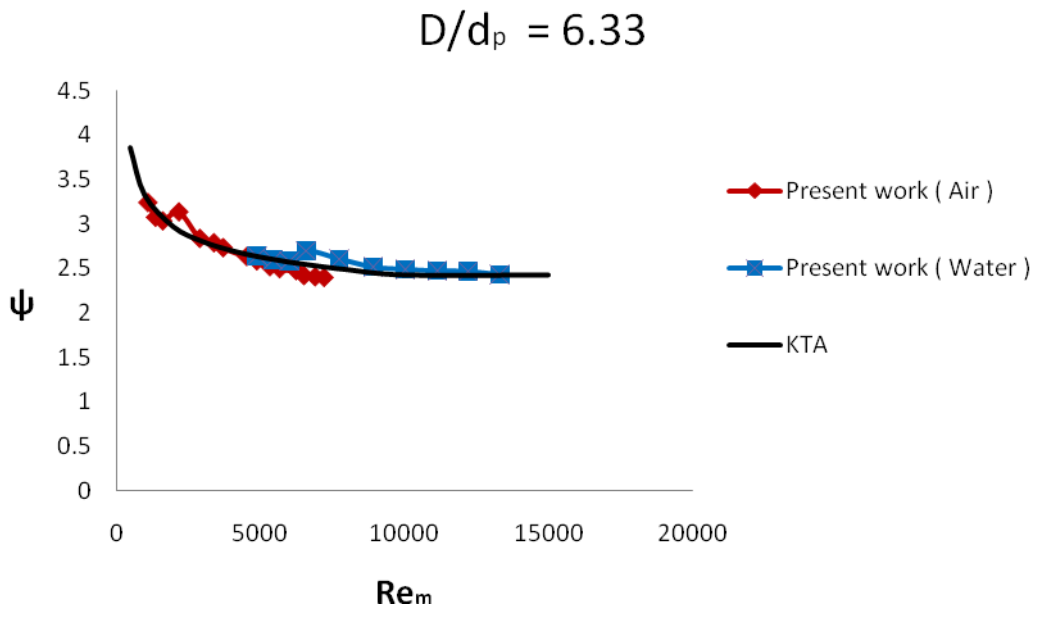

Fig. 28. The comparison of present work with KTA by using the friction correlation used in KTA (D/d_p = 6.33).

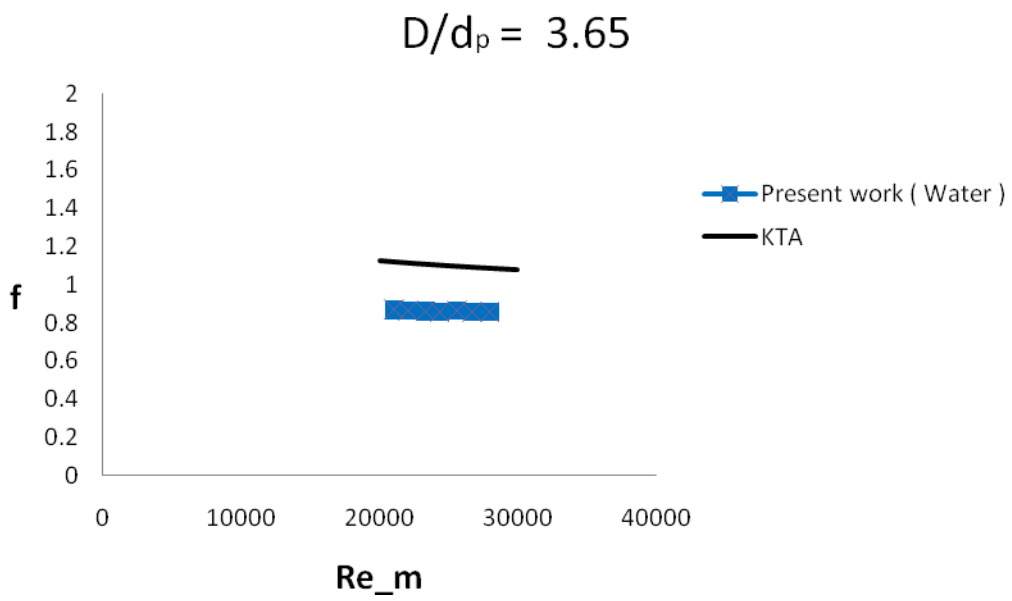

Fig. 29. The comparison of present work with KTA by using the friction factor (D/d_p=3.65).

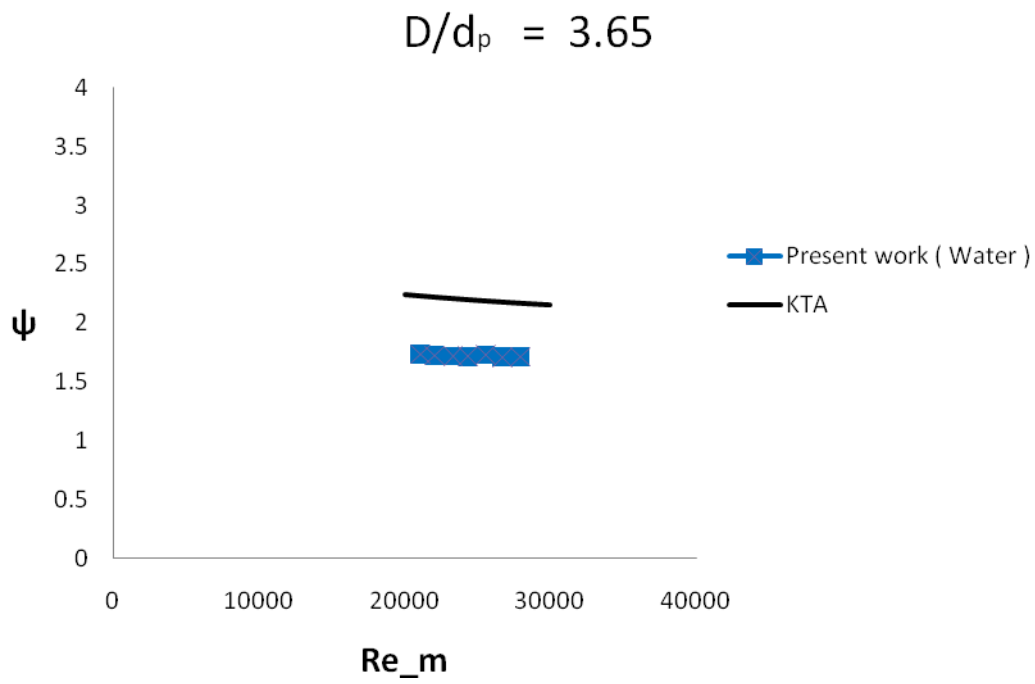

Fig. 30. The comparison of present work with KTA by using the friction correlation used in KTA (D/d_p = 3.65).

Error analysis

There are many factors to reduce error in present work. One of the most important factors is to keep the same porosity. When the bed is filled with beads, its porosity is changed even though same methods were used to fill particles into the bed. And the different porosity causes different pressure drop. It makes difficulties for us to compare air and water experiments. Therefore, the experiment of air and water were done continuously without repacking.

In addition, temperature is important factor. An exact checking of temperature gives accurate properties of air and water. The temperature of air didn't change very much. However, the water temperature was changed even while we were doing experiment. The temperature were checked when the pressure were measured. Also the differences of temperature were checked to estimate error regime of these experiments. A type of thermocouple was submerged into the reservoir tank to monitor the bulk liquid temperature. The flow rate was kept constant while the pressure transducer was reading pressures. Even while the pressure sensor was measuring the pressure, the temperature of the reservoir tank was increased about 1~2°C. Total change of the temperature over one set experiment was about 6~10 °C.

Next effort for reducing error is to wait enough time for steady state. After pump works, it has to be waited for steady state of flow. When the flow meter gives same flow rate, the pressure transducer was started to measure pressures.

Another big issue is that it has to be no air between pressure sensor and bed water. It causes pressure measuring error. While the water flows, the sensor tab has to be connected loosely and water leaks through the pressure sensor and the water makes the left air out. After then tab should be locked totally. By doing these procedures, the air can be removed from the gap between the sensor and the water of bed.

Lastly, when the water flow the bed, any bubble has to be removed from the bed. The water of tank enters into the pump. And the water rotates the test loop. When it enters into the reservoir water tank again, some bubbles are made in the tank. The air might enter the water loop.

Error analysis of air experiments

The uncertainty for the determination of the flow rate is ±4%. In addition, from the manufacturer, Dwyer Rate-master flow meter gives ±2% uncertainty. The HiQ ventury digital instrument for measurement of flow rate has ±4% uncertainty. The uncertainty for average bed porosity is ±3%.

Table 14 shows the uncertainty for porosity at each particle diameter case.

Table 14. The uncertainty for porosity measurement.

d_p	0.635cm	1.27cm	1.905cm	3.3cm
Porosity 1	0.381	.	.	.
Porosity 2	0.385	0.393	0.414	0.471
Porosity 3	.	0.397	0.416	0.465
Porosity (chosen)	0385	0.397	0.416	0.465
Regime from other's correlations	0.368~0.395	0.377~0.405	0.388~0.419	0.417~0.479
Uncertainty	2.53	1.97	0.71	2.92

The uncertainty for pressure measurement is ±1%. Table 15 shows the uncertainty for pressure measurement.

Table 15. The uncertainty for pressure measurement.

Instrument	Uncertainty(σ)
Digital manometer (chosen)	±1%
Inclined manometer	±1%
Magnehelic differential pressure gauge	±2%

The estimated uncertainty associated to the determination of the modified Reynolds number is ±5%. The uncertainty of the modified Reynolds number is consist of velocity (v) and porosity (ε). The other factors like density, viscosity of air and particle diameter are assumed that they are constant. The estimated uncertainty associated to the determination of the modified friction factor is ±5.1%. This uncertainty is composed of differential pressure, porosity and velocity.

These uncertainties were determined by the Kline and McClintock [40] method.

Error analysis for water experiments

The uncertainty for the determination of the flow rate is ±1%. From the manufacturer, G2 Industrial Grade flow meter has ±1% error. The uncertainty for average bed porosity is ±3%. Table 14 shows the uncertainty for porosity at each particle diameter case.

The accuracy of the pressure transducer (sensor: PX309 series, 30 psi) from the manufacturer is ±2%. FSO (except 1 psi = ±4.5% and 2 psi = ±3%). This error band includes linearity, hysteresis, repeatability, thermal hysteresis, and thermal errors.

The estimated uncertainty associated to the determination of the modified Reynolds number is ±5.1%. The uncertainty of the modified Reynolds number is consist of velocity(v) , porosity(ε) and density, viscosity of water. Particle diameter is assumed that it is constant and could be ignored. The density and viscosity of water is changed with water temperature. The water is increased because of pump heat while we are measuring the flow rate. And the temperature of water is measured from the reservoir not the bed.

The estimated uncertainty associated to the determination of the modified friction factor is ±5.5%. This uncertainty is composed of differential pressure, porosity, velocity and viscosity of water.

These uncertainties were determined by the Kline and McClintock[40] method.

Fig. 31 to 34 show the error estimation of present work of different particle size. In addition, Fig. 35 to 38 show the error comparison of present work with KTA. KTA has ± 15% error in their experiments. When the error is considered both KTA and present work they match very well each other except for the case of D/d_p = 3.65.

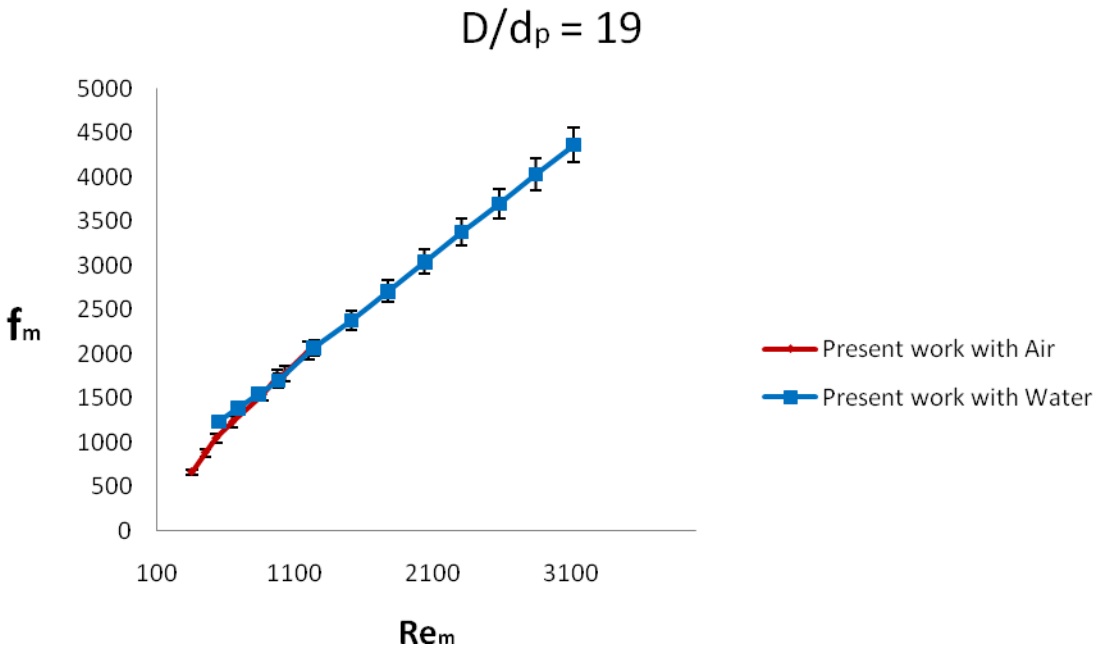

Fig. 31. An error estimation for $D/d_p = 19$.

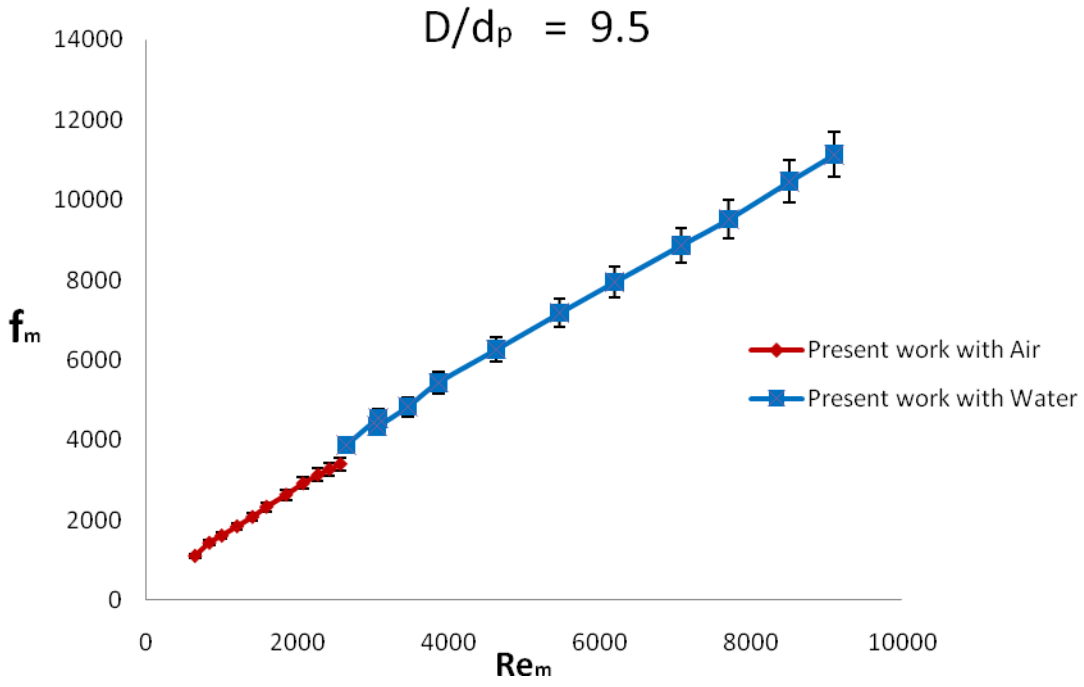

Fig. 32. An error estimation for $D/d_p = 9.5$.

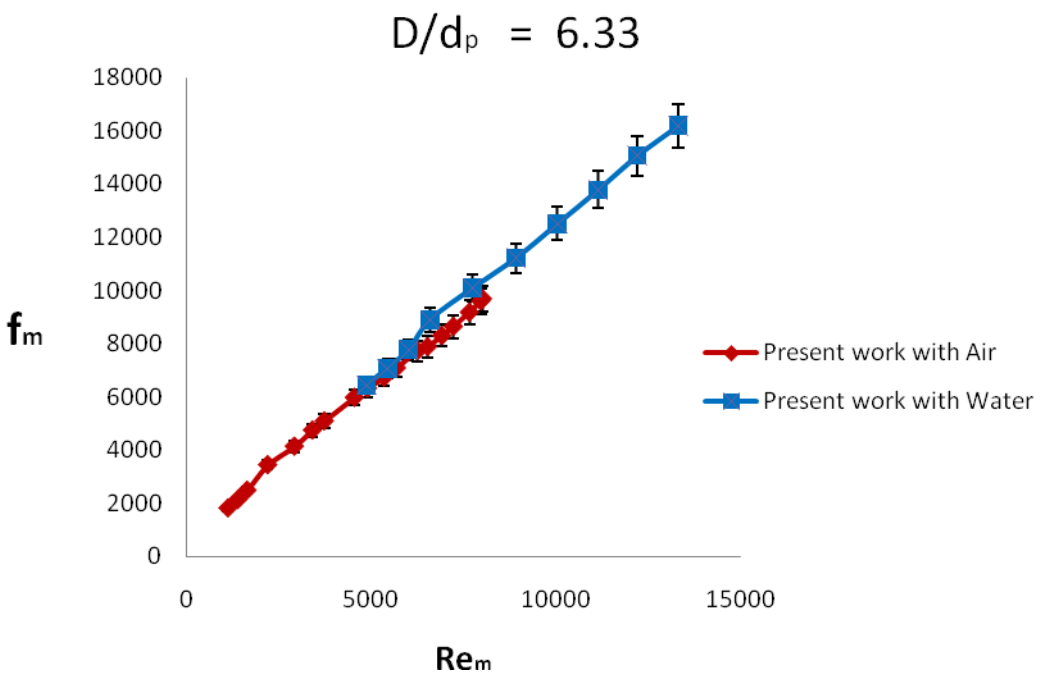

Fig. 33. An error estimation for $D/d_p = 6.33$.

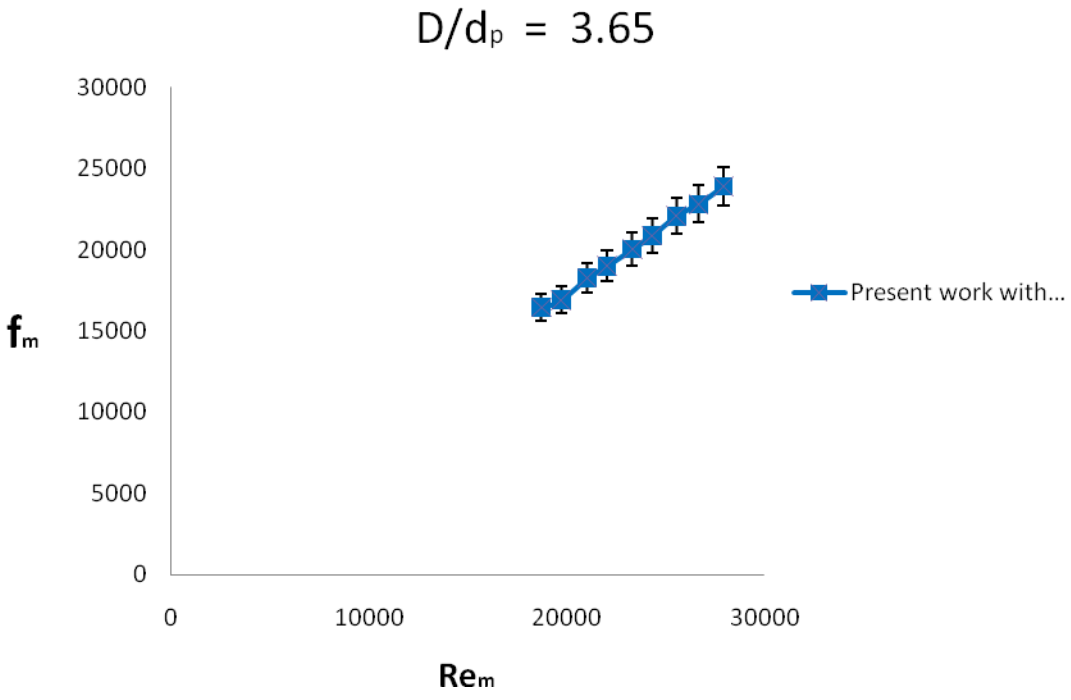

Fig. 34. An error estimation for $D/d_p = 3.65$

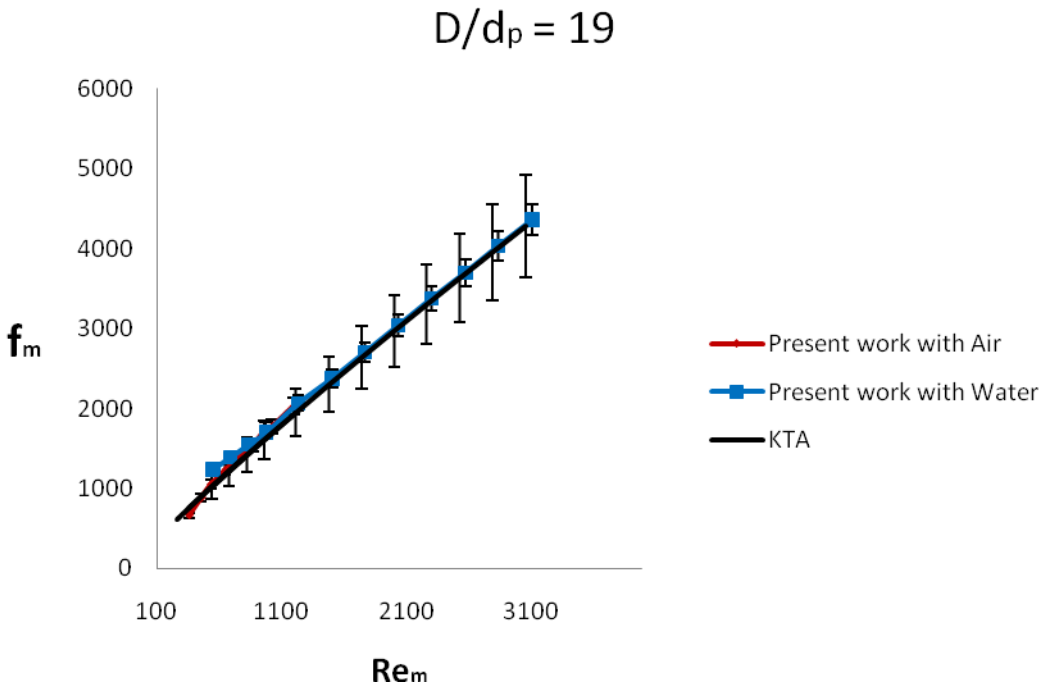

Fig. 35. A comparison with KTA including error bar ($D/d_p = 19$).

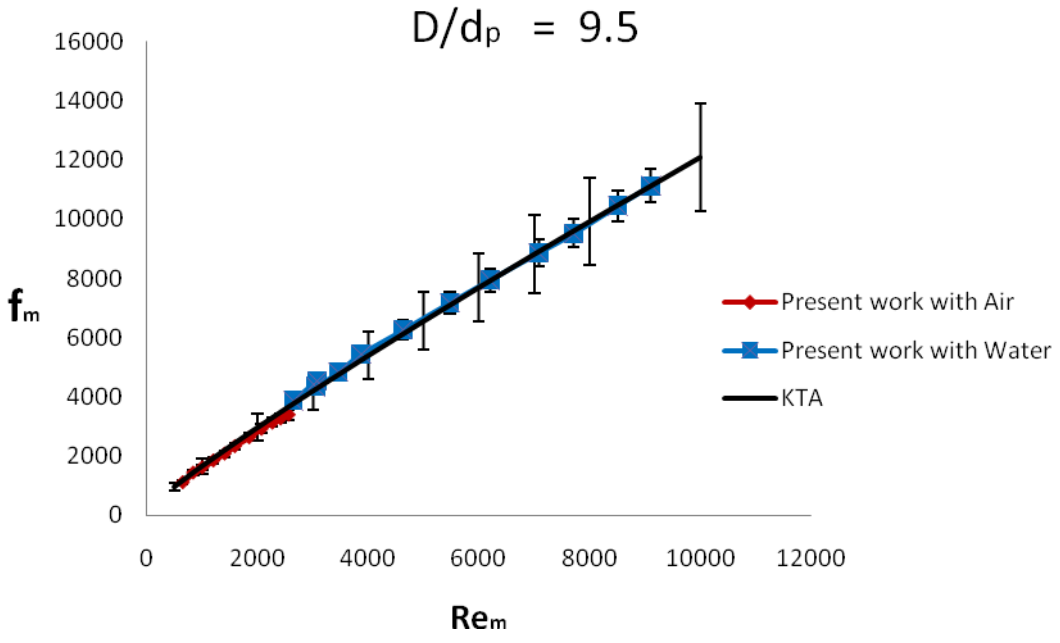

Fig. 36. A comparison with KTA including error bar ($D/d_p = 9.5$).

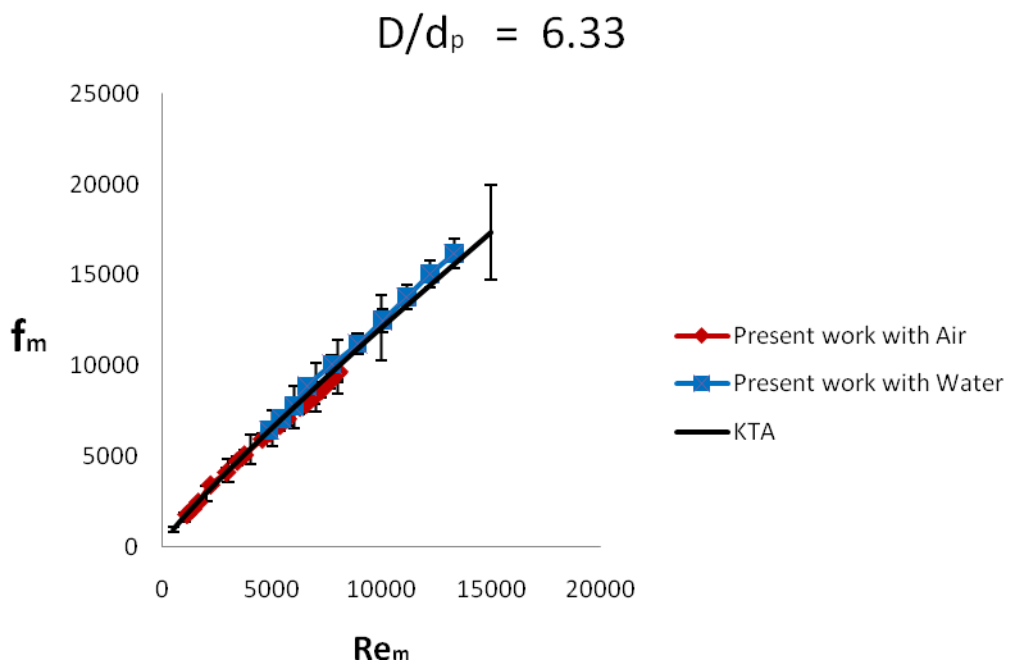

Fig. 37. A comparison with KTA including error bar ($D/d_p = 6.33$).

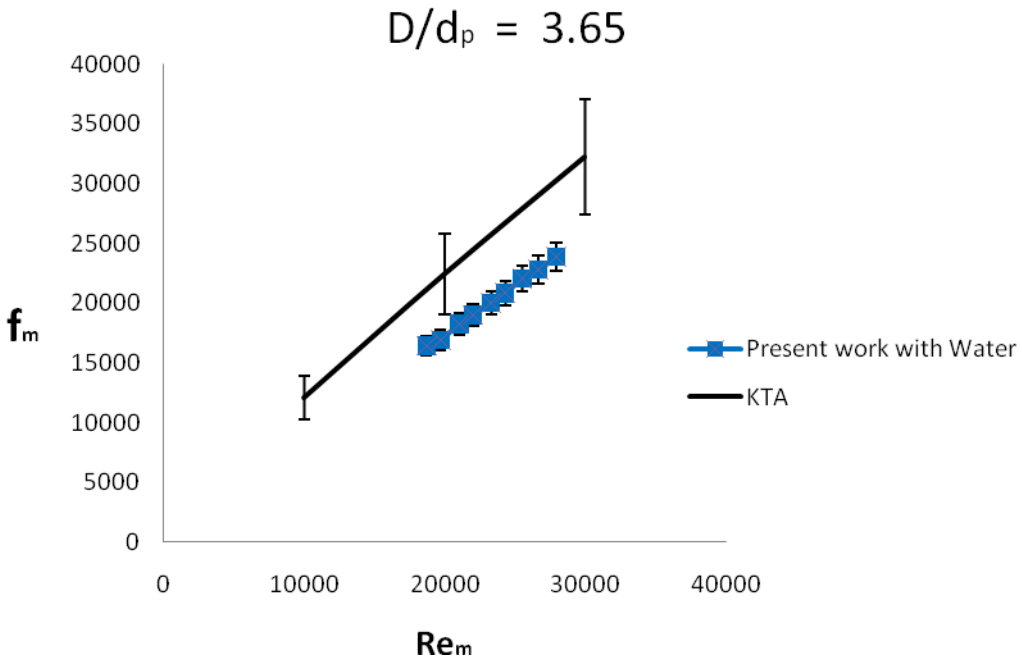

Fig. 38. A comparison with KTA including error bar ($D/d_p = 3.65$).

CHAPTER IV

CONCLUSIONS

The average bed porosities based on experiments was compared with existing correlations. In addition, from data analysis of present work, it is demonstrated that correlations for pressure drop found in the literature doesn't predict pressure drop at high Reynolds numbers correctly. Even the system has wall effects, it is more difficult to predict pressure drop accurately from existing correlations. The wall effects became more prominent at $D/d_p < 5$. This thesis is based on a series of experiments from low Reynolds numbers to high Reynolds numbers ($528 < Re_m < 29936$), with different bed-to-particle diameter ratios(19, 9.5 6.33 and 3.65). KTA [2] correlation was matched well with present work for bed-to-particle diameter ratios of 19, 9.5 and 6.33. However, in the case of $D/d_p = 3.65$, KTA [2] was over predicted because of wall effect of the system. Therefore, a new correlation for pressure drop at high Reynolds numbers ($20000 < Re_m < 29936$) and low bed-to-particle diameter ratios ($D/d_p < 5$) was developed.

REFERENCES

[1] Ergun S. Fluid flow through packed columns. *Chemical Engineering Progress* 1952; **48**(2): 89-94.

[2] Nuclear Safety Standards Commission (KTA). Reactor core design of high-temperature gas-cooled reactor. Part 3: Loss of pressure through friction in pebble bed cores. *Safety Standards, KTA 3102.3* 1987; Issue 3/81.

[3] Eisfeld B, Schnitzlein K. The influence of confining walls on the pressure drop in packed beds. *Chemical Engineering Science* 2001; **56**(14): 4321-4329.

[4] Andersson K E B. Pressure drop in packed beds. *Transactions of the Royal Institute of Technology Stockholm* 1963; (No. 201).

[5] Carman P C. Fluid flow through a granular bed. *Transactions Institutions of chemical engineers* 1937; **15**: 150–156

[6] Coulson J M. The flow of fluids through granular beds: effect of particle shape and voids in streamline flow. *Transactions Institutions of chemical engineers* 1949; **27**: 237-257.

[7] Mehta D, Hawley M C. Wall effect in packed columns. *Industrial & Engineering Chemistry Process Design and Development* 1969; **8**(2): 280-282.

[8] Foumeny E A, Benyahia F, Castro J A A, Moallemi H A, Roshani S. Correlations of pressure drop in packed beds taking into account the effect of confining wall. *International Journal of Heat and Mass Transfer* 1993; **36**(2): 536-540.

[9] Leva M. Pressure drop through packed tubes. 1. A general correlation. *Chemical Engineering Progress* 1947; **43**(10): 549-554.

[10] Sonntag G. Einfluß des lückenvolumens auf den druckverlust in gasdurchströmten füllkörpersäulen. *Chemie-Ingenieur-Technik* 1960; **32**: 317–329.

[11] Hicks R E. Pressure drop in packed beds of spheres. *Industrial & Engineering Chemistry Fundamentals* 1970; **9**(3): 500-502.

[12] Reichelt W. Calculation of pressure drop in spherical and cylindrical packings for single phase flow. *Chemie Ingenieur Technik* 1972; **44**(18): 1068-1071.

[13] Macdonald I F, El-Sayed M S, Mow K, Dullien F A L. Flow through porous media ergun equation revisited. *Industrial & Engineering Chemistry Fundamentals* 1979; **18**(3): 199-208.

[14] Fand R M, Thinakaran R. The Influence of the wall on flow through pipes packed with spheres. *Journal of Fluids Engineering-Transactions of the Asme* 1990; **112**(1): 84-88.

[15] Comiti J, Renaud M. A new model for determining mean structure parameters of fixed beds from pressure-drop measurements - Application to beds packed with parallelepipedal particles. *Chemical Engineering Science* 1989; **44**(7): 1539-1545.

[16] Shijie Liu A A, Jacob Masliyah, Steady incompressible laminar flow in porous media. *Chemical Engineering Science* 1994; **49**: 3565-3586.

[17] Hayes R E, Afacan A, Boulanger B. *An* equation of motion for an Incompressible Newtonian fluid in a packed bed. *Transport in Porous Media* 1995; **18**(2): 185-198.

[18] Niven R K. Physical insight into the Ergun and Wen & Yu equations for fluid flow in packed and fluidised beds. *Chemical Engineering Science* 2002; **57**(3): 527-534.

[19] Di Felice R, Gibilaro L G. Wall effects for the pressure drop in fixed beds. *Chemical Engineering Science* 2004; **59**: 3037–3040.

[20] Montillet A. Flow through a finite packed bed of spheres: A note on the limit of applicability of the Forchheimer type equation. *Journal of Fluids Engineering-Transactions of the Asme* 2004; **126**(1): 139-143.

[21] Rose H E, Rizk A M A. Further researches in fluid flow through beds of granular material. *Proceedings of the Institution of Mechanical Engineers Part C-Journal of Mechanical Engineering Science* 1949; **60**: 493–503.

[22] Nemec D, Levec J. Flow through packed bed reactors: 1. Single phase flow. *Chemical Engineering Science* 2005; **60**(24): 6947-6957.

[23] Choi Y S, Kim S J, Kim D. A semi-empirical correlation for pressure drop in packed beds of spherical particles. *Transport in Porous Media* 2008; **75**(2): 133-149.

[24] Wu J S, Yu B M, Yun M J. A resistance model for flow through porous media. *Transport in Porous Media* 2008; **71**(3): 331-343.

[25] Rumpf H, Gupte A R. Influence of porosity and particle size distribution in resistance law of porous flow. *Chemie Ingenieur Technik* 1971; **43**(6): 367.

[26] Liu S J, Afacan A, Masliyah J. Steady incompressible laminar flow in porous media. *Chemical Engineering Science* 1994; **49**(21): 3565-3586.

[27] Endo Y, Chen D R, Pui D Y H. Theoretical consideration of permeation resistance of fluid through a particle packed layer. *Powder Technology* 2002; **124**(1-2): 119-126.

[28] Hill R J, Koch D L, Ladd A J C. The first effects of fluid inertia on flows in ordered and random arrays of spheres. *Journal of Fluid Mechanics* 2001; **448**: 213-241.

[29] Beavers G S, Sparrow E M, Rodenz D E, Influence of bed size on flow characteristics and porosity of randomly packed beds of spheres. *Journal of Applied Mechanics-Transactions of the Asme* 1973; **40**(3): 655-660.

[30] Yuji Sato T H, Futoshi Takahashi, Mikio Toda. Pressure loss and liquid holdup in packed bed reactor with cocurrent gas-liquid down flow. *Journal of Chemical Engineering of Japan* 1973; **6**: 147-152.

[31] Zou R P, Yu A B. The packing of spheres in a cylindrical container - The thickness effect. *Chemical Engineering Science* 1995; **50**(9): 1504-1507.

[32] Chu C F, Ng K M. Flow in packed tubes with a small tube to particle diameter ratio. *Aiche Journal* 1989; **35**(1): 148-158.

[33] Foscolo P U, Gibilaro L G, Waldram S P. A unified model for particulate expansion of fluidized beds and flow in fixed porous media. *Chemical Engineering Science* 1983; **38**(8): 1251-1260.

[34] Handley D, Heggs P J. Momentum and heat transfer mechanisms in regular shaped packings. *Transactions of the Institution of Chemical Engineers and the Chemical Engineer* 1968; **46**(9): T251-T264.

[35] Yu J, Zhang M, Fan W, Zhow Y, Zhao G. Study on performance of the ball packed-bed regenerator: experiments and simulation. *Applied Thermal Engineering* 2002; **22**(6): 641-651.

[36] Tallmadge J A. Packed bed pressure drop - An extension to higher Reynolds numbers. *Aiche Journal* 1970; **16**(6): 1092-1093.

[37] Brauer H. Eigenschaften der Zweiphasen-Strömung bei der Rektifikation in Füllkörpersäulen. In H. Bretschneider(Ed.), Fortschritte der Destilliertechnik. Forschungsarbeiten aus dem Max-Planck-Institut für Strömungsforschung Göttingen, Dechema-Monographien. *VCH, Weinherm* 1960; **37**: 7-78.

[38] Morcom A R. Fluid flow through granular materials. *Transactions of the Institution of Chemical Engineers and the Chemical Engineer* 1946; **24**: 30-46.

[39] Wentz C A, Thodos G. Pressure drops in the flow of gases through packed and distended beds of spherical particles. *Aiche Journal* 1963; **9**(1): 81-84.

[40] Kline S J, Mcclintock F A. Describing uncertainties in single sample experiments. *Mechanical Engineering* 1953; **75**: 3-8.

APPENDIX

Data from the present experiments

Water experiment data

Table 16. Water experiment data for $D/d_p = 19$ experiments of vertical bed set up with up-flow direction.

HZ	Q(gpm)	Q(cfm)	Q(m^3/s)	T	μ(34C)	ρ(34C)
17.5	11.17	1.493429	0.0007048	32.3	0.000715	993.9346
20	12.97	1.734089	0.0008184	23	0.0007038	993.6555
25	16.42	2.195354	0.0010361	26	0.000752	994.77355
30	20.03	2.678011	0.0012639	33	0.0007024	993.62026
35	23.56	3.149972	0.0014866	33.2	0.0007567	994.87078
40	27.12	3.625944	0.0017113	33.1	0.0007024	993.62026
45	30.75	4.111275	0.0019403	33.5	0.0007505	994.74097
50	34.33	4.589921	0.0021662	33.5	0.0007052	993.69067
55	38	5.0806	0.0023978	33.3	0.0007324	994.34364
60	41.58	5.559246	0.0026237	33	0.0007136	993.89999

(a)

P1(PSI)	P2(PSI)	P3(PSI)	P4(PSI)	P5(PSI)
1.7632461	1.06277	0.2046166	-0.540239	-1.371802
2.6002624	1.7808707	0.8054075	-0.063736	-1.01844
4.6352071	3.5388656	2.28219	1.10657	-0.13904
7.0782088	5.6503061	4.0606152	2.5503655	0.9596776
9.9841893	8.159239	6.1557719	4.2323134	2.2293742
13.278702	11.019763	8.5919063	6.220436	3.7625058
17.034853	14.263273	11.325116	8.4029013	5.4116326
21.168358	17.877355	14.429607	10.949264	7.4191917
25.740563	21.832859	17.773202	13.631383	9.4582808
30.01416	26.25478	21.583846	16.776899	11.954107

(b)

Table 16. continued.

Re_m	Q(m^3/s)	Q(cfm)	P(Pa)	P (inches water)	f_m	v(m/s)
899.47	0.0007	1.4928	5916.23	23.77	1794	0.0617
1060.77	0.0008	1.7334	7623.39	30.63	2022	0.0716
1258.20	0.0010	2.1944	11736.16	47.16	2301	0.0906
1641.35	0.0013	2.6769	16427.80	66.01	2827	0.1106
1794.39	0.0015	3.1487	22112.27	88.85	3003	0.1300
2222.33	0.0017	3.6244	28343.78	113.89	3603	0.1497
2361.01	0.0019	4.1096	35811.84	143.89	3758	0.1697
2802.30	0.0022	4.5880	43379.30	174.30	4339	0.1895
2988.53	0.0024	5.0785	52369.28	210.42	4556	0.2097
3354.77	0.0026	5.5569	61435.81	246.85	5014	0.2295

(c)

Table 17. Water experiment data for $D/d_p = 19$ experiments of horizontal bed set-up.

HZ	Q(gpm)	Q(cfm)	Q(m^3/s)	T	μ(28C)	ρ(28C)
12.5	6.83	0.913	0.0004	32.3	0.00076	994.9352
15	8.6	1.150	0.0005	23?	0.000749	994.7083
17.5	10.42	1.393	0.0007	26?	0.000705	993.6907
20	12.2	1.631	0.0008	33	0.000749	994.7083
25	15.42	2.062	0.0010	33.2	0.000746	994.6428
30	18.81	2.515	0.0012	33.1	0.000747	994.6756
35	22.11	2.956	0.0014	33.5	0.000741	994.5438
40	25.43	3.400	0.0016	33.5	0.000741	994.5438
45	28.75	3.844	0.0018	33.3	0.000744	994.6098
50	32.16	4.300	0.0020	33	0.000749	994.7083
55	35.47	4.742	0.0022	32	0.000765	995.0312
60	38.88	5.198	0.0025	30.4	0.000791	995.5301

(a)

P1(PSI)	P2(PSI)	P3(PSI)	P4(PSI)	P5(PSI)
0.46	0.33	0.05	-0.08	-0.31
1.10	0.90	0.53	0.32	0.01
1.86	1.55	1.08	0.78	0.39
2.71	2.30	1.73	1.33	0.83
4.78	4.10	3.27	2.63	1.89
7.27	6.29	5.13	4.21	3.20
10.20	8.85	7.34	6.09	4.76
13.56	11.82	9.90	8.27	6.57
17.37	15.17	12.80	10.74	8.62
21.62	18.91	16.04	13.50	10.91
26.27	23.01	19.61	16.53	13.43
30.01	27.54	23.54	19.88	16.23

(b)

Table 17. continued.

Re_m	Q(m^3/s)	Q(cfm)	ΔP(3-5)(Pa)	ΔP(3-5) (inches water)	f_m	v(m/s)
518.0825	0.0004	0.9128	2510.7169	10.0881	1171.5105	0.0377
661.6456	0.0005	1.1493	3547.2579	14.2529	1333.5559	0.0475
850.5672	0.0007	1.3926	4791.6428	19.2528	1579.0364	0.0575
938.6135	0.0008	1.6305	6166.0695	24.7753	1634.0506	0.0673
1191.1256	0.0010	2.0608	9474.5127	38.0686	1994.6389	0.0851
1450.0716	0.0012	2.5139	13298.1944	53.4321	2290.3866	0.1038
1718.1952	0.0014	2.9549	17793.4736	71.4942	2628.5581	0.1220
1976.1965	0.0016	3.3986	22988.9251	92.3695	2952.6902	0.1404
2225.2683	0.0018	3.8423	28856.6472	115.9460	3265.0175	0.1587
2474.2467	0.0020	4.2980	35383.1653	142.1696	3557.1122	0.1775
2674.1540	0.0022	4.7404	42559.7324	171.0050	3800.2483	0.1958
2836.0785	0.0025	5.1961	50416.0331	202.5716	3971.6019	0.2146

(c)

Table 18. Water experiment data for $D/d_p = 9.5$ experiments of vertical bed set up with up-flow direction.

HZ	Q(gpm)	Q(cfm)	Q(m^3/s)	T	vis(34C)	dens(34C)
22.5	20.1	2.6874	0.0013	37.5	0.00068	993.155
25	22.49	3.0069	0.0014	35.9	0.00071	993.726
27.5	24.69	3.3011	0.0016	37.5	0.00068	993.155
30	28.29	3.7824	0.0018	32.6	0.00076	994.838
32.5	29.35	3.9241	0.0019	37.7	0.00068	993.082
35	31.65	4.2316	0.0020	36	0.00071	993.691
37.5	33.91	4.5338	0.0021	37.6	0.00068	993.119
40	38.13	5.0980	0.0024	32.8	0.00075	994.774
42.5	38.53	5.1515	0.0024	37.6	0.00068	993.119
45	40.78	5.4523	0.0026	36.1	0.00070	993.656
47.5	43.15	5.7692	0.0027	37.3	0.00069	993.227
50	47.76	6.3855	0.0030	33.6	0.00074	994.511
52.5	47.57	6.3601	0.0030	36.8	0.00069	993.407
55	49.95	6.6783	0.0032	34.6	0.00073	994.175
57.5	51.89	6.9377	0.0033	36	0.00071	993.691

(a)

P1(PSI)	P2(PSI)	P3(PSI)	P4(PSI)	P5(PSI)
3.0973	2.6856	1.7417	0.9471	0.0332
4.0323	3.6242	2.5848	1.6745	0.6477
5.1268	4.6903	3.5425	2.5259	1.3832
5.9815	5.5241	4.1851	2.9693	1.6266
7.5756	7.0970	5.6961	4.4365	3.0234
8.9590	8.4614	6.9308	5.5291	3.9696
10.4490	9.9120	8.2462	6.6970	4.9808
11.3690	10.7927	8.8601	7.0144	4.9899
13.7131	13.1164	11.1607	9.2836	7.2285
15.5280	14.9077	12.8090	10.7554	8.5176
17.3824	16.7207	14.4591	12.2211	9.7971
18.2621	17.5414	14.9220	12.2705	9.4204
21.4524	20.7231	18.1219	15.4934	12.6661
23.4917	22.7220	19.9159	17.0423	13.9702
25.9376	25.1335	22.1779	19.1239	15.8659

(b)

Table 18. continued.

Re_m	Q(m^3/s)	Q(cfm)	P(Pa)	P(inches water)	f_m	v(m/s)
3165	0.0013	2.6863	6824	27	4579	0.1109
3542	0.0014	3.0057	8400	34	5037	0.1241
3888	0.0016	3.2997	9932	40	5425	0.1363
4455	0.0018	3.7808	12684	51	6047	0.1561
4622	0.0019	3.9225	13471	54	6190	0.1620
4984	0.0020	4.2298	15460	62	6588	0.1747
5340	0.0021	4.5319	17558	71	6983	0.1872
6005	0.0024	5.0959	21728	87	7685	0.2104
6068	0.0024	5.1493	22155	89	7755	0.2127
6422	0.0026	5.4500	24631	99	8146	0.2251
6796	0.0027	5.7668	27186	109	8497	0.2382
7522	0.0030	6.3829	32973	132	9311	0.2636
7492	0.0030	6.3575	32658	131	9259	0.2626
7866	0.0032	6.6755	36035	145	9730	0.2757
8172	0.0033	6.9348	38561	155	10022	0.2864

(c)

Table 19. Water experiment data for $D/d_p = 9.5$ experiments of horizontal bed set-up.

HZ	Q(gpm)	Q(cfm)	Q(m^3/s)	T	vis(37C)	dens(37C)
17.5	15.87	2.121819	0.0010014	34.5	0.000727	994.20859
20	18.42	2.462754	0.0011623	34.8	0.000722	994.10644
20	18.31	2.448047	0.0011553	35	0.000719	994.03795
22.5	20.74	2.772938	0.0013087	36	0.000705	993.69067
25	23.18	3.099166	0.0014626	39.9	0.000654	992.26184
30	27.75	3.710175	0.001751	39.4	0.00066	992.4515
35	32.78	4.382686	0.0020684	39.3	0.00066	992.48921
40	37.14	4.965618	0.0023435	39.7	0.000657	992.33793
45	42.41	5.670217	0.002676	39.6	0.000658	992.37586
50	46.2	6.17694	0.0029152	40	0.000653	992.22368
55	51	6.8187	0.0032181	40	0.000653	992.22368
60	54.55	7.293335	0.0034421	38	0.000678	992.97252

(a)

P1(PSI)	P2(PSI)	P3(PSI)	P4(PSI)	P5(PSI)
1.636	1.555	1.250	0.944	0.627
2.354	2.330	1.836	1.467	0.988
2.382	2.291	1.895	1.497	1.087
3.217	3.115	2.618	2.118	1.602
4.124	4.061	3.371	2.790	2.093
6.330	6.220	5.300	4.490	3.538
8.818	8.651	7.454	6.342	5.070
11.930	11.705	10.265	8.853	7.272
15.072	14.771	12.978	11.164	9.167
19.215	18.856	16.815	14.682	12.354
23.038	22.593	20.140	17.544	14.732
28.102	27.587	24.863	21.894	18.706

(b)

Table 19. continued.

Re_m	Q(m^3/s)	Q(cfm)	P(Pa)	P(inches water)	f_m	v(m/s)
2524	0.00100	2.121	4298.56	17.27	3690.47	0.09
2947	0.00116	2.462	5849.37	23.50	4352.77	0.10
2941	0.00116	2.447	5568.56	22.37	4185.39	0.10
3397	0.00131	2.772	7007.37	28.16	4742.83	0.11
4087	0.00146	3.098	8812.29	35.41	5752.56	0.13
4848	0.00175	3.709	12145.13	48.80	6560.41	0.15
5727	0.00207	4.381	16437.04	66.04	7516.34	0.18
6524	0.00234	4.964	20633.43	82.91	8374.91	0.20
7436	0.00268	5.668	26275.04	105.57	9321.96	0.23
8161	0.00292	6.174	30752.66	123.56	10091.18	0.25
9008	0.00322	6.816	37283.94	149.81	11082.89	0.28
9283	0.00344	7.290	42442.47	170.53	11355.45	0.30

(c)

Table 20. Water experiment data for $D/d_p = 6.33$ experiments of vertical bed set up with up-flow direction.

HZ	Q(gpm)	Q(cfm)	Q(m^3/s)	T	vis(30C)	dens(30C)
27.5	28.15	3.763655	0.0017762	31.7	0.000769	995.126
30	30.78	4.115286	0.0019422	28.8	0.000818	996.007
35	36.2	4.83994	0.0022842	30	0.000797	995.651
40	41.73	5.579301	0.0026331	29.9	0.000799	995.682
45	47.09	6.295933	0.0029713	29.9	0.000797	995.651
50	52.3	6.99251	0.0033001	30.3	0.000792	995.561
55	57.46	7.682402	0.0036257	30.9	0.000782	995.377
60	62.38	8.340206	0.0039361	31.5	0.000773	995.189

(a)

P1(PSI)	P2(PSI)	P3(PSI)	P4(PSI)	P5(PSI)
3.753	3.001	2.050	1.205	0.284
4.588	3.761	2.723	1.780	0.768
6.594	5.601	4.354	3.212	1.994
8.910	7.731	6.254	4.878	3.419
11.535	10.138	8.414	6.767	5.045
14.429	12.810	10.815	8.865	6.852
17.639	15.772	13.484	11.200	8.863
21.321	19.207	16.616	14.002	11.346

(b)

Re_m	Q(m^3/s)	Q(cfm)	P(Pa)	P(inches water)	f_m	v(m/s)
6324	0.0018	3.7621	7218.10	29.00	8779	0.155
6915	0.0019	4.1136	8518.38	34.23	9475	0.170
8132	0.0023	4.8379	11313.58	45.46	10700	0.200
9374	0.0026	5.5770	14580.83	58.59	11963	0.230
10578	0.0030	6.2933	18265.13	73.39	13280	0.260
11749	0.0033	6.9896	22362.14	89.85	14639	0.289
12908	0.0036	7.6792	26892.77	108.06	16024	0.317
14013	0.0039	8.3367	31374.06	126.06	17220	0.344

(c)

Table 21. Water experiment data for $D/d_p = 6.33$ experiments of horizontal bed set-up.

HZ	Q(gpm)	Q(cfm)	Q(m^3/s)	T	vis(26C)	dens(26C)
22.5	23.67	3.1647	0.0015	24.1	0.00091	997.29881
25	26.4	3.5297	0.0017	24.4	0.00091	997.29881
27.5	29.18	3.9014	0.0018	24	0.00091	997.29881
30	31.99	4.2771	0.0020	26.3	0.00086	996.70648
35	37.56	5.0218	0.0024	26.5	0.00086	996.65262
40	43.27	5.7852	0.0027	26.5	0.00086	996.65262
45	48.71	6.5125	0.0031	26	0.00087	996.78656
50	54.09	7.2318	0.0034	26.9	0.00085	996.5438
55	59.22	7.9177	0.0037	25.3	0.00088	996.97016
60	64.61	8.6384	0.0041	27.8	0.00083	996.23701

(a)

P1(PSI)	P2(PSI)	P3(PSI)	P4(PSI)	P5(PSI)
2.413	1.684	2.015	0.946	1.311
3.167	2.279	2.681	1.367	1.818
3.999	2.935	3.424	1.833	2.375
4.924	4.274	3.560	2.936	2.244
6.976	6.100	5.171	4.335	3.420
9.301	8.161	6.991	5.901	4.747
11.956	10.545	9.116	7.734	6.300
14.895	13.154	11.441	9.729	7.994
18.076	16.007	13.996	11.939	9.872
22.069	19.671	17.319	14.898	12.483

(b)

Re_m	Q(m^3/s)	Q(cfm)	P(Pa)	P(inches water)	f_m	v(m/s)
4667	0.00149	3.16	4859.24	19.52	6159	0.13
5205	0.00167	3.53	5951.88	23.91	6763	0.15
5753	0.00184	3.90	7231.04	29.05	7434	0.16
6641	0.00202	4.28	8835.24	35.50	8730	0.18
7832	0.00237	5.02	11821.80	47.50	9993	0.21
9023	0.00273	5.78	15181.68	61.00	11140	0.24
10046	0.00307	6.51	19163.76	77.00	12352	0.27
11379	0.00341	7.23	23394.72	94.00	13855	0.30
12024	0.00374	7.91	28123.44	113.00	14677	0.33
13920	0.00408	8.63	32976.61	132.50	16751	0.36

(c)

Table 22. Water experiment data for $D/d_p = 3.65$ experiments of vertical bed set up with up-flow direction.

HZ	Q(gpm)	Q(cfm)	Q(m^3/s)	T	vis(33C)	dens(33C)
40	44.31	5.9242	0.0028	33	0.000749	994.7083
45	49.76	6.6529	0.0031	33.5	0.000741	994.5438
50	55.11	7.3682	0.0035	32	0.000765	995.0312
55	60.5	8.0889	0.0038	34	0.000734	994.3772
60	66.17	8.8469	0.0042	31	0.000781	995.3456

(a)

P1(PSI)	P2(PSI)	P3(PSI)	P4(PSI)	P5(PSI)
7.9423	7.1756	6.2522	5.6103	4.9277
10.2696	9.3829	8.3545	7.6202	6.8756
12.9339	11.9194	10.7720	9.9334	9.1161
15.7972	14.6463	13.3681	12.4261	11.5250
18.9943	17.6847	16.2683	15.2141	14.1998

(b)

Re_m	Q(m^3/s)	Q(cfm)	P(Pa)	P(inches water)	f_m	v(m/s)
20047	0.00280	5.922	4174.95	16.77	17184	0.2446
22512	0.00314	6.650	5239.32	21.05	19203	0.2746
24933	0.00348	7.365	6459.98	25.96	21379	0.3042
27371	0.00382	8.085	7750.76	31.14	23365	0.3339
29936	0.00418	8.843	9304.54	37.39	25646	0.3652

(c)

Table 23. Water experiment data for $D/d_p = 3.65$ experiments of horizontal bed set-up.

HZ	Q(gpm)	Q(cfm)	Q(m^3/s)	T	vis(29C)	dens(29C)
40	44.95	6.0098	0.0028	29.2	0.000815	995.948657
42.5	47.36	6.3320	0.0030	29.3	0.000815	995.948657
45	50.54	6.7572	0.0032	28.8	0.000815	995.948657
47.5	52.91	7.0741	0.0033	29.3	0.000815	995.948657
50	55.99	7.4859	0.0035	28.5	0.000815	995.948657
52.5	58.4	7.8081	0.0037	29.5	0.000815	995.948657
55	61.35	8.2025	0.0039	27.8	0.000832	996.237009
57.5	64.05	8.5635	0.0040	29.8	0.000797	995.651465
60	67.08	8.9686	0.0042	26.5	0.000860	996.652619

(a)

P1(PSI)	P2(PSI)	P3(PSI)	P4(PSI)	P5(PSI)
7.7068	7.2788	6.7101	6.3961	6.0704
8.6235	8.1389	7.5224	7.1766	6.8292
9.9445	9.3938	8.7089	8.3075	7.9096
10.9990	10.3866	9.6537	9.2150	8.7835
12.4340	11.7474	10.9411	10.4444	9.9701
13.6293	12.8794	12.0239	11.4803	10.9695
15.1823	14.3452	13.4119	12.7967	12.2396
16.5108	15.6043	14.6064	13.9451	13.3416
18.1659	17.1655	16.0875	15.3546	14.6998

(b)

Re_m	Q(m^3/s)	Q(cfm)	P(Pa)	P(inches water)	f_m	v(m/s)
18721	0.0028	6.0098	4410.65	17.72	16440	0.2482
19725	0.0030	6.3320	4779.10	19.20	16907	0.2615
21049	0.0032	6.7572	5510.13	22.14	18266	0.2791
22036	0.0033	7.0741	5999.10	24.10	18996	0.2921
23319	0.0035	7.4859	6694.58	26.90	20033	0.3092
24322	0.0037	7.8081	7269.03	29.21	20854	0.3225
25551	0.0039	8.2025	8081.42	32.47	22070	0.3387
26676	0.0040	8.5635	8719.15	35.03	22808	0.3537
27938	0.0042	8.9686	9566.44	38.44	23894	0.3704

(c)

Air experiment data

Table 24. The properties of air experiments.

D/d_p	ε	μ (kg/ms)	ρ (kg/m^3)	d_p (m)	D	A (Bed,m^2)	L (m)
19	0.385	0.0000183538	1.1726	0.00635	0.12065	0.011432587	0.508
9.5	0.397	0.0000183538	1.1726	0.0127	0.12065	0.011432587	0.508
6.33	0.416	0.0000183538	1.1726	0.01905	0.12065	0.011432587	0.508

Table 25. Air experiment data for $D/d_p = 19$.

Re_m	Q(m^3/s)	Q(cfm) (ft^3/min)	P3-P5(Pa)	P3-P5 (inches water)	f_m	v(m/s)
263	0.00454	9.6056	373.32	1.50	617	0.39669
336	0.00579	12.2542	572.42	2.30	742	0.50607
409	0.00705	14.9381	796.42	3.20	847	0.61691
478	0.00824	17.4454	1045.30	4.20	952	0.72046
542	0.00934	19.7762	1343.95	5.40	1080	0.81672
603	0.01039	22.0010	1667.50	6.70	1204	0.90860
670	0.01155	24.4731	2015.93	8.10	1309	1.01069
732	0.01262	26.7332	2364.36	9.50	1405	1.10403
793	0.01366	28.9404	2737.68	11.00	1503	1.19518

Table 26. Air experiment data for $D/d_p = 9.5$.

Re_m	Q(m^3/s)	Q(cfm) (ft^3/min)	P3-P5(Pa)	P3-P5 (inches water)	f_m	v(m/s)
647	0.0055	11.58	177	0.71	1106	0.48
836	0.0071	14.97	296	1.19	1434	0.62
1000	0.0085	17.90	398	1.6	1613	0.74
1201	0.0102	21.50	548	2.2	1846	0.89
1404	0.0119	25.13	722	2.9	2081	1.04
1590	0.0134	28.45	916	3.68	2333	1.18
1848	0.0156	33.08	1202	4.83	2634	1.37
2071	0.0175	37.07	1493	6	2920	1.53
2268	0.0192	40.60	1755	7.05	3133	1.68
2418	0.0204	43.28	1954	7.85	3272	1.79
2562	0.0217	45.85	2153	8.65	3403	1.89
2683	0.0227	48.03	2297	9.23	3467	1.98
2921	0.0247	52.28	2663	10.7	3692	2.16
3148	0.0266	56.34	3061	12.3	3938	2.33
3344	0.0283	59.84	3492	14.03	4229	2.47
3551	0.0300	63.55	3820	15.35	4357	2.62
3645	0.0308	65.23	3982	16	4424	2.69
3798	0.0321	67.97	4338	17.43	4626	2.81
4142	0.0350	74.13	5002	20.1	4891	3.06

Table 27. Air experiment data for $D/d_p = 6.33$.

Re_m	Q(m^3/s)	Q(cfm) (ft^3/min)	P3-P5(Pa)	P3-P5 (inches water)	f_m	v(m/s)
1118	0.0061	12.9198	116.97	0.4700	1811	0.53
1381	0.007533333	15.9556	169.24	0.6800	2122	0.66
1634	0.008916667	18.8855	233.95	0.9400	2478	0.78
2193	0.011966667	25.3454	435.54	1.7500	3437	1.05
2917	0.015916667	33.7115	696.86	2.8000	4135	1.39
3406	0.018583333	39.3595	933.30	3.7500	4743	1.63
3727	0.020333333	43.0660	1095.07	4.4000	5086	1.78
4296	0.023437406	49.6404	1566.88	6.2957	6314	2.05
4631	0.025267332	53.5162	1785.56	7.1744	6674	2.21
5055	0.027579476	58.4133	2077.27	8.3465	7113	2.41
5396	0.029440957	62.3559	2324.62	9.3403	7457	2.58
6005	0.032760549	69.3868	2793.41	11.2239	8053	2.87
6224	0.033956541	71.9200	2970.99	11.9374	8263	2.97
6633	0.03618687	76.6438	3314.45	13.3175	8650	3.17
6968	0.038018933	80.5241	3608.56	14.4992	8964	3.33
7462	0.040711047	86.2260	4060.33	16.3144	9419	3.56
7833	0.042734944	90.5126	4415.32	17.7408	9758	3.74
7902	0.043111963	91.3111	4482.91	18.0123	9821	3.77

Experiment for the annular bed

Methodology

Pressure drop experiment was also done by the annular packed bed. Fig. 39 shows the diagram of experiment apparatus. The outer diameter of this bed is 35 inches (88.9 cm) and inner diameter is 10.inches (26.67 cm). The bed height is 86 inches (218.44 cm). The sphere particle diameter is 3.302 cm.

The bed has 10 tabs to measure wall pressures at each point. The distance of tab to tab was 6.5inches (16.51 cm). The working fluid was air. The flow rate of air was controlled by pump power controller. The only way to find flow rate was to measure velocity of the air in the tube. It was very difficult to measure velocities in the annular bed. Instead of measuring bed velocities, the pipe velocities were measured. At this point, the velocity measurement of the tube was also very difficult due to the size of the bed tube. The velocities were measured 16 points to get average velocity for this bed (Fig. 40). The velocities were fluctuated significantly. Therefore it was repeated 10 times. After then, the velocities in the annular bed were calculated. At last the flow rate was found by multiplying this average velocity to the area of the bed. And the flow rate of the inlet and the outlet flow rate were compared. The discrepancy was within 5 %. Table 29 shows the average velocities and area of the annular bed and pipe. The wall pressures (Table 30) were checked from the manometer at each tab. Table 31 shows final results of this experiment. Fig. 41 represents the modified friction factor of this packed bed as a function of the modified Reynolds number.

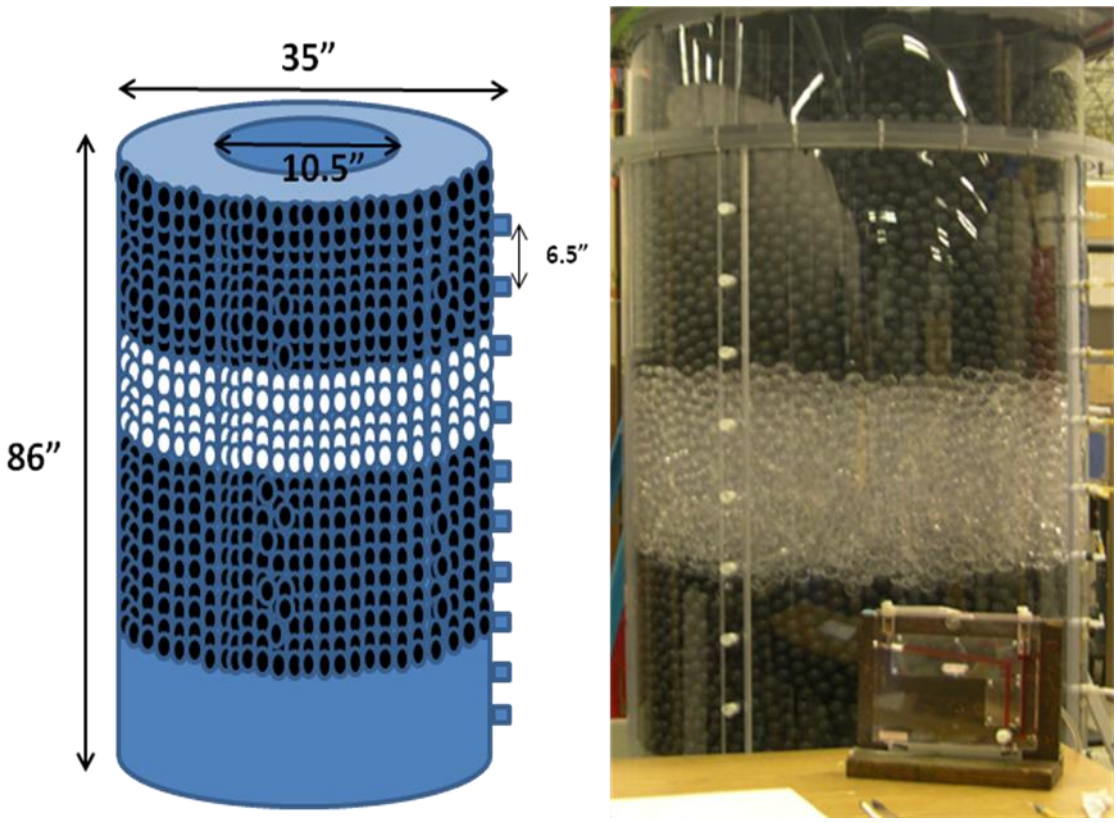

Fig. 39. A diagram and a picture of annular packed bed.

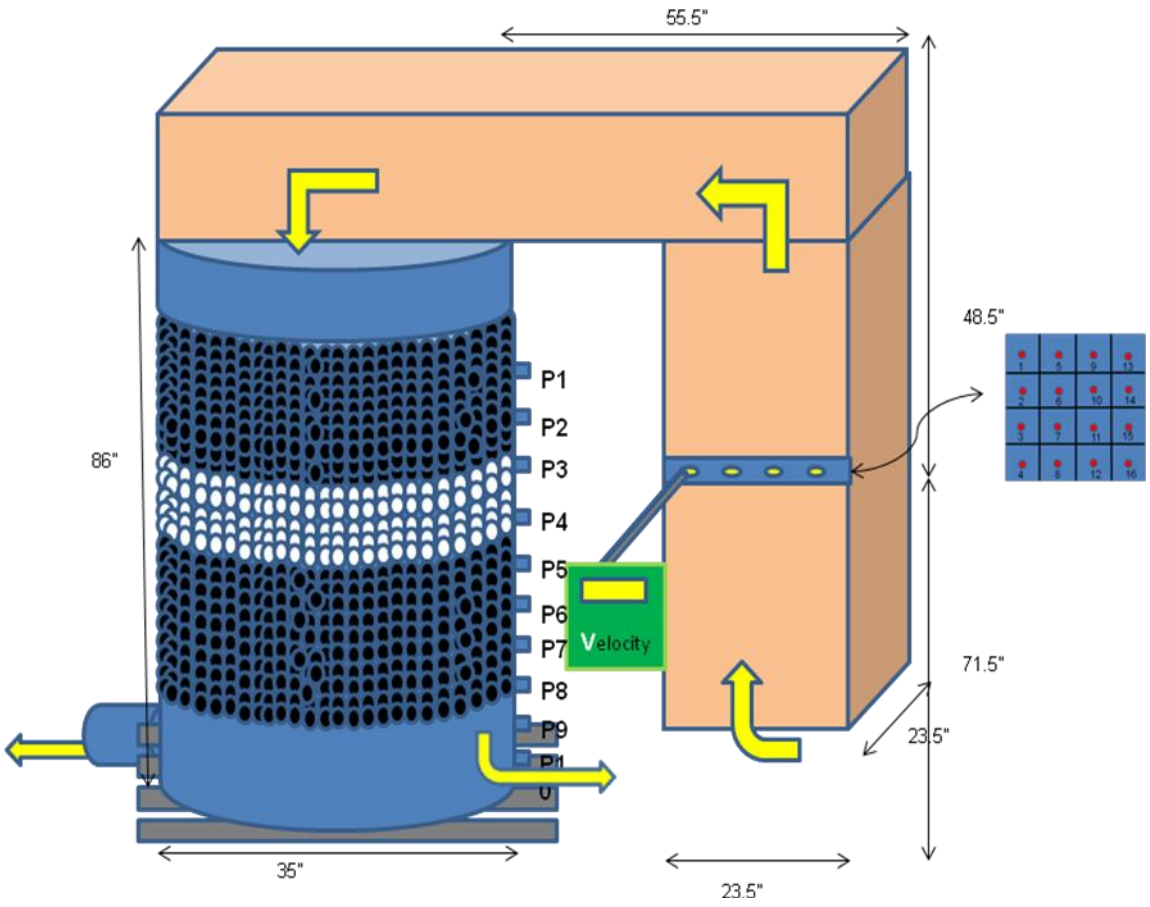

Fig. 40. A diagram of annular packed bed expeirment.

Results and Analysis

The porosity of the annular bed was 0.404. It was measured from particle counting method. The volume of the annular bed can be calculated from the bed dimensions. The only thing to know is the number of sphere. The number of sphere were filled were 31020. The measured porosity was 0.404. It used to calculated pressure drop and applied to other correlations to get the pressure drop and to compare pressure drops. Table 28 shows the properties of these experiments.

Table 28. The properties of the experiments

ε	μ_g(kg/ms)	ρ_g(kg/m^3)	d_p(m)	D	A(Bed,m^2)	A(pipe,m^2)
0.404	0.00001803	1.18376	0.03302	0.6223	0.565	0.356

Table 29. The average velocities and areas

(v1 : the average velocity of the pipe, A1 : the area of the pipe,

v2 : the average velocity of the annular bed and A2 : the area of the annular bed).

V1 (m/s)	A1 (m^2)	V2 (m/s)	A2 (m^2)
0.2927	0.3563	0.1846	0.5649
0.5999		0.3784	
0.8537		0.5385	
1.1249		0.7096	
1.5336		0.9673	
1.7983		1.1343	

Table 30. The measured pressures at each tab (unit : inches water).

P1	P2	P3	P4	P5	P6	P7	P8	P9	P10
0.13	0.11	0.1	0.09	0.08	0.07	0.055	0.045	0.03	0.025
0.47	0.44	0.39	0.35	0.3	0.26	0.22	0.18	0.11	0.105
1.05	0.95	0.85	0.76	0.66	0.58	0.48	0.41	0.25	0.23
1.8	1.6	1.5	1.38	1.2	1.05	0.855	0.738	0.46	0.43
2.73	2.58	2.3	2.1	1.85	1.65	1.4	1.2	0.73	0.68

Table 31. The final summarized results (velocity, flow rate, the modified Reynolds number, pressure difference (P1 to P8) and the modified friction factor).

V(m/s)	Q(m^3/s)	Re_m	ΔP(Pa)	ΔP (inches water)	f_m
0.185	0.104	671.625	21.155	0.085	1112.793
0.378	0.214	1376.467	72.175	0.290	1852.485
0.539	0.304	1958.756	159.283	0.640	2872.911
0.710	0.401	2580.905	264.311	1.062	3618.053
0.967	0.546	3518.441	415.630	1.670	4173.387
1.134	0.641	4125.904	547.536	2.200	4688.413

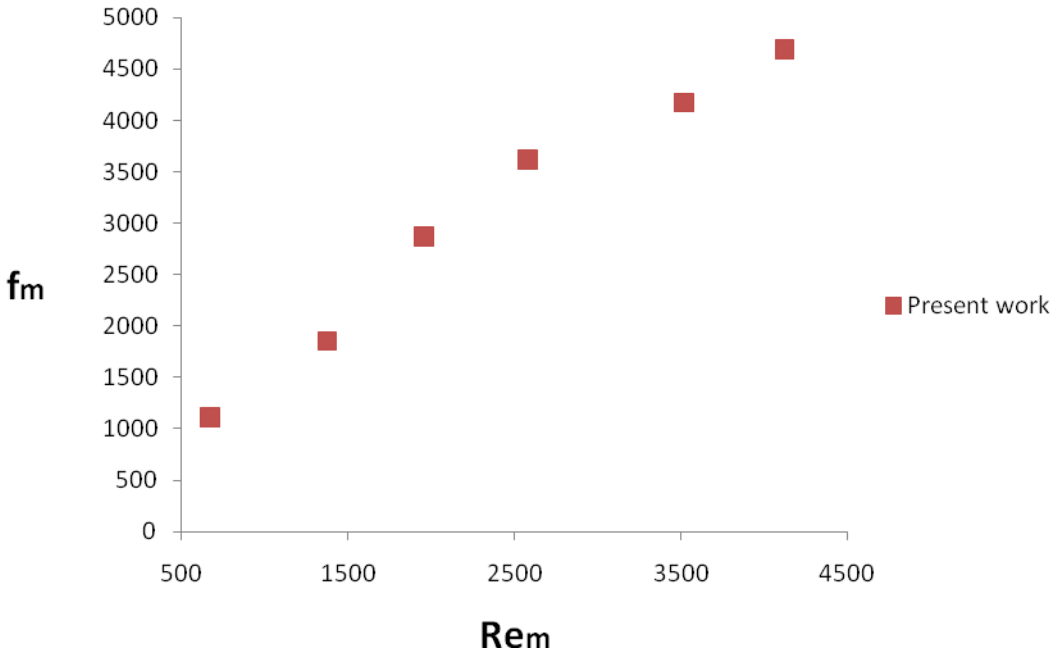

Fig. 41. The annular bed pressure drop results:

The modified friction factor as a function of the modified Reynolds number.

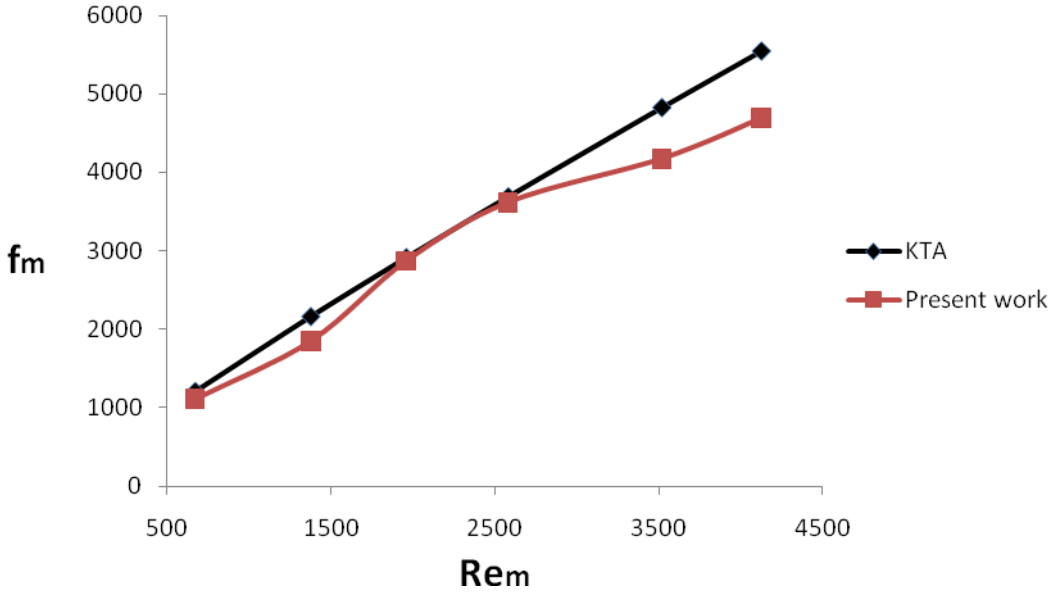

Fig. 42. The comparison of present work to KTA.

Fig. 42. shows the comparison of present work to KTA (1981)[2]. The modified friction factors of the present work were similar with KTA[2] by 3000 of the modified Reynolds number. However, as the modified Reynolds number increases, the difference of the modified friction factor between present work and KTA[2] increases. One of the possible reasons that made this difference is the velocity measurement error. As the velocity increases, there was more leaked air from the tube. The flow rate at the high velocity (=high pump power) was not accurate. In addition, the velocity measurement was not exact. The velocities from 16 points were not enough to get the exact average velocity of the pipe. The velocities of each point were fluctuated significantly. It caused the error of the pressure drop measurement. The new issue of this experiment is to get the flow rate exactly. The experiment set up has to be changed in order to get exact flow rate by reducing leaked air.

Summary of the existing pressure drop correlations

Ergun(1952)

$$\frac{\Delta P}{L} = 150\frac{(1-\varepsilon)^2}{\varepsilon^3}\frac{\mu}{d_p^2}U + 1.75\frac{(1-\varepsilon)}{\varepsilon^3}\frac{\rho}{d_p}U^2$$

$$\frac{\Delta P}{L} = 150\frac{(1-\varepsilon)^2}{\varepsilon^3}\frac{\mu_f}{d_p^2}U \text{ (for laminar)}$$

$$\frac{\Delta P}{L} = 1.75\frac{(1-\varepsilon)}{\varepsilon^3}\frac{\rho}{d_p}U^2 \text{ (for turbulent)}$$

$$f = \frac{\Delta P d_p^2 \varepsilon^3}{L\,\mu\,U(1-\varepsilon)^2} = 150 + 1.75\frac{\rho_f U d_p}{\mu(1-\varepsilon)}$$

$Re_m < 500$

Foscolo(1982)

$$\frac{\Delta P}{L} = 17.3\frac{(1-\varepsilon)}{\varepsilon^{4.8}}\frac{\mu_f}{d_p^2}U + 0.336\frac{(1-\varepsilon)}{\varepsilon^{4.8}}\frac{\rho_f}{d_p}U^2$$

$$\frac{\Delta P}{L} = 17.3\frac{(1-\varepsilon)}{\varepsilon^{4.8}}\frac{\mu_f}{d_p^2} \text{ (for laminar)}$$

$$\frac{\Delta P}{L} = 0.336\frac{(1-\varepsilon)}{\varepsilon^{4.8}}\frac{\rho_f}{d_p}U^2 \text{ (for turbulent)}$$

$$f = \frac{\Delta P d_p^2 \varepsilon^3}{L\,\mu\,U(1-\varepsilon)^2} = 17.3\frac{1}{(1-\varepsilon)\varepsilon^{1.8}} + 0.336\frac{\rho_f U d_p}{\mu(1-\varepsilon)\varepsilon^{1.8}}$$

$0.2<Re<500$

Foumeny et al. (1993, 1995)

$$\frac{\Delta P}{L} = 211\frac{(1-\varepsilon)^2}{\varepsilon^3}\frac{\mu_f}{d_p^2}U + \left(3.81 - \frac{5.265}{\frac{D}{d_{pe}}} - \frac{7.047}{(\frac{D}{d_{pe}})^2}\right)\frac{(1-\varepsilon)}{\varepsilon^3}\frac{\rho_f}{d_p}U^2$$

Where d_{pe} = equivalent diameter, $6V_p/S_p$ (S_p = surface area of particle)

$$1995.f = \frac{\Delta P d_p^2 \varepsilon^3}{L\,\mu\,U(1-\varepsilon)^2} = 211 + \left(3.81 - \frac{5.265}{\frac{D}{d_{pe}}} - \frac{7.047}{(\frac{D}{d_{pe}})^2}\right)\frac{\rho_f U d_p}{\mu(1-\varepsilon)}$$

$5 < Re_m < 8500$

For cylindrical particle

$$\frac{\Delta P}{L} = 130\frac{(1-\varepsilon)^2}{\varepsilon^3}\frac{\mu_f}{d_p^2}U + \frac{\frac{D}{d_p}}{0.335\frac{D}{d_p} + 2.28}\frac{(1-\varepsilon)}{\varepsilon^3}\frac{\rho_f}{d_p}U^2$$

$$1993.f = \frac{\Delta P\, d_p^2\, \varepsilon_m^3}{L\,\mu\,u\,(1-\varepsilon_m)^2} = \frac{\frac{D}{d_p}}{0.335\frac{D}{d_p} + 2.28}\frac{\rho\, u\, d_p}{\mu\,(1-\varepsilon_m)} + 130$$

$5 < Re_m < 8500$

$3 < \frac{D}{d_p} < 24$

Handley and Heggs(1968)

$$\frac{\Delta P}{L} = 368\frac{(1-\varepsilon)^2}{\varepsilon^3}\frac{\mu}{d_p^2}U + 1.24\frac{(1-\varepsilon)}{\varepsilon^3}\frac{\rho}{d_p}U^2$$

$$f = \frac{\Delta P d_p^2 \varepsilon^3}{L\,\mu\,U(1-\varepsilon)^2} = 368 + 1.24\frac{\rho_f U d_p}{\mu(1-\varepsilon)}$$

$1000 < Re_m < 5000$

Hicks(1970)

$$\frac{\Delta P}{L} = 6.8 \frac{(1-\varepsilon)^{1.2}\rho_f{}^{0.8}U^{1.8}\mu^{0.2}}{\varepsilon^3 d_p{}^{1.2}}$$

$$f = \frac{\Delta P d_p^2 \varepsilon^3}{L \mu U (1-\varepsilon)^2} = 6.8\left(\frac{\rho_f U d_p}{\mu(1-\varepsilon)}\right)^{0.8}$$

$300 < Re_m < 60000$

J.Wu et al. (2008)

$$\frac{\Delta P}{L} = 72\tau\frac{(1-\varepsilon)^2}{\varepsilon^3}\frac{\mu}{d_p^2}U + 3\tau\frac{(1-\varepsilon)}{4\varepsilon^3}\frac{\rho}{d_p}U^2\left(\frac{3}{2}+\frac{1}{\beta^4}-\frac{5}{2\beta^2}\right)$$

Where, β is the ratio of the pore diameter to the throat diameter

$$\beta = \frac{1}{1-\sqrt{1-\varepsilon}}$$

$$f = \frac{\Delta P d_p^2 \varepsilon^3}{L \mu U (1-\varepsilon)^2} = 72\tau + \frac{3\tau}{4}\left(\frac{3}{2}+\frac{1}{\beta^4}-\frac{5}{2\beta^2}\right)\frac{\rho_f U d_p}{\mu(1-\varepsilon)}$$

$0 < Re_m < 4000$

Lakota (2002)

$$\frac{\Delta P}{L} = 160\frac{(1-\varepsilon)^2}{\varepsilon^3}\frac{\mu}{d_p^2}U + 1.6\frac{(1-\varepsilon)}{\varepsilon^3}\frac{\rho}{d_p}U^2$$

For nonporous spheres with $d_p = 6mm$.

$$f = \frac{\Delta P d_p^2 \varepsilon^3}{L \mu U (1-\varepsilon)^2} = 160 + 1.6\frac{\rho_f U d_p}{\mu(1-\varepsilon)}$$

$18 < Re < 110$

Leva(1947)

$$\frac{\Delta P}{L} = \frac{3.50\, G^{1.9}\, \mu^{0.1}\, \square^{1.1}(1-\varepsilon)}{d_p^{1.1}\, \rho_f g_c \varepsilon^3}$$

$$\frac{\Delta P}{L} = 200\frac{(1-\varepsilon)^2}{\varepsilon^3}\frac{\mu}{d_p^2} U + 1.75\frac{(1-\varepsilon)}{\varepsilon^3}\frac{\rho}{d_p} U^2$$

$$f = \frac{\Delta P d_p^2 \varepsilon^3}{L\, \mu\, U(1-\varepsilon)^2} = 200 + 1.75\frac{\rho_f U\, d_p}{\mu(1-\varepsilon)}$$

$1 < Re < 17635$

Macdonald(1979)

$$\frac{\Delta P}{L} = 180\frac{(1-\varepsilon)^2}{\varepsilon^3}\frac{\mu_f}{d_p^2} U + 1.8\frac{(1-\varepsilon)}{\varepsilon^3}\frac{\rho_f}{d_p} U^2$$

$$f = \frac{\Delta P d_p^2 \varepsilon^3}{L\, \mu\, U(1-\varepsilon)^2} = 180 + 1.8\frac{\rho_f U\, d_p}{\mu(1-\varepsilon)}$$

$Re < 500$

Montillet (2004)

$$\frac{\Delta P}{L} = \left\{\frac{1410}{Re} + 16 + \frac{45}{Re^{0.45}}\right\}\frac{\rho_f U^2}{d_p}$$

$$F'' = \frac{\Delta P\, d_p}{L \rho_f U^2} = \frac{1410}{Re} + 16 + \frac{45}{Re^{0.45}}$$

$$f = \frac{\Delta P d_p^2 \varepsilon^3}{L\, \mu\, U(1-\varepsilon)^2} = \left\{\frac{1410}{Re} + 16 + \frac{45}{Re^{0.45}}\right\}\frac{d_p\, \varepsilon^3 \rho_f\, U}{\mu\, (1-\varepsilon)^2} = \left\{\frac{1410}{Re} + 16 + \frac{45}{Re^{0.45}}\right\} Re_m \frac{\varepsilon^3}{(1-\varepsilon)}$$

$120 < Re < 1540$

Rose(1949)

$$\frac{\Delta P}{L} = f(\varepsilon)\left\{\frac{1000}{Re} + \frac{60}{Re^{1/2}} + 12\right\}\frac{\rho_f U^2}{d_p}$$

$$f = \frac{\Delta P d_p^2 \varepsilon^3}{L \mu U(1-\varepsilon)^2} = f(\varepsilon)\left\{\frac{1000}{Re} + \frac{60}{Re^{1/2}} + 12\right\}\frac{d_p \varepsilon^3 \rho_f U}{\mu (1-\varepsilon)^2} = f(\varepsilon)\left\{\frac{1000}{Re} + \frac{60}{Re^{1/2}} + 12\right\} Re_m \frac{\varepsilon^3}{(1-\varepsilon)}$$

f(ε) is 1 for ε = 0.4

1000<Re<6000

Brauer(1960)

$$\frac{\Delta P}{L} = \{160 + 3.1\{Re_m\}^{0.9}\}\frac{\mu U(1-\varepsilon)^2}{d_p^2 \varepsilon^3}$$

$$f = \frac{\Delta P d_p^2 \varepsilon^3}{L \mu U(1-\varepsilon)^2} = 160 + 3.1\left\{\frac{\rho_f U d_p}{\mu(1-\varepsilon)}\right\}^{0.9}$$

$2 < Re_m < 20000$

Reichelt(1972)

$$\frac{\Delta P}{L} = \left\{\frac{154 A_w^2 \mu(1-\varepsilon)}{\rho_f U d_p} + \frac{A_w}{B_w}\right\}\frac{\mu U(1-\varepsilon)^2}{d_p^2 \varepsilon^3}$$

$$f = \frac{\Delta P d_p^2 \varepsilon^3}{L \mu U(1-\varepsilon)^2} = \frac{154 A_w^2 \mu(1-\varepsilon)}{\rho_f U d_p} + \frac{A_w}{B_w}$$

where, $A_w = 1 + \frac{2}{3\frac{D}{d_p}(1-\varepsilon)}$ $B_w = \left\{1.15\left(\frac{d_p}{D}\right)^2 + 0.87\right\}$ for Spheres beads

$0.01 < Re < 17635$

Mehta and Hawley(1969)

$$\frac{\Delta P}{L} = \frac{150\, G\, \mu\, (1-\varepsilon)^2}{d_p^2\ \rho\, \varepsilon^3}\left(\frac{4d_p}{6D(1-\varepsilon)}+1\right)^2 + 1.75\ \frac{G^2}{\rho\, d_p}\ \frac{1-\varepsilon}{\varepsilon^3}\left(\frac{4d_p}{6D(1-\varepsilon)}+1\right)$$

$$f = 150\left(\frac{4d_p}{6D(1-\varepsilon)}+1\right)^2 + 1.75 Re_m \left(\frac{4d_p}{6D(1-\varepsilon)}+1\right)$$

0.18<Re<9.55

Yu et al.(2002)

$$\frac{\Delta P}{L} = 203\frac{(1-\varepsilon)^2}{\varepsilon^3}\ \frac{\mu_f}{d_p^2}\ U + 1.95\ \frac{(1-\varepsilon)}{\varepsilon^3}\ \frac{\rho_f}{d_p} U^2$$

$$f = \frac{\Delta P d_p^2\, \varepsilon^3}{L\, \mu\, U(1-\varepsilon)^2} = 203 + 1.95\frac{\rho_f\, U\, d_p}{\mu(1-\varepsilon)}$$

797 < Re < 2449

Shijie Liu(1994)

$$\frac{\Delta P}{L} = \frac{\mu\, U(1-\varepsilon)^2}{d_p^2\ \varepsilon^{\frac{11}{3}}}\left\{85.2\left(1+\frac{\pi(d_p/D)}{6(1-\varepsilon)}\right)^2 + 0.69\left[1-\frac{\pi^2(d_p/D)}{24}\left(1-0.5(d_p/D)\right)\right] Re_m \frac{Re_m^2}{16^2+Re_m^2}\right\}$$

$$f = \frac{1}{\varepsilon^{\frac{2}{3}}}\left\{85.2\left(1+\frac{\pi(d_p/D)}{6(1-\varepsilon)}\right)^2 + 0.69\left[1-\frac{\pi^2(d_p/D)}{24}\left(1-0.5(d_p/D)\right)\right] Re_m \frac{Re_m^2}{16^2+Re_m^2}\right\}$$

$Re_m < 1600$

KTA(1981)

$$\frac{\Delta P}{L} = \left\{\frac{320}{\left(\frac{Re}{1-\varepsilon}\right)} + \frac{6}{\left(\frac{Re}{1-\varepsilon}\right)^{0.1}}\right\} \left\{\left(\frac{(1-\varepsilon)}{\varepsilon^3}\right)\left(\frac{1}{d_p}\right)\left(\frac{1}{2\rho}\right)(\rho U)^2\right\}$$

$$f = \frac{\Delta P d_p^2 \varepsilon^3}{L \mu U(1-\varepsilon)^2} = 160 + 3Re_m^{0.9}$$

$10 < Re_m < 100000$

$0.36 < \varepsilon < 0.42$

Chilton and Colburn(1931)

For low Reynolds number

$$\frac{\Delta P}{L} = \frac{425 \mu U}{d_p^2}$$

$$f = \frac{\Delta P d_p^2 \varepsilon^3}{L \mu U(1-\varepsilon)^2} = \frac{425\varepsilon^3}{(1-\varepsilon)^2}$$

For high Reynolds number

$$\frac{\Delta P}{L} = \frac{19\ Re^{0.85} \mu U}{d_p^2}$$

$$f = \frac{\Delta P d_p^2 \varepsilon^3}{L \mu U(1-\varepsilon)^2} = \frac{19\ Re^{0.85}\varepsilon^3}{(1-\varepsilon)^2}$$

Wentz and Thodos(1963)

$d_p = 3.12cm$

$\varepsilon = 0.354, 0.48, 0.615, 0.728$

$$\frac{\Delta P}{L} = \frac{\mu U(1-\varepsilon)^2}{d_p^2 \varepsilon^3} \frac{0.396\ Re_m}{Re_m^{0.05} - 1.20}$$

$$f = \frac{\Delta P d_p^2 \varepsilon^3}{L \mu U (1-\varepsilon)^2} = \frac{0.396\ Re_m}{Re_m^{0.05} - 1.20}$$

1460<Re<7661

Re. Hayes(1995)

$$\frac{\Delta P}{L} = \frac{\mu U (1-\varepsilon)^2}{d_p^2 \varepsilon^3} \left\{ \frac{1}{\tau} \left[456 + \frac{17.8(3\tau-1)}{\tau(1-\varepsilon)(1-\tau)} Re \right]^{0.5} \frac{1}{\varepsilon} + 1.3 \left(\frac{\tau}{3\tau-1} \right) Re_m \right\}$$

$$f = \frac{\Delta P d_p^2 \varepsilon^3}{L \mu U (1-\varepsilon)^2} = \frac{1}{\tau} \left[456 + \frac{17.8(3\tau-1)}{\tau(1-\varepsilon)(1-\tau)} Re \right]^{0.5} \frac{1}{\varepsilon} + 1.3 \left(\frac{\tau}{3\tau-1} \right) Re_m$$

30<Re<1000

Tallmadge(1970)

$$\frac{\Delta P}{L} = \frac{\mu U (1-\varepsilon)^2}{d_p^2 \varepsilon^3} (150 + 4.2 (Re_m)^{0.833})$$

$$f = \frac{\Delta P d_p^2 \varepsilon^3}{L \mu U (1-\varepsilon)^2} = 150 + 4.2 (Re_m)^{0.833}$$

$0.1 < Re < 10^5$

Carman(1970)

$$\frac{\Delta P}{L} = (180 + 2.87 (Re_m)^{0.9}) \frac{\mu U (1-\varepsilon)^2}{d_p^2 \varepsilon^3}$$

$$f = \frac{\Delta P d_p^2 \varepsilon^3}{L \mu U (1-\varepsilon)^2} = 180 + 2.87 (Re_m)^{0.9}$$

Morcom(1946)

$$\frac{\Delta P}{L} = \left(\frac{800}{Re} + 14\right)\frac{\rho U^2}{d_p}$$

$$f = \frac{\Delta P d_p^2 \varepsilon^3}{L \mu U (1-\varepsilon)^2} = (800 + 14Re)\frac{\varepsilon^3}{(1-\varepsilon)^2}$$

Y.S. Choi(2008)

$$\frac{\Delta P}{L} = 150\frac{(1-\varepsilon)^2}{\varepsilon^3}\frac{\mu M^2}{d_p^2} U + 1.75\frac{(1-\varepsilon)}{\varepsilon^3}\frac{\rho M C_w}{d_p} U^2$$

$Re_m < 1000$

Du plessis(1994)

$$\frac{\Delta P}{L} = 207\frac{(1-\varepsilon)^2}{\varepsilon^3}\frac{\mu_f}{d_p^2} U + 1.88\frac{(1-\varepsilon)}{\varepsilon^3}\frac{\rho_f}{d_p} U^2$$

$$f = \frac{\Delta P d_p^2 \varepsilon^3}{L \mu U (1-\varepsilon)^2} = 207 + 1.88\frac{\rho_f U d_p}{\mu(1-\varepsilon)}$$

Table 32. Experimental parameters of referenced literature.

Author	Bed type	Fuel type	ε	d_p	D/d_p	Re
Oman/Waston (1944)	Cylindrical	Spherical	0.3775~0.379	5.50	18.47	4.99~14.37
Coulson(1949)	Cylindrical	Spherical	0.393~0.420	1.59~7.94	6.4~ 31.95	0.0095~1.125
Andersson (1963)	Cylindrical	Spherical	0.351~0.410	0.709~ 5.49	6.53~ 56.9	1.5~1313
Handley/ Heggs(1968)	Cylindrical	Spherical	0.390	3.17 9.52	8 24	1000~5000
Mehta/Hawley (1969)	Cylindrical	Spherical	·	0.14~1.65	7.7~91	0.18~9.55
Reichelt(1972)	Cylindrical	Spherical	0.366~0.485	9.71~ 24.05	3.32~ 14.32	0.01~17635
Beavers(1973)	Cylindrical	Spherical	0.364~0.376	3	19.02~4 4.33	64~208
Foumeny (1995)	Cylindrical	Spherical	0.386~0.456	2.1~15.48	3.23~ 23.8	5~8500
Yu(2002)	Cylindrical	Spherical	0.364~0.379	12~20	30	797~2449
Lakota(2002)	Cylindrical	Spherical	0.375	3	57.33	18~110
Montillet (2004)	Cylindrical	Spherical	0.367	4.92	12.2	30~1500
Nemec/Levec (2005)	Cylindrical	Spherical	0.382~0.40	1.66~3.50	11.7~ 24.7	3~147
Y.S.Choi(2008)	Cylindrical	Spherical	·	·	3.2~91	0.01~1000
Wu(2008)	Cylindrical	Spherical	0.42	10		0~4000
Burke/Plummer (1928)	Cylindrical	Spherical	0.363~0.421	·	5.379~3 9.179	0.8~1070
Ergun/Orning (1949)	Cylindrical	Spherical	0.330~0.352	·	44.561~ 51.107	0.4~30
Gupte(1970)	Cylindrical	Spherical	0.366~0.640	·	50~250	0.01~184
Leva(1951)	Cylindrical	Spherical	0.354~0.651	·	1.624~1 3.466	1~17635
Wentz/Thodos (1963)	Cylindrical	Spherical	0.354~0.882	·	·	2550~64900
Fand(1989)	Cylindrical	Spherical	0.3571~0.6168	2.098~ 4.029	1.4~ 41.28	0.62~869
Morcom (1946)	Cylindrical	Spherical	0.425~0.450	0.56~1.01	·	100~500
Wintersberg /Tsotsas(2000)	Cylindrical	Spherical	0.37	·	4~40	1, 1000
Shijie Liu(1994)	Cylindrical	Spherical	0.6007	3.184	1.4039	0~6000
Eisfeld (2001)	Annular	·	0.330~0.882	·	1.624~2 50	0.01~17635
Tallmadge (1970)	·	·	·	·	·	0.1~100000
Hicks(1970)	·	·	·	·	·	300~60000
R.E. Hayes(1994)	Cylindrical	Spherical	0.402, 0.408,0.427, 0.385	2.97, 4.82, 6.01, 2.5	·	3~1000
KTA(1981)	Annular,	Spherical	0.36~0.42	·	·	10~100000

VITA

Changwoo Kang was born in Gwangju, South Korea. He received the degree of Bachelor in Civil Engineering from The Korea Military Academy in 2006. He entered the nuclear engineering department at Texas A&M University in September 2008. During his graduate studies at Texas A&M University, the author was a Graduate Research Assistant in the Department of Nuclear Engineering under the direction of Professor Yassin A. Hassan. His research interests include pebble bed modular reactors, pressure measurement, porosity measurement and computational fluid dynamics.

This thesis was written as a requirement for his degree of Master of Science. His email is kcw8305@gmail.com.

Name: Changwoo Kang

Address: Department of Nuclear Engineering, Texas A&M University,
3133 TAMU, College Station, TX 77843-3133

Email Address: kcw8305@gmail.com